Dissertation
submitted to the
Combined Faculties for the Natural Sciences and for Mathematics
of the Ruperto-Carola University of Heidelberg, Germany
for the degree of
Doctor of Natural Sciences

Role of CHRAC14 and histone methyltransferase Su(var)3-9 in facilitating ectopic loading of CENP-A

Presented by
Abhishek Sharma
Born in: Lucknow, India

Dissertation
submitted to the
Combined Faculties for the Natural Sciences and for Mathematics
of the Ruperto-Carola University of Heidelberg, Germany
for the degree of
Doctor of Natural Sciences

Role of CHRAC14 and histone methyltransferase Su(var)3-9 in facilitating ectopic loading of CENP-A

Presented by
Abhishek Sharma
(M.Sc. in Genetic Manipulation and Molecular Cell Biology)
Born in: Lucknow, India
Date of oral-examination: 26 January 2017

Role of CHRAC14 and histone methyltransferase Su(var)3-9 in facilitating ectopic loading of CENP-A.

Referees:
Prof. Dr. Elmar Schiebel
Dr. Sylvia Erhardt

Dedicated

To my lovely mom Mrs. Usha Sharma
and dear father Mr. Ashutosh Sharma

Acknowledgment

First of all, I would like to thank my mentor Dr. Sylvia Erhardt for giving me the opportunity to work in her team and financially supporting me. I am thankful for her critical and supportive suggestions throughout my Ph.D. Additionally, I am thankful for her patience and valuable time she put in correcting my thesis.

I would also like to thank my first supervisor Prof. Dr. Elmar for his valuable support and suggestions in my PhD project. Further, I am thankful to my TAC member Dr. Karsten Rippe for his inputs in my project.

Beside my supervisors and TAC members, I am thankful to all the current and past members of Dr. Erhardt's lab. Special thanks to Anne-Laure for her support and patience. Thanks for always being there for discussions, suggestions and guidance, which often made life easy in the lab. I am also thankful to all the technical helps provided by Andrea. Dear Ana and Engin, I am thankful to you guys for all the scientific and non-scientific conversations we had at our free times. You guys have been great support in my good and bad times. It would have been harder to handle the stress without you guys.

Further, I would like to thank the members of Elmar's lab, especially Gurkan, Takumi, Marko and Shoji for their support. Further thanks to all my friends which I made during my stay in Heidelberg University, in some or the other way, everybody of you have made my life easier and nicer.

In the end, I am thankful to my parents and siblings, without their support I would have never made it so far. Their motivation, hard work and love always keeps me motivated.

Summary

Kinetochore formation is required for the attachment of microtubules to the chromosome at centromere where CENP-A (also known as CID in Drosophila) is the key factor for the formation of kinetochore. CENP-A is a variant of histone H3 and its accumulation at the centromere leads to the initiation of kinetochore formation. CENP-A localization to centromere in Drosophila requires CENP-C and CAL1. Ectopic localization of CENP-A has been reported to give rise to pseudo-kinetochore, which results in chromosome segregation defect and could lead to aneuploidy. Breast, prostate and colon cancer show higher level of CENP-A with ectopic localization. In 2014 our lab reported that depletion of CHRAC14 leads to ectopic localization in Drosophila cells. CHRAC14 is a subunit of two chromatin remodelling complex, CHRAC and ATAC complex.

In this study, we have investigated the potential role of CHRAC14 in maintaining chromatin structure and how it's absence lead to CENP-A ectopic localization. We show that depletion of CHRAC14 leads to increase in transcript level of histone methyltransferase Su(var)3-9. Su(var)3-9 is responsible for histone H3 lysine 9 (H3K9) methylation. Using Immunoblotting and immunofluorescence we show that lack of CHARC14 leads to overall increase in histone H3 lysine (H3K9) di methylation and reduction in H3K9 acetylation, thereby highlighting the importance of CHRAC14 in maintaining heterochromatin and euchromatin balance.

Further, we examined if the increase in Su(var)3-9 expression level could lead to ectopic CENP-A localization. Using Su(var)3-9 overexpressing Drosophila S2 cells, we show that overexpression of Su(var)3-9 can cause ectopic localization of CENP-A and CENP-C. Moreover, live-cell imaging analysis revealed that Su(var)3-9 overexpressing cells show cell segregation defect with delayed metaphase and lagging chromosome. Further analysis of the observed lagging chromosomes in Su(var)3-9 overexpressing cells revealed presence of higher number of CENP-A foci, indicating it to be the cause of cell segregation defect. Overall, this study reveals the role of CHRAC14 in maintaining the chromatin structure and highlights the significance of maintaining the physiological level of Su(var)3-9 for proper CENP-A localization.

Zusammenfassung

Kinetochore bilden die strukturelle Basis für das Binden von Mikrotubuli an Zentromere. Zentromere werden durch den Schlüsselfaktor CENP-A (auch bekannt als CID in Drosophila) definiert. CENP-A ist eine H3 Histonvariante und seine Anreicherung am Zentromer führt zur Ausbildung des Kinetochores. Für die Zentromerlokalisation von CENP-A sind in Drosophila zwei Proteine sehr wichtig: CENP-C und CAL1. Ektopische Lokalisation von CENP-A führt zu Chromosomsegregations-Defekten und Aneuploidie. In Brust-, Darm- und Prostatakrebs ist das CENP-A Proteinlevel erhöht und CENP-A lokalisiert zu Regionen außerhalb des Zentromeres. 2014 berichtete unser Labor, dass in Drosophila-Zellen eine Reduzierung von CHRAC14 ebenfalls zu ektopischer Lokalisation von CENP-A führt. CHRAC14 bildet eine Untereinheit von jeweils zwei verschiedenen Komplexen, dem ATAC und dem CHRAC Komplex.

In dieser Doktorarbeit haben wir die Rolle von CHRAC14 in Bezug auf die Aufrechterhaltung von Chromatin-Strukturen erforscht und wie das Fehlen von CHRAC14 ektopische CENP-A Lokalisation bedingen könnte. Hier zeigen wir, dass ein Mangel an CHRAC14 zum Anstieg des Transkriptlevels der Methyltransferase Su(var)3-9 führt. Su(var)3-9 ist für die Methylierung von Histone H3 an Lysin 9 verantwortlich. Durch das Anwenden von Immunoblotting und Immunfluoresenz zeigen wir, dass das Fehlen von CHRAC14 einen globalen Anstieg von H3 Lysin Di-Methylierung und einen Abfall in H3K9 Acetylierung bewirkt. Dieses Ergebnis betont die Bedeutung von CHRAC14 die Balance zwischen Eu- und Heterochromatin beizubehalten.

Darüber hinaus untersuchten wir, ob der Anstieg des Su(var)3-9 Expressionslevels möglicherweise zu ektopischer CENP-A Lokalisation führen könnte. Indem wir Su(var)3-9 in Drosophila-Zellen über-exprimieren, zeigen wir, dass dies ektopische Lokalisation von CENP-A und CENP-C verursacht. Des Weiteren deuten Lebend-Zell-Bildgebungs-Experimente darauf hin, dass Su(var)3-9-Überexpression zu Chromosomsegregations-Defekten führt und durch eine verzögerte Metaphase wie auch durch ‚Lagging Chromsomes' gekennzeichnet ist. Eine genaue Untersuchung der observierten ‚Lagging Chromosomes' offenbart zudem eine vergrößerte Menge an CEÑP-A Foki in Su(var)3-9 überexprimierenden Zellen. Dies ist möglicherweise die Grundlage für die beobachteten Defekte.

Zusammenfassend zeigt diese Studie, dass CHRAC14 wichtig für die Beibehaltung von Chromatin-Strukturen ist und unterlegt dessen Bedeutung für die Aufrechterhaltung physiologischer Su(var)3-9-Level, sodass CENP-A korrekt lokalisiert.

1. Introduction

1.1. Chromatin organization

1.1.1 High order chromatin structure

Genetic information is retained in DNA sequence which makes it important for cells to strictly maintain its sequence information. The length of DNA is far greater than what could fit into the size of a nucleus (length of DNA in human chromosome is around 2 meters). The high compaction of DNA to chromatin is a multistep process which renders the cells able to carry and manage the flow of genetic information. First, the DNA is wrapped around repeating units called nucleosomes as proposed by Roger D. Kornberg (Kornberg 1974). These repeating units are composed of H2A, H2B, H3 and H4 histone octamer around which 146 bp DNA sequence is wrapped (Luger et al. 1997). DNA that connects two nucleosomes is called linker DNA which is 10-80bp and nucleosomes form a 10nm structure resembling beads on a string. Histone H1 binds to the linker DNA. Histone H1 stabilizes nucleosomes and facilitates the higher order packing of nucleosomes into 30nm fibers which are helical in structures (Bednar et al. 1998; Olins & Olins 1974)(Figure 1.1). The evidences for the existence of 30nm fiber are limited (Maeshima et al. 2010; Woodcock 1994; Scheffer et al. 2011) and might not be present uniformly (Razin & Gavrilov 2014). Nevertheless, the 30nm fiber is further folded and packed into the final structure which is seen in metaphase chromosome (Hood & Galas 2003a).

An ordered chromatin organization is necessary for packing all DNA information in the nucleus compartment. However, the DNA packaging changes during cellular processes like DNA transcription, replication and during different stress conditions like DNA damage with the help of chromatin remodelers (Swygert & Peterson 2014; Peterson 2002). The phenomenon of changing the chromatin structure in response to different environmental conditions to alter the expression of genes without altering the underlying DNA sequence is termed as epigenetic (Goldberg et al. 2007). Epigenetics can also be explained as change in phenotype without

changing the genotype by effecting how cells read the gene. Chromatin remodelers play a crucial role in changing the chromatin structure. These remodelers have five common properties: 1) DNA dependent ATPase domain which is required for breaking the DNA-histone contact thereby helping in remodeling, 2) domains/proteins that regulate the ATPase domain, 3) domains that recognize the covalent histone modification 4) domains or subunits that help to interact with chromatin associated factors and 5) affinity to nucleosome. Chromatin remodelers are classified into four families on the basis of their distinct domains associated with ATPase domain. These families are a) switching defective/sucrose non fermenting (SWI/SNF) remodelers, b) imitation switch (ISWI) remodelers, c) chromodomain, helicase, DNA binding (CHD) remodelers, and d) inositol requiring 80 (INO80). Chromatin remodelers work by moving, ejecting, or re-structuring the composition of nucleosome which is well explained in several reviews (Clapier & Cairns 2009; Narlikar et al. 2013) (Figure 1.2). In general, ATPase domain binds to DNA at the site inside the nucleosome and is responsible for translocation. The ATPase translocation domain remains attached to a fixed site on the nucleosome octamer and from this site it conducts directional DNA translocation. This process can create transient DNA loops on the nucleosome which then propagate around the nucleosome. This loop propagation requires nucleosome sliding, or disruption of one or two histones from the nucleosome, resulting in change in chromatin packing without changing the underlying sequence. Additionally, certain enzymes alter the affinity between the nucleosome

histones and DNA through posttranslational modification of histone amino acids. Some of them are discussed later in this chapter.

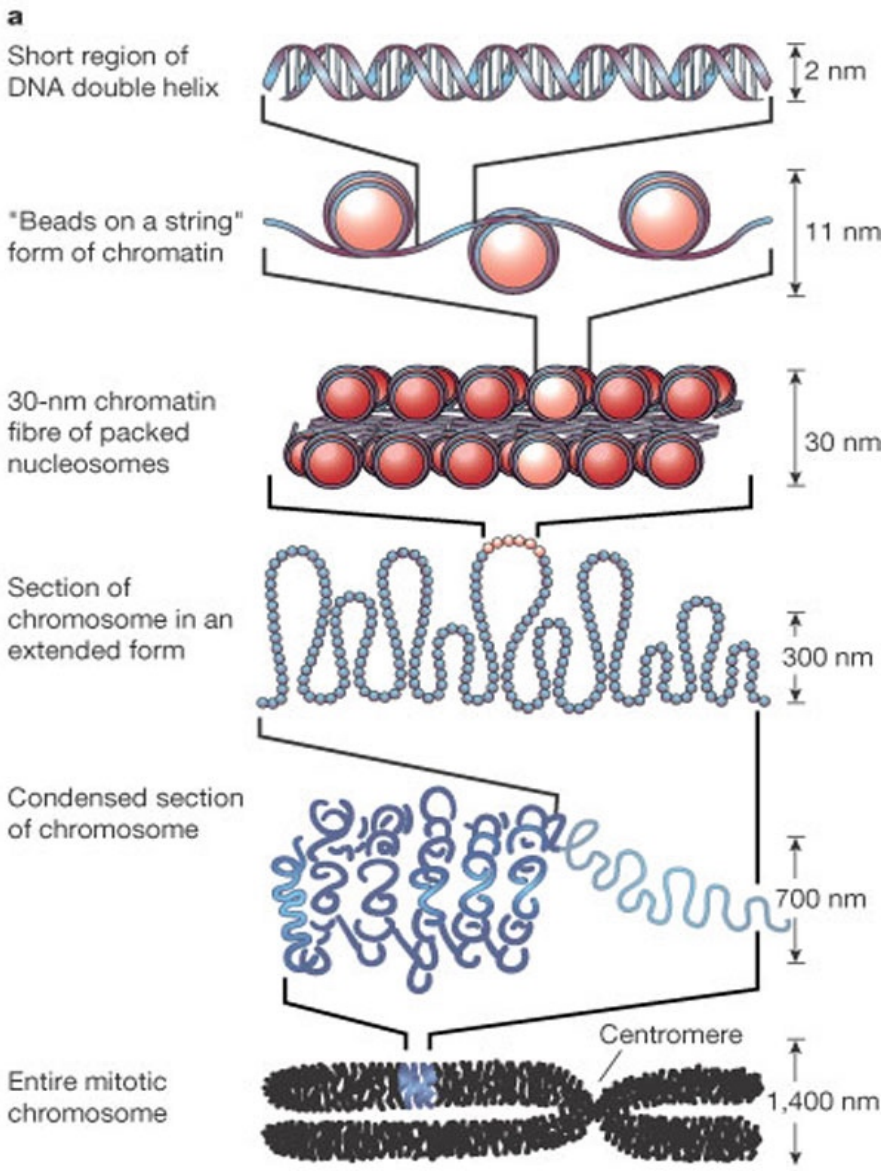

Figure 1.1: Organization of DNA into chromatin structure (Hood & Galas 2003b). The picture represents the levels of chromatin packaging from DNA helix to arrangement of the helix on a histone octamer (nucleosome) to 30nm fibers and resulting in final packaging into a mitotic chromosome.

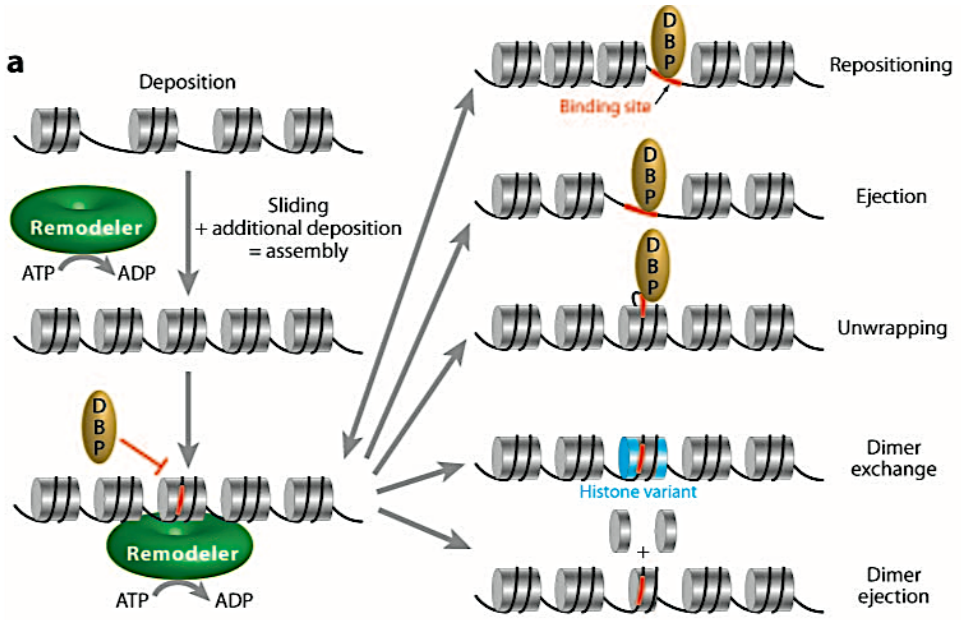

Figure 1.2 (Adapted from Clapier & Cairns 2009). Mechanisms utilized by different chromatin remodelers to access the genomic site or alter the composition of nucleosomes. For access of genomic sites, remodelers (*green*) can change the chromatin structure by moving already deposited nucleosomes, ejecting the histone units from the nucleosome, unwrapping the DNA from the histone octamer. Remodelers alter the composition of nucleosomes by histone dimer exchange with histone variants (in blue) and by ejection of a histone dimer.

1.1.2 Heterochromatin and euchromatin

In eukaryotes, traditionally, the chromatins are divided into two categories: heterochromatin and euchromatin. Heterochromatin represents inactive or dense chromatin regions and comprises 10 to 25% of total chromatin depending on age, cell type and species (Yunis & Yasmineh 1971; Gabor et al. 1979). Heterochromatin is further subdivided into two categories: constitutive and facultative. Constitutive heterochromatin is referred to the chromatin regions that stay transcriptionally inert throughout the cell life. Facultative heterochromatin represents a region of euchromatin, which is silenced via condensation and can be transcriptionally active when required by cell conditions. Euchromatin comprises the active chromatin regions. In general, euchromatin contains several histone H3 lysine (K) methylation and acetylation modifications like, H3K4me2, H3K4me3, H3K27ac and H3K9ac whereas heterochromatin or inactive chromatin regions contain H3K9me2/3 and H3K27me3 (Shilatifard 2008; Wang et al. 2014; Schneider

& Grosschedl 2007; Hood & Galas 2003b). These modifications are collective results of activities of histone acetyltransferase (HAT), histone deacetylase (HDAC), and histone methyltransferase (HMT). Heterochromatin and euchromatin is a simplified view of chromatin structure, recent studies have further characterized subtypes of chromatin structures based on associated proteins. According to Fillion and colleagues, Drosophila chromatin can be divided into 5 types, which gives further insight into the types of heterochromatin and euchromatin (Filion et al. 2010). The study suggests that heterochromatin can be divided into three types 1) heterochromatin protein 1 (HP1) associated chromatin, 2) polycomb group (PcG)-associated chromatin and 3) predominantly associated with H1 and suppressor of underreplication (Suur). Furthermore, they divide euchromatin into 2 types: 1) chromatin region enriched with H3K36me3 and, 2) active chromatin region that contains no H3K36me3 but is associated with Brahma which is a nucleosome remodeler. This gives a hint on specialized roles of different chromatin remodelers and histone modification enzymes in maintaining the chromatin structure, some of which are discussed below.

1.1.3 **Histone acetyltransferases**

HATs are enzymes that acetylate histones. Hyperacetylation of histones is associated with active or accessible chromatin regions (Oliva et al. 1990). Acetylation of the lysine residue of histones removes the positive charge and this in turn reduces the interaction of the histone with negatively charged DNA thereby making chromatin relaxed. This in combination with other chromatin remodelers overall affect the chromatin assembly and structure (Eberharter & Becker 2002), further making DNA information available for the transcription machinery (Bannister & Kouzarides 2011). HAT1 and GCN5 were the first two discovered HATs (Kleff et al. 1995; Brownell et al. 1996), since then a number of HATs has been identified in various organisms (Table 1.1). HATs can be categorized into two families, the Gcn5 N-acetyltransferase (GNAT) and MYST HAT family (named after

founding members MOZ, Ybf2/Sas3, Sas2 and Tip60). GNATs can be sub-categorized into following a) GCN5 containing, b) PCAF containing, **c)** Hat1a containing d) Elp3 containing and e) Hpa2 containing HAT complexes. MYST HATs can be categorized into complexes with a catalytic subunit a) Esa1 b) Sas3 **c)** Sas2 d) TIP60 e) HBO1 f) MOZ/MORF g) MSL (Lee & Workman 2007). Beside these HATs, nejire (KAT3) is the single Drosophila CBP/p300 homologue.

Different HAT complexes are composed of many different subunits with DNA-binding domains which are important for HAT recruitment and its activity. Multiple functions identified for HATs explain the requirements of many subunits. Associated subunits help HATs to be recruited to an appropriate genomic location and contain domains like bromodomain, chromodomains (CD), WD40 repeats, Tudor domain and PHD fingers. HATs have been reported to co-localize with H3K9ac at the promoter regions. Complementing with this, HATs are important for transcription activation, cell cycle and growth control (Carrozza et al. 2003; Xue-Franzén et al. 2013). Loss of HATs activity impairs the DNA damage repair ability (Dinant et al. 2008; Carrozza et al. 2003). Furthermore, CBP dependent H3K56ac is found to localize at the DNA damage repair sites in Drosophila and human cells. The deposition of H3K56ac to DNA damage repair sites is mediated by chromatin assembly factor 1(Caf1) (Das et al. 2009). In a nutshell, current findings suggest a strong role for HATs mediated histone acetylation in maintaining genome stability and cell cycle progression by changing the chromatin structure.

GNAT HATs		MYST HATs	
Catalytic subunits found in GNAT family HATs	**Associated complex**	**Catalytic subunits found in MYST family HATs**	**Associated complex**
GCN5	SAGA, ATAC, SLIK, ADA. HAT-A2, STAGA,	Esa1	NuA4
PCAF	PCAF	Sas3	NuA3
Hat1a	HATB	Sas2	SAS
Elp3	Elongator	TIP60	TIP60
Hpa2	Hpa2	HBO1	HBO1
-	-	MOF	MSL

Table 1.1 The Histone acetyltransferases (HATs) are grouped into GNAT (Gcn5 N-acetyltransferase) and MYST (Morf-Ybf2-Sas2-Tip60) families. This table represents catalytic subunits of various HAT complexes from the two families. Further details on HATs can be found in the reviews. (Lee & Workman 2007; Carrozza et al. 2003; Biterge 2016)

1.1.4 Histone deacetylases

Histone deacetylases (HDACs) catalyze the removal of functional acetyl groups (O=C-CH3) from histones. HDACs are metal dependent (Zn^{2+}) enzymes that hydrolyze acetyl-L-lysine side chains in histones to yield lysine and acetate (Lombardi & Cole 2011). HDACs in eukaryotic organisms have been classified in four classes (Class I – IV) based on shared homology with yeast HDACs. Class I represents HDACs which share homology with Rpd3, like Rpd3, HDAC1, HDAC2 and HDAC3 (Kasten et al. 1997). Using the Drosophila model system, it has been postulated that class I HDACs play a role in inactivation of genes via interaction with histone methyltransferases (HMT) (Czermin et al. 2001). Class II HDACs are HDACs which share similarity with yeast Hda1 and bind to MEF2 family of transcription factors through a MEF2 binding domain (Wang et al. 1999; Miska et al. 2001). HDAC4 from class II has also been shown to play a role

in the circadian cycle in Drosophila and mammals (Fogg et al. 2014). Class III HDACs share similarity with yeast Sir2 and play a role in longevity, apoptosis and skeletal myogenesis in yeast, *C. elegans*, Drosophila and mammals (Luo et al. 2001; Whitaker et al. 2013; Guarente 2001; Fulco et al. 2003). Class IV HDACs are a new class of HDACs and contain only one member - HDAC11. This newly discovered HDAC is exclusively expressed in brain, kidney and testis (Gao et al. 2002) and plays a role in immune system. In Drosophila, it has been shown that individual HDACs modulate transcription of distinct genes (Cho et al. 2005).

The wide variety of HDAC functions in cell proliferation, cancer and other diseases (Ververis et al. 2013) led to the need of HDAC inhibitors for research and clinical purposes. N-butyrate is the earliest discovered inhibitor, which causes a reversible increase in histone acetylation (Riggs et al. 1977). Trapoxin A (TPX) and trichostatin A (TSA) were discovered following N-butyrate (Yoshidas 1990; Kijima et al. 1993). TSA is shown to create hyperacetylation of the chromatin environment by inhibiting a wide range of HDACs, in turn to reduce the heterochromatin environment concomitant with a reduction in H3K9 methylation (Görisch et al. 2005; Tóth et al. 2004; Felisbino et al. 2016; Wu et al. 2008). TSA is one of the extensively used drugs in studying the overall role of HDACs in chromatin change, DNA repair, gene activation, cell proliferation and cancer treatment (Tao et al. 2004; Pile et al. 2001; Vigushin et al. 2001; Kondo et al. 2003; Görisch et al. 2005; Klement et al. 2014; Taddei et al. 2005; Szyf 2003).

1.1.5 **Histone methyltransferases**

Histone methyltransferases (HMTs) are a class of enzymes that add a methyl (CH_3) group to histones. HMTs transfer CH_3 from the cofactor S-adenosylmethionine (SAM) to the terminal amine of a specific substrate lysine (K) or arginine (R) residue. An early evidence of histone methylation was discovered in 1960s, were the importance of histone methylation in RNA synthesis was shown (Murray 1964; Allfrey et al. 1964). Su(var)3-9 is

the first reported HMT (Rea et al. 2000). Most of the HMTs contain a SET domain that is a 130 amino acid catalytic domain initially found to be conserved in **S**u(var)3-9, **E**(z) (enhancer of zeste) and **T**rithorax (Jenuwein 2006). Su(var)3-9, E(z), and trithorax are lysine HMTs (KHMTs). Lysine methylation on histones is one of the posttranslational modifications that regulate important epigenetical phenomena like gene silencing and heterochromatin formation. KHMTs can be divided into two groups: KHMTs with a SET domain and KHMTs without a SET domain (Nguyen & Zhang 2011b).

Subsequently, I will focus on modifications catalyzed by SET domain containing KHMTs, their substrates and their significance in regulating cell cycle progression and development. Methylation of lysine residues of Histone H3 K4, K9, K27, K36 and K79, and K20 in H4 histone are well-studied sites (Table 1.2) and reviewed in detail by Black et al. 2012 and Izzo & Schneider 2010. Methylation of H3 K9, K27 and H4K20 plays a role in the formation of heterochromatin and transcriptional silencing, while methylation of H3K4, H3K36 and H3K79 are important for transcription activation (Black et al. 2012; Biterge 2016).

Table 1.2: Substrate, site and functions of SET containing KHMT

Histone lysine	**Histone Lysine methyltransferases**	**Function/s**
H3K9	Dm Su(var)3-9, Hs and Mm Su(var)3-9H1 and Su(var)3-9h2, Sp Clr4	Heterochromatin and euchromatin silencing; DNA methylation (Lundberg et al. 2013).
	Mm and Hs G9a, Hs GLP1	Euchromatin silencing and DNA methylation (Seum et al. 2007).
	Mm, Dm and Hs SETDB1	Euchromatin silencing (Loyola et al. 2009).

	Nc DIM-5	Heterochromatin silencing and DNA methylation (Ruesch et al. 2015).
H3K27	Dm E(z); Hs EZH1 and EZH2 (catalytic subunits if Polycomb repressive complex 2)	Euchromatin Silencing (Gaydos et al. 2014).
	Hs and Mm G9a	Euchromatin Silencing (Wu et al. 2011).
H3K4	Hs EZH2 (catalytic subunits of Polycomb repressive complex 3)	Transcriptional silencing (Reinberg 2011).
	Dm Trxk Hs MLL1, MLL2 and MLL3	Transcriptional activation (Sandstrom et al. 2014; Lee et al. 2013).
	Hs SET1, Sc SET1	Transcriptional activation and elongation (Thornton et al. 2014).
	Hs SET7/9	Transcriptional activation (Gu & Lee 2013).
	Dm ASH1	Transcriptional activation (Dillon et al. 2005).
H3K36	Sc SET2	Transcriptional silencing and elongation (Bell et al. 2007).
	Mm NSD1 and Dm MES-4	Transcriptional regulation (Wagner & Carpenter 2012).
H3K79	Dm, Hs and Mm DOT1 (KHMT without SET domain)	Demarcation of Euchromatin (Nguyen & Zhang 2011a).
H4K20	Dm, and Hs SET8	Cell cycle-dependent silencing, mitosis and cytokinesis (Jørgensen et al. 2013).

	Dm, Mm and Hs Su(var)4-20 H1 and Su(var)4-20	Heterochromatin silencing (Jørgensen et al. 2013).
	Mm NSD1	Transcription regulation (Rayasam et al. 2003).
	Dm ASH1	Transcription activation (Beisel et al. 2002).
	SpSET9	Recruitment of checkpoint protein Crb2 to sites of DNA damage (Sanders et al. 2004).
H1K26	Hs and Dm EZH2	Transcriptional silencing (Kuzmichev et al. 2004).

Table 1.2: The Histone lysine methylation sites listed according to their lysine histone methyltransferase and function of the methylation. Species abbreviation: Dm: Drosophila melanogaster, Hs: Homo sapiens, Mm: Mus musculus, Nc: Neurospora crassa Sp: Schizosaccharomyces pombe. (Black et al. 2012; Izzo & Schneider 2010)

1.1.5.1 Histone K9 methylation

Among heterochromatin histone modifications, H3K9 methylation is one of the most extensively studied histone modification. Su(var)3-9, G9a and SETDB1 are the predominant HMTs responsible for H3K9 methylation (Du et al. 2015). Mono- (H3K9me1), di- (H3K9me2) or tri- (H3K9me3) methyl groups can be added which often has a different function. In mammals, H3K9me2 and H3K9me3 represent facultative and constitutive heterochromatin, respectively (Peters et al. 2003). This H3 modification has been shown to be one of the epigenetically inherited modifications in yeast via cryptic loci regulator 4 (Clr4) HMT (homolog of Su(var)3-9) (Audergon et al. 2015). In the study, authors show that H3K9me is a persistent histone modification that can be stably copied through meiosis and mitotic cell divisions after the loss of Clr4. Su(var)3-9 is demonstrated to be conserved from yeast to human. Su(var)3-9h1 which is a homolog of Drosophila Su(var)3-9, requires the H3K9me1 modification by SETDB1 for adding

H3K9me2/3 at pericentric heterochromatin (Loyola et al. 2009; Lundberg et al. 2013). Su(var)3-9 physically interacts with H1 linker histone playing a key role in formation of heterochromatin (Lu et al. 2013). H3K9me is important for maintaining constitutive heterochromatin, while it is also important for silencing euchromatin regions. In Drosophila, Su(var)3-9 is the dominant HMT and is detected in all major heterochromatin regions and several euchromatin regions (Hwang et al. 2001; Schotta et al. 2003). Lack of Su(var)3-9 results in an aberrant chromosome segregation during meiosis and increases genome instability in mammals (Peters et al. 2001; Schotta et al. 2002). Its activity is important for peri-centric and telomeric H3K9 methylation. Overexpression of Su(var)3-9 in mammals causes a cell segregation defect with chromosome bridges with micro- and poly-nuclei. Interestingly, Su(var)3-9 double null murine cells also show similar defects during mitosis with micro- and poly-nuclei (Rea et al. 2000). The Su(var)3-9 mediated H3K9me formation is important for maintaining DNA methylation (Du et al. 2015). It is important to note that DNA methylation is not present in all the organisms or restricted to an early development stage, for instance, in *Drosophila melanogaster* (Lyko et al. 2000; Raddatz et al. 2013; Takayama et al. 2014; Capuano et al. 2014), indicating the presence of an alternative DNA compaction strategy, possibly, larger role of histone methylation in DNA compaction.

Formation of heterochromatin requires H3K9me2/3 by Su(var)3-9, which is followed by binding of Heterochromatin protein 1 (HP1) {also termed as Su(var)2-5} which interacts with both Su(var)3-9 and methylated H3K9 and this provides a positive feedback loop mechanism for maintenance and spread of heterochromatin (Lachner et al. 2001; Nielsen et al. 2002; Schotta et al. 2003; Lundberg et al. 2013). Su(var)3-9 and HP1 both bind to surrounding common repetitive regions in Drosophila cells (Greil et al. 2003). In addition, HP1 interacts with both H3K9me2 and H3K9me3, although it has a

stronger affinity to bind to H3K9me3 than H3K9me2 via its chromodomain (Pérez-Toledo et al. 2009; Fischle et al. 2003). HP1 also interacts with CAF1 chromatin-remodeler and regulates HP1 mediated heterochromatin stability (H. Huang et al. 2010; Quivy et al. 2008). Furthermore, HP1 interacts with repetitive RNAs (Shareef et al. 2001), this interaction between heterochromatin elements and non-coding repetitive RNA is postulated to be important for maintaining heterochromatin structure, as well as in maintaining heterochromatin and euchromatin boundaries (Keller et al. 2013; Blattes et al. 2006; Zhou et al. 2009). Recent findings also suggest a role of HP1 in regulating euchromatin regions positively and more evidences are emerging to show functions of HP1 independent of H3K9me2/3, in positive regulation of gene expression (Yuan & O'Farrell 2016; Liu & Zhang 2015).

G9a, another SET domain containing HMT which methylates H3K9 and has a dominating role in euchromatin silencing via H3K9 mono- and di-methylation (Tachibana et al. 2001) with different localization than HMT Su(var)3-9. G9a can auto-methylate itself which resembles H3K9me3. Auto-methylated G9a peptide interacts with HP1 and shows potential of recruiting HDAC1 and DNMT1 (Chin et al. 2007). G9a also methylates many transcription factors, which inhibit their transcription activity, for example, CEBP-β is methylated at K39 by G9a which interferes with transcription of myeloid genes (Leutz et al. 2011). G9a also methylates p53 at K373 leading to its transcriptional inactivation (J. Huang et al. 2010). In addition, G9a also contributes to H3K27 methylation (Wu et al. 2011). G9a is essential for embryogenesis in mammals and is important for embryonic stem cell differentiation (Yamamizu et al. 2012; Chen et al. 2012). Contrary to this, G9a does not seem to be essential for the Drosophila organism (Tachibana et al. 2002; Seum et al. 2007).

1.2 CHRAC14 containing complexes and their role in chromatin maintenance

CHRAC14 is a subunit of Ada2s-containing (ATAC) and chromatin accessibility (CHRAC) chromatin remodeling complex (Figure 1.3). The ATAC complex contains 13 subunits which includes two HAT subunits, Gcn5 and ATAC2 (Suganuma et al. 2008; E. Vamos & Boros 2012; Ciurciu et al. 2008). CHRAC belongs to ISWI chromatin remodeling family. CHRAC contains ACF, CHRAC14 and CHRAC16 subunits (Kukimoto et al. 2004; Varga-Weisz et al. 1997; Corona et al. 2000). The presence of CHRACI4 enhances the nucleosome sliding activity of CHRAC. The CHRAC14/16 subunit also helps the CHRAC complex to bind to genomic sites on the chromatin (Hartlepp et al. 2005). In mammals, depletion of ACF1 delays the replication of heterochromatin regions, indicating its role in opening heterochromatin structures (de la Serna & Imbalzano 2002; Collins et al. 2002).

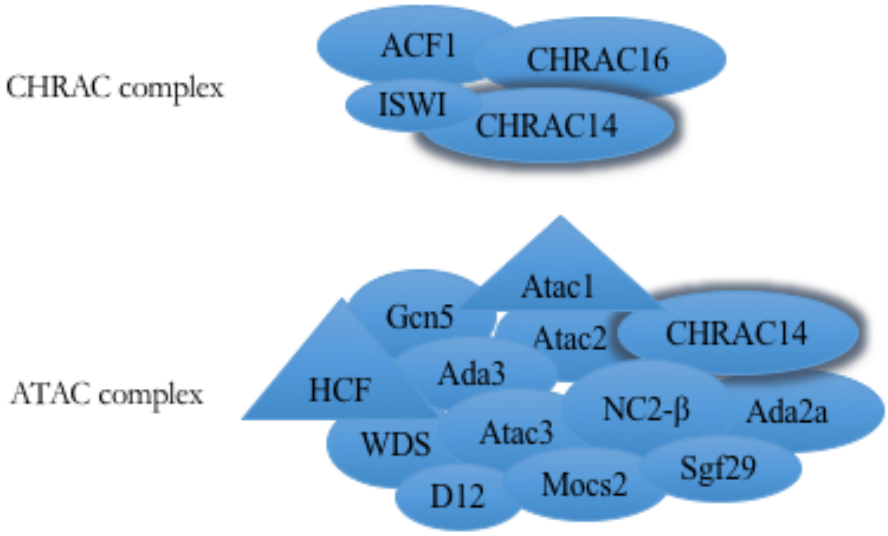

Figure 1.3: Summary of CHRAC14 containing chromatin-remodeling complexes. The arrangement of subunits represents only to date identified subunits, not necessarily how they interact with each other in the complex. References: CHRAC complex (Längst & Becker 2001) ATAC complex (Ciurciu et al. 2008; Guelman et al. 2009; Spedale et al. 2012).

In accordance with the idea of chromatin opening/accessibility, mammalian Gcn5, which is a catalytic subunit of many HAT including ATAC complexes, co-localizes at DNA damage sites upon DNA damage induced with increased H3K9 acetylation (H3K9ac) that in turn recruits DNA repair proteins (Guo et al. 2011). Further, loss

of Ada3, which is another ATAC complex subunit, show impaired DNA damage repair ability upon Ionizing radiation (IR) treatment in murine cells (Mirza et al. 2012). Moreover, Gcn5 containing the ATAC complex subunit ADA2B shows genetic interaction with p53 (Pankotai et al. 2005) and absence of CHRAC14 shows impaired DNA damage repair in Drosophila (Mathew et al. 2014). Taken together, these reports suggest a role for CHRAC14 containing complexes in maintaining chromatin structure in need of transcription activation and accessibility to DNA damage sites. However, whether CHRAC14 solely or as a part of ATAC and CHRAC complex is essential for maintaining chromatin structure remains to be elucidated.

1.3 Centromere and its DNA

The centromere was first defined as a primary constriction of the chromosome by a German biologist Walter Flemming in 1880s (Flemming 1882). The centromere is important for the formation of the kinetochore, which is required for attachment of microtubules and chromosome segregation during cell division. Centromeres have no defined sequence and are enriched in satellite repeats in all animals except the yeast *S. cerevisiae*. (Pardue & Gall 1970; Rošić & Erhardt 2016). Some animals like orangutan, horse, and chicken have a mixture of repetitive and non-repetitive sequences (Montefalcone et al. 1999; Piras et al. 2010; Locke et al. 2011). These repetitive sequences are not specifically conserved among species, although reports on human-specific 171bp alpha-satellite and yeast *S. pombe* centromere regions suggest a role in the de-novo specification of the centromere (Hahnenberger et al. 1989; Haaf et al. 1992). In budding yeast, centromere specific DNA element III sequence is directly recognized by Centromere binding factor 3 (Cbf3) (Lechner & Carbon 1991). In addition, human artificial chromosome is capable with an alpha satellite repeat of inducing de-novo assembly of active centromere/kinetochore structure (Masumoto et al. 1998).

Converse to genetic sequence, centromeres in all the species have some common features, which possibly make the centromeres unique for localization of kinetochore proteins. One of the common similarities is the presence of heterochromatin regions bordering the centromere from two sides. This

centromere flanking heterochromatin is termed as pericentric-heterochromatin, which is a conserved epigenetic feature in both yeast and human. Pericentric-heterochromatin is predominantly marked by H3K9me2 (Sullivan & Karpen 2004), while H3K9me3 is present on only one side as seen in human and Drosophila cells. Sullivan and Karpen's study on mammalian and fruit fly cells reveals that centromeric DNA contains no heterochromatin modifications. Moreover, centromeric DNA does not contain any active chromatin mark i.e. no detectable H3 or H4 acetylation mark (Blower et al. 2002; Sullivan & Karpen 2004) reflecting a hypoacetylated region at the centromere.

Identity and functionality of centromere can also be addressed by localization of kinetochore forming proteins or by the presence of a sequence that binds to kinetochore forming proteins. Because of variation in underlying centromere sequences between different species, it is challenging to study the potential role of underlying centromere sequence. On the other hand, the centromere/kinetochore interacting proteins are widely conserved from yeast to human and have been extensively used in understanding centromere/kinetochore functionality.

1.4 CENP-A at the centromere

Centromeric protein-A (CENP-A) is a H3 histone variant specifically localizing to the centromere. Other than pericentric-heterochromatin, what makes centromere very unique from rest of the chromosome sites is the presence of CENP-A containing nucleosome. CENP-A is conserved from yeast to human. In various organisms, CENP-A nucleosome is not present uniformly but shows an interspersed pattern (Blower et al. 2002; Greaves et al. 2007; Yan & Jiang 2007). The composition of a CENP-A nucleosome is still unclear. However, *in vivo* studies in yeast and mammalian cells suggest presence of a tetramer nucleosome at centromere i.e. CENP-A nucleosome contains one of each H2A, H2B, CENP-A and H4 histone (Henikoff et al. 2014; Bodor et al. 2014; Tachiwana et al. 2011; Padeganeh, De Rop, et al. 2013; Sekulic et al. 2010) that is also referred as hemisome. Moreover, cell cycle dependent fluctuation of tetramer to octamer has also been postulated (Bui et al. 2012). By contrast, presence of hemisome and

tetramer to octamer fluctuation at centromere have been challenged by many other studies (Padeganeh, Ryan, et al. 2013; Bassett et al. 2012; Tachiwana et al. 2011) suggesting the presence of an octamer nucleosome throughout the cell cycle (Dunleavy et al. 2013).

CENP-A is a key component for the establishment of a kinetochore at the centromere, thereby important for attachment of microtubule and chromosome segregation in anaphase (Pauleau & Erhardt 2011). CENP-A has a CENP-A targeting domain (CATD), which is required for CENP-A centromeric localization. A chimera of CENP-A CATD domain and canonical H3 histone is sufficient to lead to centromeric localization (Black et al. 2007; Vermaak et al. 2002). Holliday junction recognition protein (HJURP) interacts with CENP-A via its CATD domain and plays a role as CENP-A assembly factor (Dunleavy et al. 2009). CENP-A is also known as CID (centromere identifier) in Drosophila, and requires Chromosome alignment defect 1 (CAL1) and Centromeric protein-C (CENP-C) for its localization at centromere (Dunleavy et al. 2009; Erhardt et al. 2008; Bassett et al. 2012). Cal1 and CENP-C are hypothesized to have a similar function as HJURP and M18BP1, despite the lack of sequence homology (Pauleau & Erhardt 2011). CENP-A bears 60% amino acid similarity with canonical H3 histone and it's the N-terminal tail part of CENP-A which has no similarity with H3 (Malik et al. 2002; Sullivan et al. 1994). Further, CENP-A has an interesting unstructured C-terminal part which is important in long term maintenance of CENP-A centromere function (Fachinetti et al. 2013) and interaction with CENP-C (Saitoh et al. 1992; Guse et al. 2011). CENP-C is also a part of the core centromere and interacts with CENP-A and kinetochore proteins. Lack of CENP-C affects the function of centromere and formation of kinetochore (Orr & Sunkel 2011). CENP-C possibly plays a role as a connecting platform between CENP-A containing nucleosome and core kinetochore component (Przewloka et al. 2011; Samb et al. 2015; Falk et al. 2016).

1.4.1 **Regulation of CENP-A**

CENP-A deposition is cell cycle dependent. In Drosophila cells, CENP-A is recruited to the centromere during mitosis after degradation of Cyclin A (Erhardt et al. 2008; Mellone et al. 2011). In human cells, CENP-A is recruited to the centromere in G1 phase. The recruitment is regulated by CDK dependent phosphorylation of M18BP1 that is a subunit of MIS18 complex (Silva et al. 2012). Phosphorylation of M18BP1 inhibits the

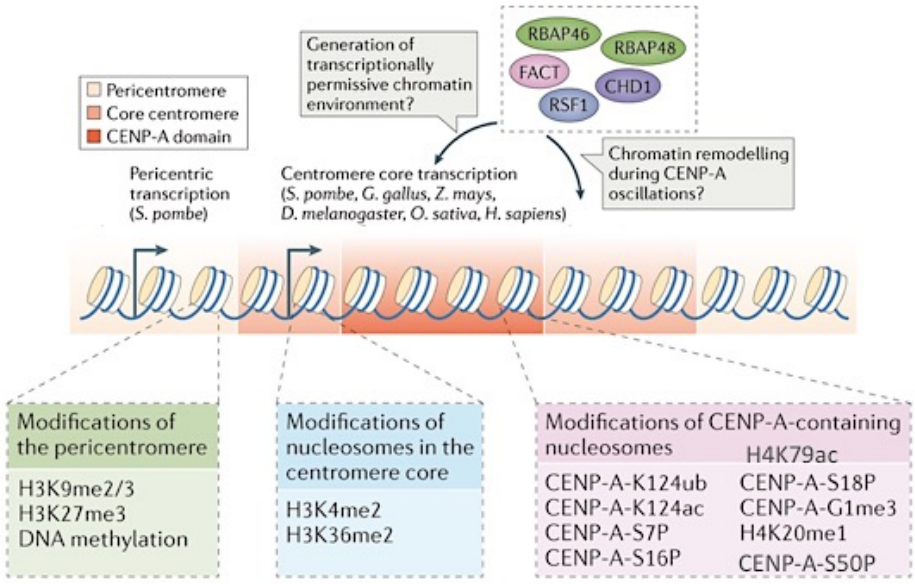

Figure 1.4: (From McKinley & Cheeseman 2016). Overview of so far reported epigenetical modification in centromere and peri-centromeric region. Peri-centromeric region contains heterochromatin histone and DNA modification (DNA methylation, H3K9me2/3 and H3K27me3). Centromeric canonical histone H3 and H4 contain H3K4me2, H3K36me2 and H4K20me1 suggesting transcriptionally active regions. Centromere specific H3 variant CENP-A is ubiquitylated at K124 and acetylated at K124, phosphorylated at S7, S16, S18, and trimethylated at G1 for proper CENP-A regulation, centromeric and kinetochore function.

recruitment of other MIS18 complex subunits MIS18α and MIS18β outside G1 phase, which is important for CENP-A assembly. Additionally, Polo-like kinase 1 promotes deposition of CENP-A by phosphorylating Mis18 complex in G1 phase (McKinley & Cheeseman 2014). Although CENP-A defines a centromere and is essential for kinetochore formation, its assembly factors play a crucial role in maintaining functionality, but there are certain factors which further ensure a proper centromere function like

posttranslational modifications of histones associated with the centromere (Figure 1.4).

Intermittent canonical histone H3 present at centromere contains H3K36me2 (Bergmann et al. 2011) and H3K4me2 (Ribeiro et al. 2010; Sullivan & Karpen 2004; Blower et al. 2002) in Drosophila and human cells suggesting transcriptionally active sites at the centromere (Wang et al. 2014). Adding to this, studies on chicken and human cells suggest the presence of H4K20 methylation in CENP-A nucleosome (Hori et al. 2014; Bailey et al. 2015), which has been demonstrated to be part of transcriptionally active chromatin (Wang et al. 2008). Recently, reports suggesting transcription at centromere have emerged and the transcription originating from centromere is important for mitosis. RNA polymerase II and many transcription factors have been reported to be localized at centromere during mitosis and perturbation of this leads to chromosome segregation defects (Chan et al. 2012; Liu et al. 2015). In addition, recently it was reported that non-coding RNA SatIII that originates from peri-centromeric repeats of x-chromosome seems to be playing a crucial role in the localization of CENP-A in Drosophila cells (Rošić et al. 2014).

In human cells, phosphorylation of CENP-A at the NH_2 terminus at S7 is important for its CENP-C interaction and functional kinetochore (Kunitoku et al. 2003). This phosphorylation is Arora B dependent. Studies using CENP-A S7 mutants show that the CENP-A nucleosome might be bridged by CENP-C via phospho-binding 14-3-3 protein (Goutte-Gattat et al. 2013). Furthermore, CENP-A is also phosphorylated at S68 by CDK1 (Cyclin-dependent kinase 1) that controls its recruitment to the centromere until onset G1 phase. In G1 phase, CENP-A S68 is dephosphorylated by PP1α (Protein phosphatase 1 alpha) leading to its centromeric recruitment (Zeitlin et al. 2001; Yu et al. 2015). Studies also show that CENP-A K124 ubiquitylation by CUL4A-RBX1-COPS8 complex is important for CENP-A centromere localization (Niikura et al. 2015). In Drosophila, CENP-A gets

ubiquitylated by E3 ligase CUL3/RDX in presence of CAL1 and this modification is important for stabilization of CENP-A and its maintenance at the centromere (Bade et al. 2014). In 2012, it was also reported that CENP-A K124 and H4K79 in CENP-A nucleosome are acetylated at G1/S phase, which could have structural consequences by neutralizing the positively charged lysine surface and reducing affinity between histone and DNA. This, in turn, would increase the accessibility of CENP-A nucleosome interior to chromatin modifiers and other proteins (Bui et al. 2012). Human cells have also been shown to be tri-methylated at the α-amino of the G1 and phosphorylated at S16 and S18 on the N-terminal tail of CENP-A (Bailey et al. 2013). It is postulated that S16 and S18 phosphorylations affect the chromatin organization thereby assisting inter- and intra-molecular interactions.

In yeast, the CENP-A homolog is methylated on R27 and this methylation plays a crucial role in the localization of kinetochore components at centromere (Samel et al. 2012). In maize, a CENP-A homolog has been identified to be phosphorylated at S50 and reported to be important for chromosome segregation, alignment, and motility (Zhang et al. 2005).

1.4.2 **Role of heterochromatin associated factors in CENP-A/kinetochore deposition**

CENP-A localizes precisely to centromeres and regulates the position of kinetochore formation in wild-type (WT) conditions. Except in budding yeast (Folco et al. 2008), until now, there is no sequence specificity identified at the centromere for localization of CENP-A. However, all organisms including yeast, show well defined epigenetic centromere flanking pericentric-heterochromatin marks (Sullivan & Karpen 2004). This pericentric-heterochromatin is heterochromatinized by Su(var)3-9 and HP1 (Aagaard et al. 1999). Moreover, tethering of HP1 via Lac-I/Lac-O system in Drosophila cells shows deposition of CENP-A and it is known that H3K9 methylation is vital for HP1 localization (Olszak et al. 2011). Whether Drosophila Su(var)3-9 tethering can also lead to similar conclusions is still

unclear. Notably, localization of clr4 in yeast is responsible for H3K9 methylation and causes deposition of CENP-A (Kagansky et al. 2009). In contrast to yeast and Drosophila, tethering of HP1 and Su(var)3-9h1 using the HAC tetR-tetO system in mammalian cells disrupts kinetochore or reduces CENP-A deposition (Ohzeki et al. 2016; Nakano et al. 2008; Ohzeki et al. 2012). Although, tethering of another HMT G9a in mammals using the HAC system shows de-novo CENP-A assembly at an ectopic site (Shono et al. 2015). In mammalian cells, centromeric protein CENP-B which interacts with Su(var)3-9h1 shows a dual role by maintaining the H3K9me3 DNA methylation while it also modulates the assembly of CENP-A on alphoid DNA (Okada et al. 2007). So far, there is no protein identified with a similar dual functionality in Drosophila. Beside CENP-B, CENP-T/CENP-W complex in human cells also interacts with another HMT EZH2 (Prendergast et al. 2016). The CENP-T/CENP-W complex is known to have a key role in recruiting downstream constitutive centromere-associated network proteins (CCAN) which are essential for kinetochore formation. Importantly, CCAN is critical for KNL1/Mis12 complex/Ndc80 complex (KMN) network which acts as a microtubule-binding interface at the kinetochore (Cheeseman et al. 2006). No direct interactions of any HMT with any inner kinetochore associated proteins including CENP-A have been reported, yet, in Drosophila.

Mislocalization or ectopic localization of CENP-A can lead to the formation of a functional kinetochore at a wrong place in Drosophila cells and this gives rise to a delayed mitotic phase and anaphase with lagging chromosome defects. One such situation of ectopic loading of CENP-A can be achieved by CENP-A overexpression (Heun et al. 2006). Mislocalization of CENP-A also results in increased genomic instability as a result of chromosome segregation defects and is a known phenotype of many cancer forms (Tomonaga et al. 2003; Lacoste et al. 2014; Heun et al. 2006; McGovern et al. 2012). Ectopic CENP-A predominantly localizes to heterochromatin boundaries and preferentially localizes near pericentric-

heterochromatin or telomeres. Moreover, hyperacetylation environment via TSA treatment can lead to a decrease in ectopic CENP-A sites in Drosophila (Olszak et al. 2011). In conclusion, these studies suggest a potential role of heterochromatin-associated factors in the de-novo deposition of centromeric and ectopic CENP-A locations. Although it is still not clear whether factors like Su(var)3-9, SETDB1 and G9a can facilitate ectopic CENP-A localization in Drosophila cells.

1.5 Relationship between CHRAC14 and CENP-A

Recently, our lab discovered that depletion of CHRAC14 causes ectopic CENP-A localization in Drosophila cells and that depletion of CHRAC14 shows endogenous accumulation of DNA damage and G2-M checkpoint failure upon induction of DNA damage (Mathew et al. 2014). Our lab has also reported *in vivo* and *in vitro* interaction of CENP-A and CHRAC14 upon DNA damage suggesting a possible role of CHRAC14 in monitoring incorporation of CENP-A to ectopic sites upon DNA damage.

1.6 Aim of the study

CHRAC14 depletion leads to ectopic loading of CENP-A in combination with impaired DNA damage repair capacity in a Drosophila model system. During this Ph.D. study, I aimed to investigate following major questions:

1. Why does lack of CHRAC14 lead to CENP-A ectopic loading?
2. Does Su(var)3-9 histone methyltransferase play a role in ectopic CENP-A localization and could this ectopic CENP-A give rise to a functional ectopic kinetochore?
3. Is maintaining the level of Su(var)3-9 physiologically important for Drosophila S2 cells?

Until now, no one has explored the role of Su(var)3-9 in facilitating ectopic loading of CENP-A in Drosophila. In the second part of this study, I explored a potential synergistic effect of increased histone methyltransferase levels and increased heterochromatin on ectopic CENP-A.

2. Results

2.2 CHRAC14 knockdown changes the level of euchromatin and heterochromatin markers

2.1.1 Depletion of CHRAC14 reduces histone H3 lysine 9 acetylation

CHRAC14 is a defined subunit of the ATAC complex. The ATAC complex contains two histone acetyltransferases, GCN5 and ATAC2. Disruption of the ATAC complex in GCN5 mutants reduced the overall H3K9 acetylation (Suganuma et al. 2008; Ciurciu et al. 2008). Further CHRAC14 depletion results in CENP-A ectopic localization (Mathew et al, 2014) but if the CHRAC depletion effect the H3K9ac was never investigated. To check if lack of CHRAC14 would give a similar effect on H3K9 acetylation, whole fly lysates from CHRAC14$^{-/-}$ and Oregon R (WT) were analyzed by immunoblotting against H3K9ac. Results obtained suggest a decrease in H3K9ac (Figure 2.1.A). To confirm these results, CHRAC14 was knocked down by RNAi in S2 cells, histone extracted and analyzed via western blot using H3K9ac and pan H3 antibodies. S2 cells treated with CHRAC14 RNAi also show a decreased H3K9acetylation level

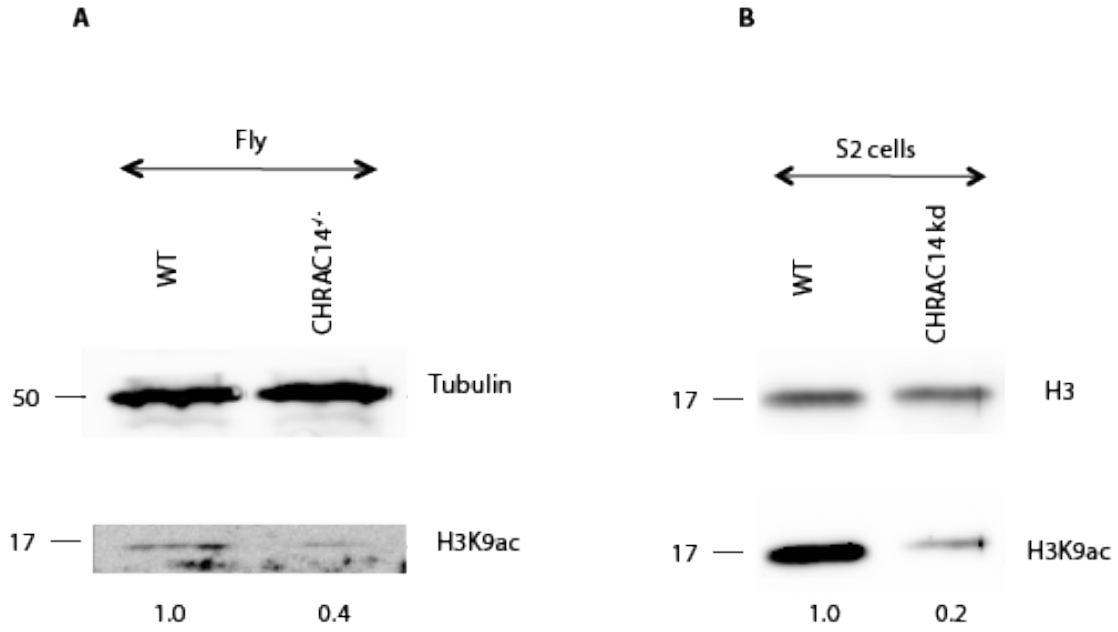

Figure 2.1: CHRAC14$^{-/-}$ flies show reduced H3K9 acetylation. **A)** Lysate from whole adult Oregon R (WT) and CHRAC14 $^{-/-}$ Drosophila were analyzed via western blot and probed with anti-H3K9ac and tubulin (loading control). **B)** 4 days CHRAC14 RNAi-treated S2 cells along with control (no RNAi) were subjected to acid histone extraction and analyzed for the level of H3K9ac, stripped and re-probed for H3 level (loading control).

(Figure 2.1B), overall suggesting that reduction of CHRAC14 influences histone H3K9 acetylation levels.

2.1.2 Lack of CHRAC14 results in an overall increase in histone H3 lysine9 di-methylation

Lack of ACF1, a subunit of the CHRAC complex, shows a reduction in heterochromatin replication (Collins et al. 2002). ADA2A and GCN5 mutants, which are subunits of the ATAC complex, show enhanced histone H3K9me2 modifications (Ciurciu et al. 2008), which is a marker of heterochromatin. Considering that CHRAC14 is part of both complexes, a depletion of CHRAC14 may result in overall increased heterochromatin levels which also complements my observation of reduced H3K9ac, as deacetylation of K9 is perquisite for addition of a methyl group on the lysine residue (Park et al.

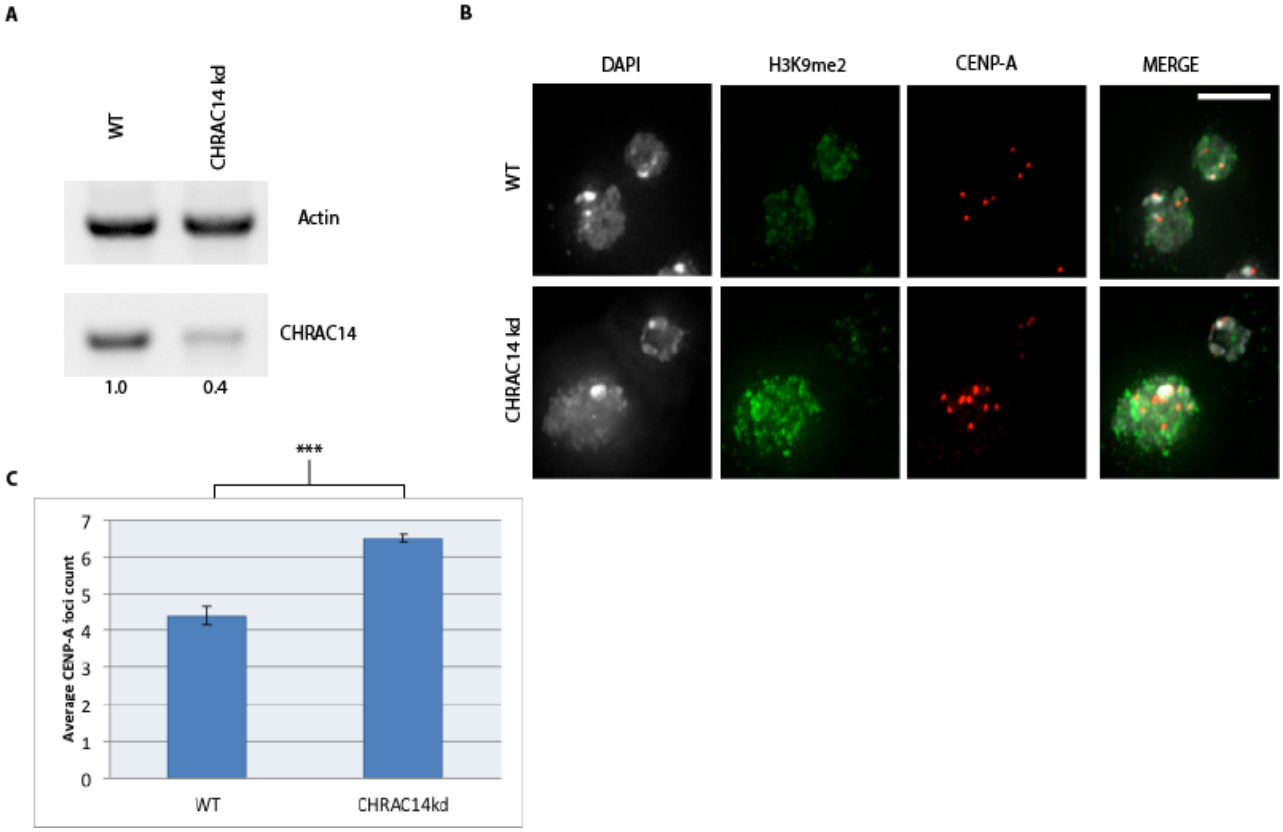

Figure 2.2: CHRAC14 depletion leads to enhanced H3K9me2 staining and increase CENP-A foci number. **A)** RT-PCR of Chrac14-depleted S2 cells. **B**) IF of CHRAC14 depleted cells stained against anti-H3K9me2 (green), CENP-A (red) and DAPI (DNA, grey). Bar= 5µM **C)** Quantification of CENP-A foci from control and CHRAC14 RNAi treated cells from 3 or more biological repeats. Error bars represent ±SEM and a p-value <0.05.

2011). Overall this would raise the possibility of a change in heterochromatin level. Further, it has been reported that heterochromatin boundaries are a

hotspot of ectopic CENP-A localization (Olszak et al. 2011). Mathew et. al. reported that CHRAC14 depletion causes ectopic CENP-A localization (Mathew et al, 2014). Considering these facts, I assessed the level of H3K9me2 in CHRAC14-depleted S2 cells via immuno-fluorescence (IF).

Control cells show H3K9me2 staining and CENP-A foci overlapping with the H3K9me2 staining. Noticeably, CHRAC14 RNAi-treated cells show enhanced H3K9me2 staining (Figure 2.2B) and an increased CENP-A foci number (Figure 2.2B and C), indicating a correlation between H3K9 methylation and number of CENP-A foci. To confirm the observation of increased H3K9me2, the level of H3K9me2 using whole adult fly lysates was measured via western blot, and measured a 1.5-fold increased H3K9me2 level in absence of CHRAC14 (Figure 2.3A).

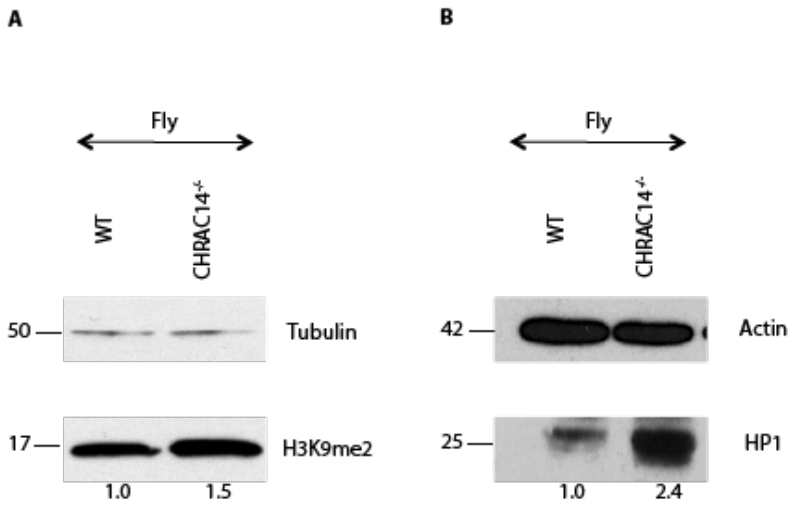

Figure 2.3: CHRAC14$^{-/-}$ flies show increased heterochromatin marker. **A)** Lysate from whole adult Oregon R (WT) and CHRAC14 $^{-/-}$ flies were analyzed via western blot. The blot was probed with anti-H3K9me2 and anti-Tubulin (loading control). **B)** CHRAC14$^{-/-}$ flies show increased HP1 level. CHRAC14$^{-/-}$ and Oregon R (WT) adult fly lysate was analyzed for HP1 protein level via western blot. The blot was probed against anti-HP1 antibody and Actin (loading control). Pictures are representative of three or more biological replicates.

An increase in the H3K9me2 levels in CHRAC14$^{-/-}$ cells indicates an elevated level of heterochromatin. Heterochromatin protein 1 (HP1) binds to methylated H3K9 and is required for heterochromatin formation (Lachner et al. 2001; Schotta et al. 2002). The HP1 protein level in CHRAC14$^{-/-}$ and Oregon

R (control) lysates was examined via immuno-blotting. Results suggest more than a two-fold increase in the level of HP1 (Figure 2.3B), indicating that CHRAC14 depletion might lead to an increase in heterochromatin markers in Drosophila cells.

2.1.3 Decrease in CHRAC14 level leads to increased Su(var)3-9 transcripts

The classic process for formation of heterochromatin includes recruitment of HP1 by methylated H3K9 which further recruits Su(var)3-9 Histone methyltransferase. Su(var)3-9 methylates more H3K9 which recruits more HP1. This leads to a positive feedback loop mechanism of heterochromatin formation and maintenance (Lachner et al. 2001; Ebert et al. 2004). Since I observed an increased level of H3K9 methylation and HP1, I tested mRNA levels of the Su(var)3-9 histone methyltransferase.

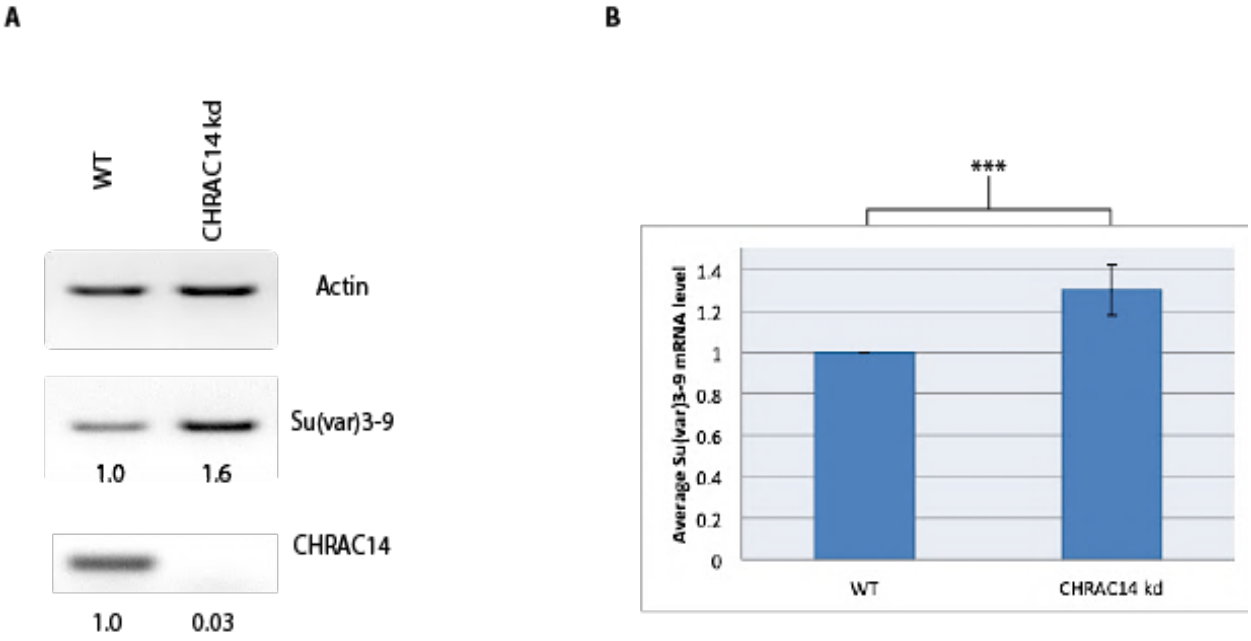

Figure 2.4: CHRAC14 kd cells show an increased expression of histone methyltransferase Su(var)3-9. **A)** RT PCR from CHRAC14 RNAi treated and control (no RNAi treatment) S2 cells using CHRAC14, Su(var)3-9 and Actin specific primers. Results show an increase in Su(var)3-9 transcripts. **B)** Quantification of the average Su(var)3-9 mRNA level, obtained from five biological repeats via RT PCR , normalized to Actin. Error bars are ±SEM and a p-value <0.05

To examine the level of Su(var)3-9 mRNA, CHRAC14 RNAi treated and control (no RNAi) S2 cells were subjected to semi-quantitative RT-PCR amplification

for CHRAC14, Su(var)3-9 and Actin (control). The obtained results show a slight, though significant, increase in transcription level of Su(var)3-9 in absence of CHRAC14 (Figure 2.4A and B). The increased expression level of Su(var)3-9 explains an increased level of H3K9me2 in CHRAC14$^{-/-}$ and CHRAC14 kd cells.

2.2 Change in level of Su(var)3-9 and histone acetylation in CHRAC14 depleted cells may affect CENP-A localization

2.2.1 Ectopic CENP-A foci in CHRAC14 depleted cells are Su(var)3-9 dependent

Mathew et.al. showed that CHRAC14 depletion leads to ectopic CENP-A foci. The previous experiments show that a CHRAC14 knockdown enhances H3K9me2 and increases Su(var)3-9 expression concomitant with an increase in CENP-A foci. It has been reported that Su(var)3-9 does not play a role in maintaining centromeric CENP-A localization (Andreyeva et al. 2007). I therefore tested, whether increased Su(var)3-9 transcripts play a role in the ectopic loading of CENP-A in absence of CHRAC14 by a co-depletion of Su(var)3-9 with CHRAC14. As seen previously, CHRAC14 depletion shows enhanced regions of H3K9me2 overlapping with DAPI region, in addition to increased CENP-A foci. Moreover, lack of Su(var)3-9 did not affect the endogenous CENP-A foci numbers, i.e. cells retained similar numbers of CENP-A foci as in control (WT) cells (Figure 2.5A, first and third panel from top). However, as expected, cells treated with Su(var)3-9 RNAi show reduced H3K9me2 staining (Figure 2.5A, third panel from top). Interestingly, cells co-treated with CHRAC14 and Su(var)3-9 RNAi also show a decrease in H3K9me2 staining in the nucleus (Figure 2.5A, last panel from top) indicating an antagonistic role of Su(var)3-9 and CHRAC14 in maintaining heterochromatin structures. Furthermore, I quantified the number of CENP-A foci in control (WT), CHRAC14 RNAi, Su(var)3-9 RNAi and co-CHRAC14/Su(var)3-9 RNAi treated cells. As reported earlier, CHRAC14 RNAi cells show an increase in CENP-A foci when compared to WT and Su(var)3-9 RNAi treated cells. Surprisingly, cells co-treated with Su(var)3-9 RNAi and CHRAC14 RNAi show a reduction in overall CENP-A foci number per cell (Figure 2.5B). These results

indicate a role of Su(var)3-9 in ectopic loading of CENP-A in CHRAC14 depleted cells.

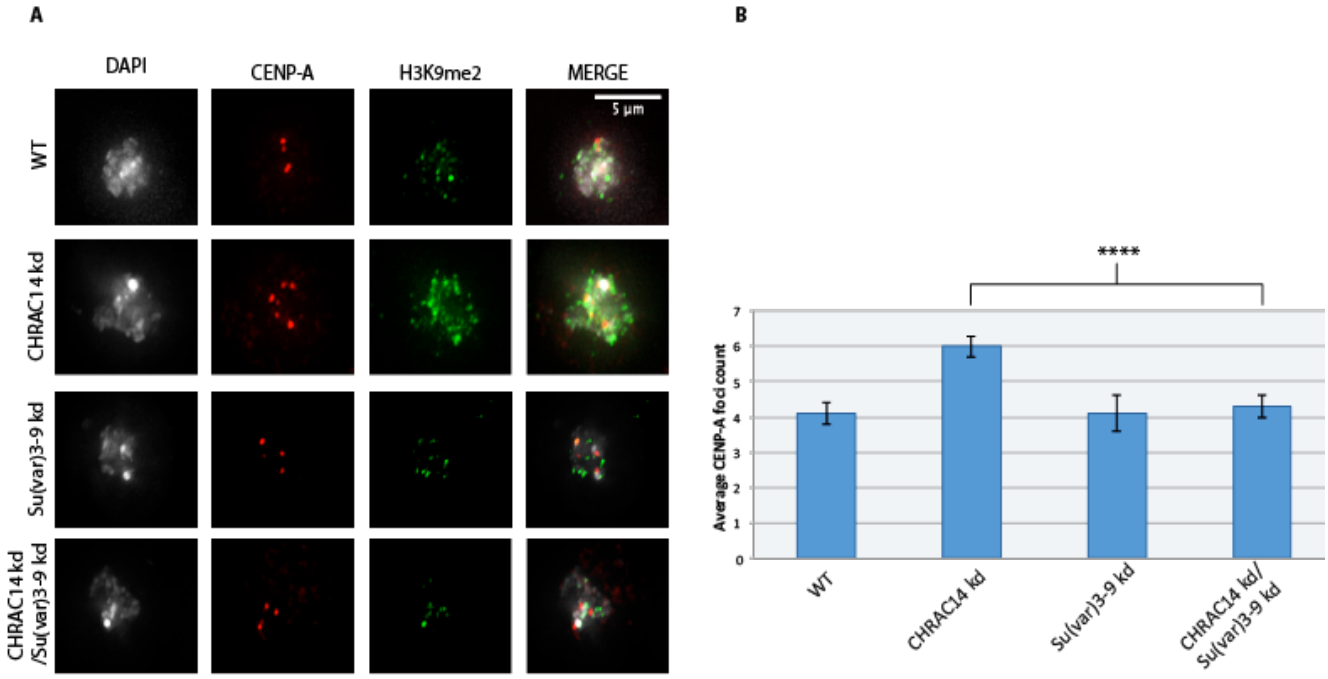

Figure 2.5: Increase in CENP-A foci in CHRAC14 RNAi treated cells is Su(var)3-9 dependent. **A)** First, second, third and fourth panel represent control (no RNAi treatment), CHRAC14 RNAi, Su(var)3-9 RNAi and co-treatment of CHARC14 and Su(var)3-9 RNAi treated S2 cells, respectively. All samples were subjected to IF against anti-H3K9me2 antibody (green), CENP-A (red) and nuclei were co-stained with DAPI (grey). Bar= 5µM. **B)** Quantification of average CENP-A foci counts from 50 cells/sample/three biological repeats of Figure A. Error bars represent ±SEM and a p-value <0.05.

2.2.2 HDAC inhibitor TSA reduces the CENP-A foci number in CHRAC14 depleted cells

To further validate the rescue effect observed on CENP-A foci numbers obtained by co-depletion of Su(var)3-9 and CHRAC14, the effect of the histone deacetyltransferase (HDAC) inhibitor TSA (Trichostatin A) was analyzed. Deacetylation of acetylated H3K9 is prerequisite for its methylation (Park et al. 2011; O'Byrne et al. 2011). HDAC removes H3K9 acetylation, after the deacetylation event, histone methyltransferases like Su(var)3-9 methylate

H3K9 (Lombardi & Cole 2011). Inhibition of HDAC inhibits deacetylation and this in turn prevents spread of H3K9 methylation (Taddei et al. 2001). It has been shown that TSA treatment can reduce ectopic CENP-A islands (Olszak et al. 2011). In the next step, it was tested whether the HDAC inhibitor TSA can affect the CENP-A phenotype observed in CHRAC14 depleted cells. To address this, I treated WT (control) and CHRAC14 RNAi cells with 0.500nM TSA for 6 hours and quantified the number of CENP-A foci in TSA untreated and treated cells.

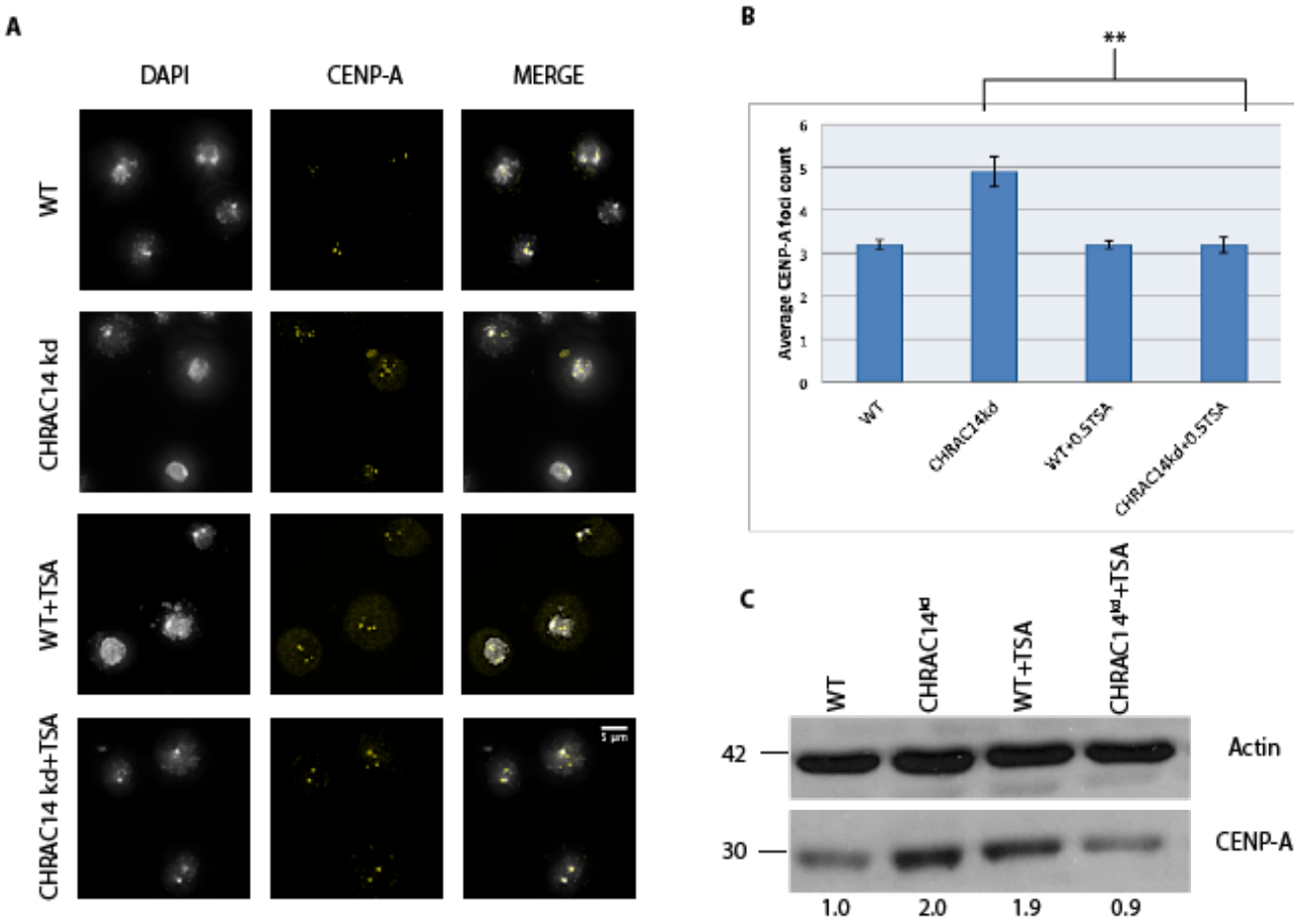

Figure 2.6: TSA treatment reduces the increased CENP-A foci count in CHRAC14 depleted cells. IF on CHRAC14 RNAi treated and WT (no RNAi) S2 cells were subjected to 0.5 µM TSA for 6 hours, controls were treated with DMSO and stained against anti-CENP-A (yellow) and DAPI (grey). Bar= 5µM. **B)** Quantification of the average CENP-A foci number. The graph is a compilation of three repeats. Error bars represent ±SEM and a p-value <0.05. **C)** Western blot of cells with and without CHRAC14 RNAi, and 0.5 µM TSA treatment. The blot was probed with anti-CENP-A and anti-Actin (loading control) antibodies.

The average CENP-A foci number in control cells with and without TSA remains unchanged. Interestingly, the quantification of CHRAC14 RNAi cells with and without TSA shows a significant reduction in the average CENP-A foci count upon TSA treatment (Figure 2.6A and B).

Further, it was checked whether the effect observed via IF is because of reduction in overall CENP-A protein level. This was analyzed via CENP-A western blot on whole lysate from CHRAC14 RNAi S2 cells treated with and without 0.5 µM TSA along with the controls. Cells with no RNAi treatment but TSA show an increase in CENP-A protein level (Figure 2.6C). Moreover, western blot analysis of CHRAC14 RNAi treated cells shows a reduction in level of CENP-A upon TSA treatment in CHRAC14 depleted cells, consistent with our observation of a decreased CENP-A foci number in CHRAC14 RNAi TSA treated cells (Figure 2.6C). Overall results suggest that the HDAC inhibitor TSA rescues the average effect of an increased CENP-A foci count in CHRAC14 depleted cells.

2.2.3 **Acetylation of CENP-A in CENP-A overexpressing S2 cells**

During this study, it was observed that CENP-A localization is affected by TSA treatment in CENP-A overexpressing cells (see Appendix 6.3). Additionally, there is nothing known about CENP-A acetylation in Drosophila cells. This led to a question whether CENP-A is potentially acetylated. For this, S2 cells with pMT-CENP-A-V5-His were used. pMT is a metal inducible promoter and genes can be expressed from it by adding $CuSO_4$. These S2 cells were subjected to 8 hours' induction for CENP-A-V5-His overexpression and later CENP-A-V5-His was subjected to denaturing immunoprecipitation in presence and absence of TSA. The samples were probed for any lysine acetylation using Pan acetyl-lysine antibody. To our surprise, samples treated with TSA showed a higher amount of acetylated lysine band at the size similar to CENP-A-V5-His (Figure 2.7). The same membrane was then re-probed with the V5 antibody to check if the band obtained via Pan acetyl-lysine antibody overlaps in size with the

CENP-A-V5-His band. Interestingly, bands obtained by CENP-A and Pan-acetyl lysine antibody locate at the same size on membrane projecting CENP-A as a potential acetylation substrate under the given conditions (Figure 2.7).

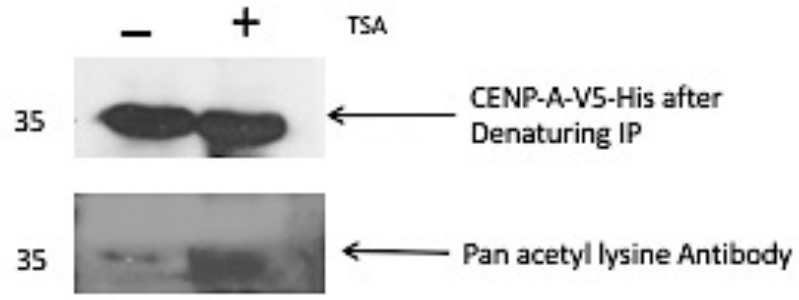

Figure 2.7: CENP-A, a substrate for acetylation. CENP-A-V5-His was overexpressed under control of pMT promoter in S2 cells and incubated with/without the HDAC inhibitor TSA 1mM. Lysates were immuno-precipitated under denaturing conditions. Thereafter, the IP was probed with V5 and pan-acetyl lysine antibody.

2.3 Increase in Su(var)3-9 level may induce ectopic CENP-A and CENP-C independent of CHRAC14 depletion

2.3.1 Su(var)3-9 overexpression leads to increased CENP-A foci

CHRAC14 depletion shows an increase in Su(var)3-9 mRNA levels with an increase in CENP-A foci number and ectopic CENP-A localization. Additionally, co-depletion of CHRAC14 and Su(var)3-9 shows a decrease in CENP-A foci number. It was therefore tested, whether an increased Su(var)3-9 expression, irrespective of CHRAC14 depletion, can lead to a similar effect on CENP-A localization.

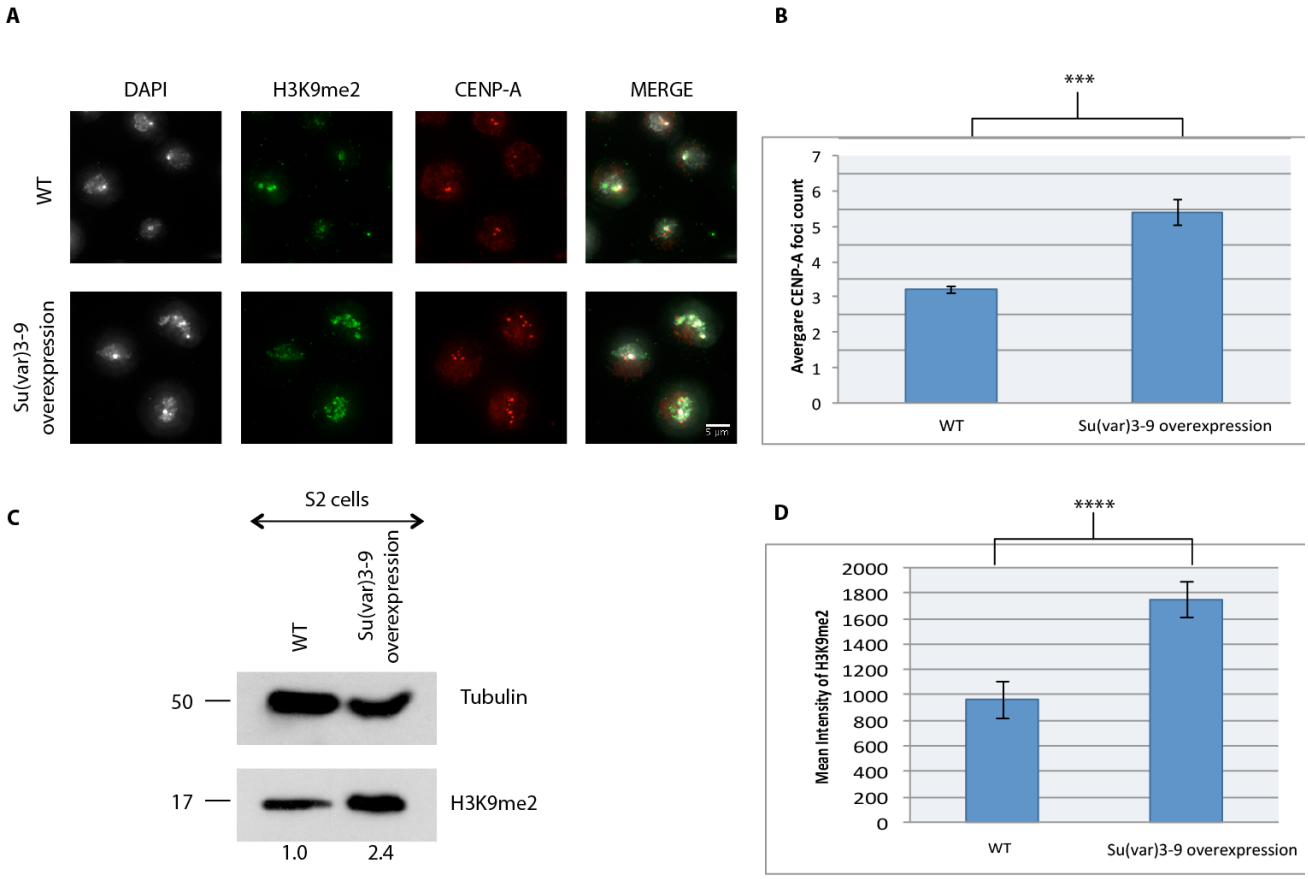

Figure 2.8: Su(var)3-9 overexpression leads to an increase in overall CENP-A foci. **A)** IF on S2 cells with and without Su(var)3-9 overexpression were stained with anti-CENP-A (red), anti-H3K9me2 (green) antibody and co-stained with DAPI (grey). Bar= 5µm. **B)** Quantification of average CENP-A foci count from control and Su(var)3-9 overexpressing cells from 3 biological replicates. Error bars represent ±SEM and a p-value <0.05. **C)** Control and Su(var)3-9 overexpressing cells were analyzed for increased H3K9me2 via western blot using anti-H3K9me2 antibody and anti-Tubulin antibody (loading control). **D)** Quantification of average signal intensity of H3K9me2 from control and Su(var)3-9 overexpressing cells from three IF repeats. Error bars represent ±SEM and a p-value <0.05.

For this purpose, S2 cells were transfected with a pMT-Su(var)3-9-V5-His construct. Su(var)3-9 was overexpressed by using 0.5mM $CuSO_4$ for 8 hours

and the level of H3K9me2 checked via western blot and IF (Figure 2.8A, C and D). As expected, western blot analysis shows an increase in H3K9me2 levels upon Su(var)3-9 overexpression. Cells with and without Su(var)3-9 overexpression were further analyzed for CENP-A foci. Comparative analysis between control (no over-expression) and Su(var)3-9 overexpressing cells show overall increased CENP-A foci numbers in cells with increased Su(var)3-9 expression (Figure 2.8A and B). This indicates that elevated Su(var)3-9 expression can lead to a similar phenotype as discovered in CHRAC14 depleted cells (compare Figure 2.2B and 2.8A).

2.3.2 **An elevated Su(var)3-9 level causes ectopic CENP-A foci**

Overexpression of Su(var)3-9 increases the overall CENP-A foci counts. Every chromosome has an endogenous centromeric CENP-A site. Increased CENP-A foci in cells as analyzed via IF could mean that there are more CENP-A sites on individual chromosomes suggesting ectopic CENP-A localization (Tomonaga et al. 2003; Mathew et al. 2014; Heun et al. 2006; Pauleau & Erhardt 2011) . To confirm this observation, metaphase chromosome spreads obtained from the cells with and without Su(var)3-9 overexpression were compared. Metaphase spreads were fixed and co-stained with DAPI and CENP-A antibody. As expected, metaphase spreads from control cells show two CENP-A foci at centromere constrictions of sister chromatids reflecting endogenous WT type localization of CENP-A (Figure 2.9A upper panel lane). Su(var)3-9 overexpressing cells show CENP-A at endogenous centromeric constriction as seen in control. In addition to centromeric localization, CENP-A also localizes to metaphase chromosome arms in Su(var)3-9 overexpressing cells (Figure 2.9). Ectopic CENP-A foci were often sited near telomere ends which is a known predominant site for ectopic CENP-A loading (Olszak et al. 2011) {Figure 2.9A image zoomed from Su(var)3-9 overexpression}. It was repeatedly observed that ectopic CENP-A foci were less intense in comparison to centromeric CENP-A.

Images were analyzed via ImageJ, brightness and contrast was adjusted accordingly to visualize ectopic CENP-A in the samples with and without Su(var)3-9 overexpression. Nevertheless, only good quality metaphase spreads from Su(var)3-9 overexpressing cells (Figure 2.9A, lower panel).

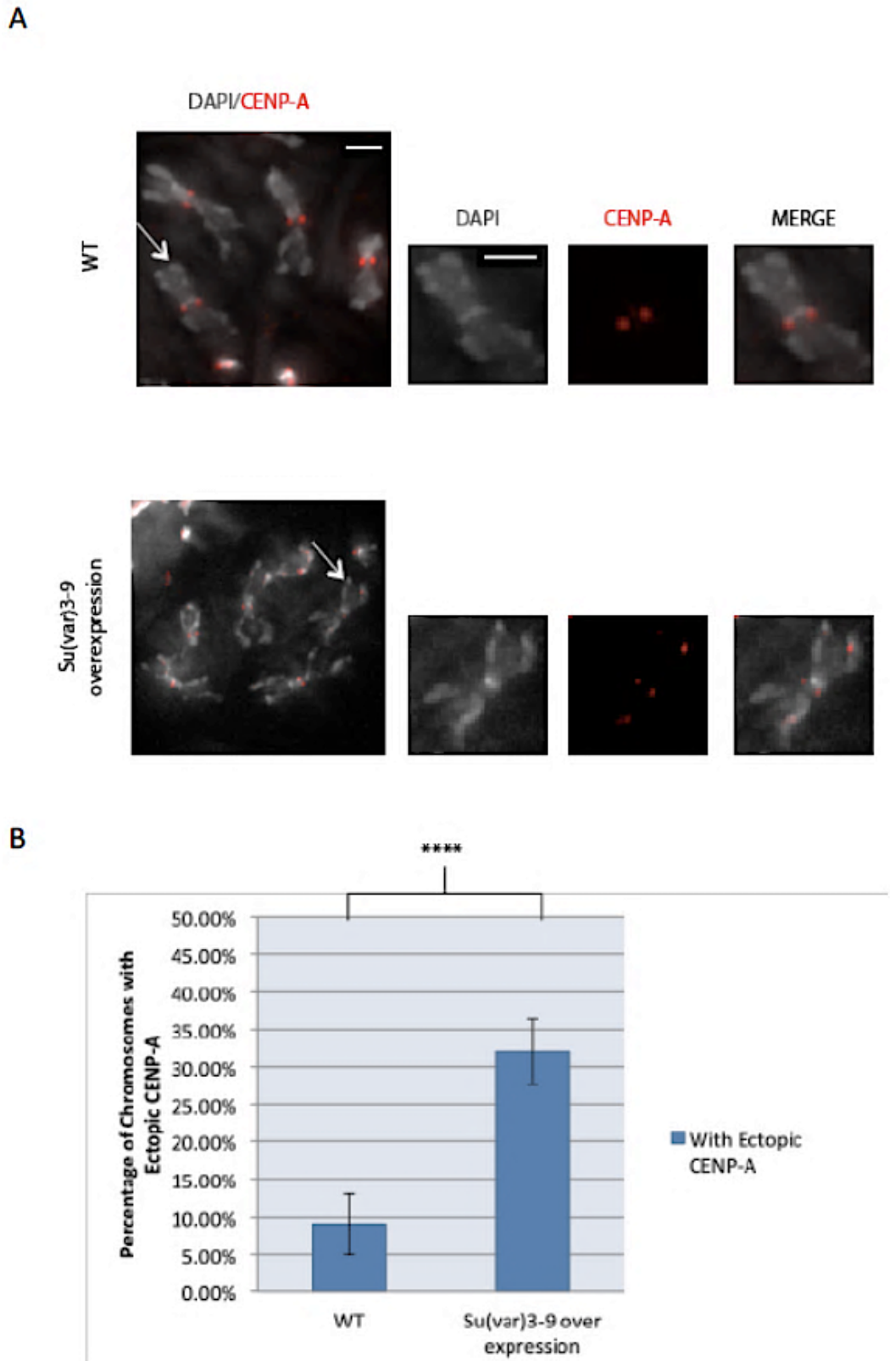

Figure 2.9: Increased Su(var)3-9 overexpression causes CENP-A ectopic localization. **A)** S2 cells with and without Su(var)3-9 overexpression were inhibited in metaphase. Thereafter, chromosomes were subjected to IF with anti-CENP-A antibody (red) and DAPI (grey). Arrowheads indicate the zoomed metaphase spread. Size bar= 2µm. **B)** Quantification of ectopic CENP-A on metaphase chromosomes obtained from WT (control with no Su(var)3-9 overexpression) and Su(var)3-9 overexpressing cells. Ectopic CENP-A on chromosome arms, with weak signal intensity were also considered in quantification. The total number of chromosomes screened is >100 from 5 repeats. Error bars represent ±SEM and a p-value <0.05. Su(var)3-9 overexpressing cells show a 3 times increase in ectopic CENP-A sites.

Quantification of five biological replicates of the experiment suggests that around 10% of chromosomes without Su(var)3-9 overexpression show ectopic CENP-A foci. Intriguingly, metaphase chromosomes obtained from Su(var)3-9 overexpressing cells show a significant increase in ectopic CENP-A localization, with around 3 times more chromosomes showing ectopic CENP-A localization. (Figure 2.9B).

2.3.3 Increased Su(var)3-9 level leads to ectopic CENP-C localization

The centromere is marked by CENP-A H3 variant, however CENP-C is also essential for centromere identity (Orr & Sunkel 2011). CENP-A and CENP-C are incorporated concomitantly at the centromere (Pauleau & Erhardt 2011) and ectopic CENP-A and CENP-C localization has been reported to result in cell segregation defects (Heun et al. 2006). Therefore, it was analyzed next whether the elevated Su(var)3-9 levels can also lead to ectopic CENP-C localization. For this question, the metaphase spreads were repeated with and without Su(var)3-9 overexpression, afterwards stained with CENP-C antibody and DAPI to visualize chromosomes. ImageJ analysis of the DAPI region (metaphase spreads) shows clear localization of CENP-C to centromeres in WT {control with no Su(var)3-9 overexpression}, however, no CENP-C signal was observed to be localized on the sister chromatid arms, suggesting centromere-specific CENP-C localization (Figure 2.10 upper panel

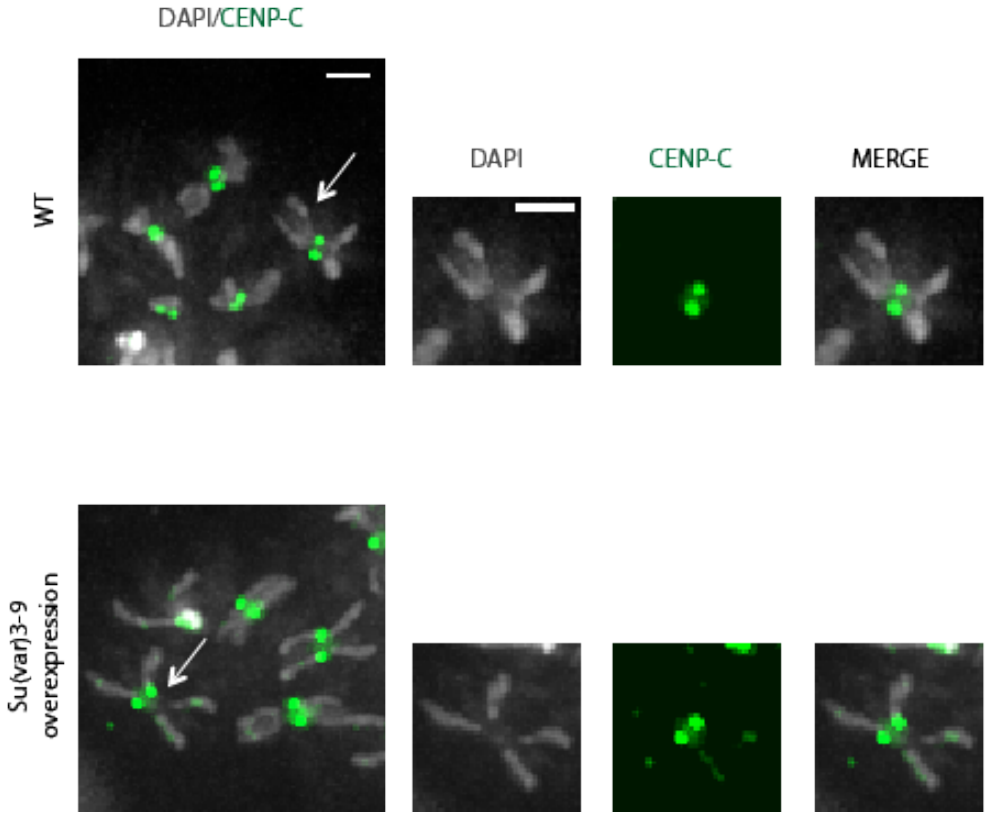

Figure 2.10: Increased Su(var)3-9 overexpression causes CENP-C ectopic localization. S2 cells with and without Su(var)3-9 overexpression inhibited in metaphase and the metaphase spread were subjected to IF with anti-CENP-C antibody (green) and DAPI (grey). The arrowheads indicate the zoomed metaphase spreads. Size bar= 2µm.

lane). Conversely, in metaphase chromosomes obtained from Su(var)3-9 overexpressing cells, ectopic CENP-C signals were observed in addition to centromeric CENP-C signals (Figure 2.10 lower panel lane, see the zoomed panel), suggesting increased Su(var)3-9 level can lead to miss-localization of centromeric CENP-C protein (Figure 2.10).

2.4 Increased Su(var)3-9 level lead to cell segregation defects

2.4.1 Higher levels of Su(var)3-9 show delay in mitotic phase and lagging chromosome defects

Ectopic CENP-A and CENP-C localization discovered under the influence of increased Su(var)3-9 expression would indicate a functional kinetochore, which in turn should result in multiple microtubule attachments to a chromosome leading to cell segregation defects either with lagging chromosome or with chromosome breakage.

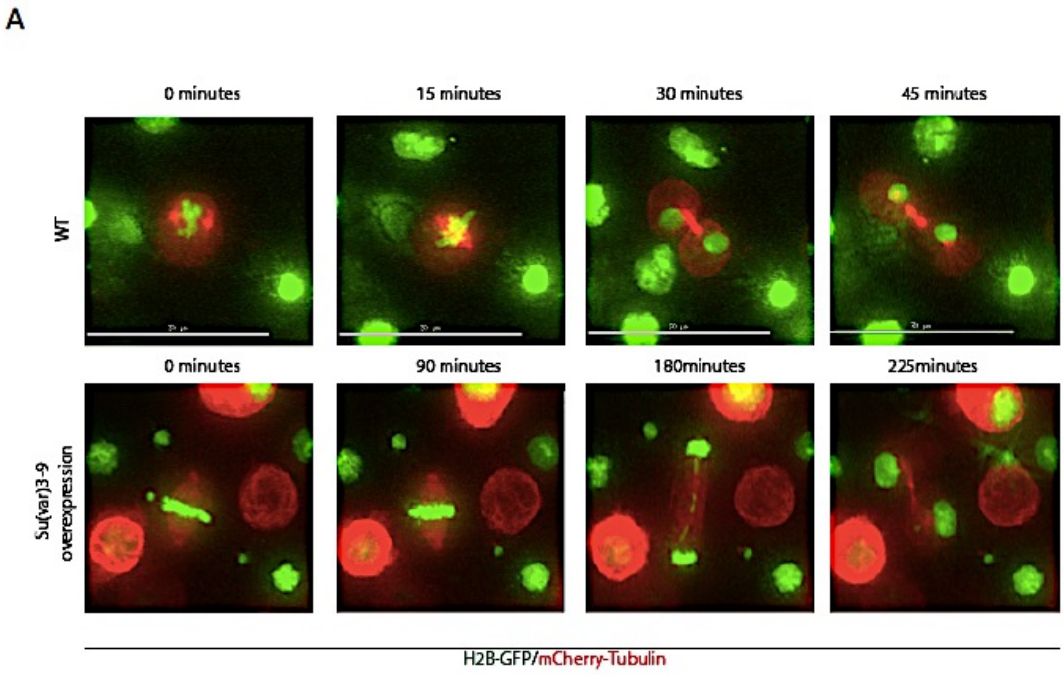

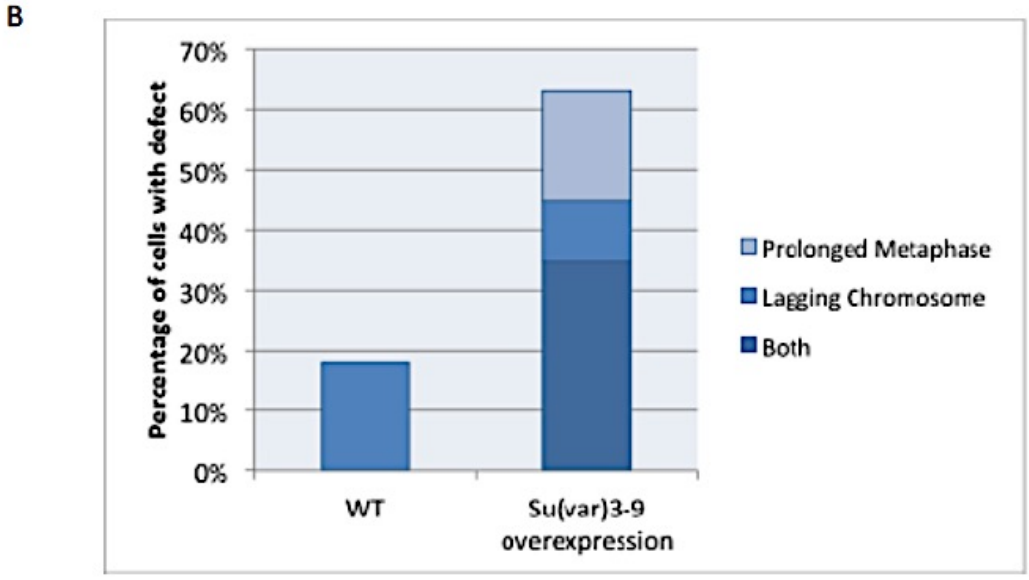

Figure 2.11: Su(var)3-9 overexpression leads to chromosome segregation defect. **A)** Live-cell analysis of Su(var)3-9 overexpressing cells. S2 cells co-transfected with histone H2B-GFP (green), mCherry-Tubulin (red), pMT-Su(var)3-9-V5-His were imaged every 15 minutes for 12 hours. WT (no $CuSO_4$) and Su(var)3-9 overexpression (with $CuSO_4$). WT cells show normal prophase to anaphase progression. Cells with Su(var)3-9 overexpression show longer metaphase or lagging chromosome defect or both. Top panel represents images from WT cells {with no Su(var)3-9 overexpression} and bottom panel represents images from Su(var)3-9 overexpressing cells. 0 minutes represents the time point of alignment of chromosomes at metaphase plate. Size bar = 30µm. **B)** Quantification of chromosome segregation defect in WT and Su(var)3-9 overexpressing cells. A defect was categorized as longer metaphase (prolonged metaphase), lagging chromosome and prolonged metaphase with lagging chromosome (both) n>30 from three independent biological experiments.

To check the occurrence of cell segregation defects in Su(var)3-9 overexpressing cells, S2 cells were co-transfected with H2B-GFP, mCherry-Tubulin and pMT-Su(var)3-9-V5-His. These cells were then subjected to live-cell imaging to capture any cell segregation defect in absence and presence of Su(var)3-9 overexpression. WT cells show normal prophase to anaphase progression with an average duration of 15 to 30 minutes (Figure 2.11A upper panel). As expected, Su(var)3-9 overexpressing cells show cell segregation defects as observed during live-cell imaging (Figure 2.11A lower panel). Defects observed include: a) longer metaphase, b) anaphase with lagging chromosomes, c) longer metaphase followed by lagging chromosome defect in anaphase (Figure 2.11B). In this analysis, control cells show 18% of segregations with lagging chromosome defects. Whereas, in Su(var)3-9 overexpressing cells, a total of 45% of cell segregations observed had lagging chromosome defects (Figure 2.11B). In total, the quantification is showing a 2.5-fold increase in lagging chromosome defects which is complementary to fold increase seen in ectopic CENP-A foci formation upon Su(var)3-9 overexpression (Figure 2.9B).

2.4.2 Lagging chromosomes show increased CENP-A foci

Lagging chromosomes can be the result of failure of microtubule attachment to kinetochore or the result of multiple microtubule attachment sites on a chromosome (Pauleau & Erhardt 2011; Maiato et al. 2004). Ectopic CENP-A and CENP-C caused by Su(var)3-9 overexpression as seen in earlier experiments could cause a segregation defect. To further validate the presence and role of ectopic CENP-A in the cell segregation defect observed in Su(var)3-9 overexpressing cells, the presence of CENP-A in observed lagging chromosomes was analyzed. For this experiment, Su(var)3-9 overexpressing cells were subjected to IF along with control (WT). These cells were stained

for anti-Tubulin (to identify the late anaphase cells), anti-CENP-A and DAPI (to visualize the DNA).

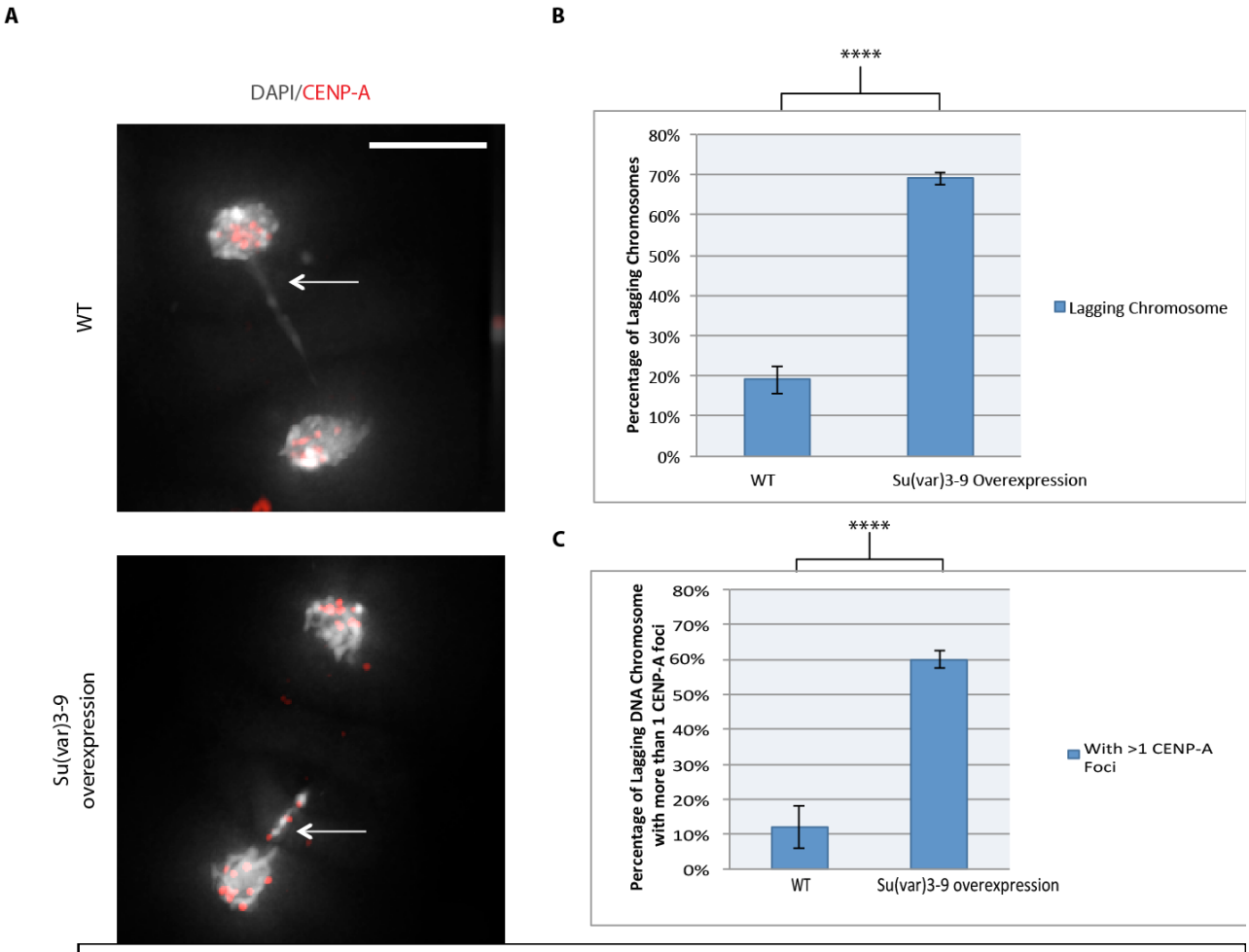

Figure 2.12: Su(var)3-9 overexpression leads to lagging chromosomes with increased CENP-A foci. A) S2 cells with normal (WT) and overexpressed Su(var)3-9 levels were plated on concanavalin A coated glass slides. Stained with CENP-A (red), Tubulin (not shown in this picture) and DAPI (grey). Lagging chromosomes were visualized by adjusting brightness and contrast. Bar=5µm B) Quantification of total anaphase cells screened for lagging chromosomes in WT and Su(var)3-9 overexpressing cells. C) Quantification of lagging chromosomes with more than one CENP-A foci observed in WT and Su(var)3-9 overexpressing cells. Error bars represent ±SEM and a p-value <0.05, n>40 from three independent biological replicates.

First, the overall lagging chromosomes were quantified in WT and Su(var)3-9 overexpressing cells, where only anaphase cells were used. To visualize the lagging chromosomes, brightness and contrast was increased via Image J. WT cells show less than 18% lagging chromosomes, however, cells with elevated Su(var)3-9 level show an elevated lagging chromosome defect, with around 70%. (Figure 2.12B). In addition, cells which showed a lagging chromosome were quantified using foci/spot detection plugin, and checked for the

presence of a CENP-A signal on them. To avoid the reading of any unspecific CENP-A signal, CENP-A foci co-localizing with both, microtubule signals and lagging chromosomes (DAPI signal) were taken into account. Quantification of CENP-A on lagging chromosomes revealed that lagging chromosomes have more than one CENP-A foci (Figure 2.12 A). In normal cells segregating chromosomes in anaphase should possess a single CENP-A-kinetochore site built at the centromere. Considering this, lagging chromosomes were categorized between a) Lagging chromosome with one CENP-A foci and b) Lagging chromosomes with more than one CENP-A foci. The presence of more than one CENP-A foci on a lagging chromosome would reflect more than one potential kinetochore site. Quantification of lagging chromosomes with more than one CENP-A foci shows that WT situation includes around 12% of lagging chromosomes with more than one CENP-A foci. Interestingly, 60% of lagging chromosome analyzed from Su(var)3-9 overexpressing cells show more than one CENP-A foci (Figure 2.12 C), the remaining 10% are common between the two conditions with no increased CENP-A foci. Overall, this is suggesting a strong correlation between a lagging chromosome defect and increased CENP-A foci under given Su(var)3-9 conditions (Compare Figure 2.12 B and C).

2.4.3 **Changed Su(var)3-9 level result in CENP-A and Su(var)3-9 interaction**

In order to examine the interaction between Su(var)3-9 and CENP-A, a pull-down assay was performed using Su(var)3-9-V5-His overexpressing cells followed by western blot. A V5 antibody was used for immunoprecipitation. Pulldown of Su(var)3-9-V5-His showed co-precipitation of methylated H3K9 which is known to interact with Su(var)3-9(not shown in the figure) (Lachner et al. 2001; Schotta et al. 2002; Al-Sady et al. 2013). Interestingly, I observed co-precipitation of CENP-A with Su(var)3-9-V5-His that suggests an interaction between endogenous CENP-A and Su(var)3-9 under given Su(var)3-9 conditions (Figure 2.13). Additionally, the pulldown of CENP-A in CENP-A overexpressing cells shows a potential direct/indirect interaction with Su(var)3-7 {known interactor of Su(var)3-9} as analyzed via mass spectrometry (Appendix 6.5).

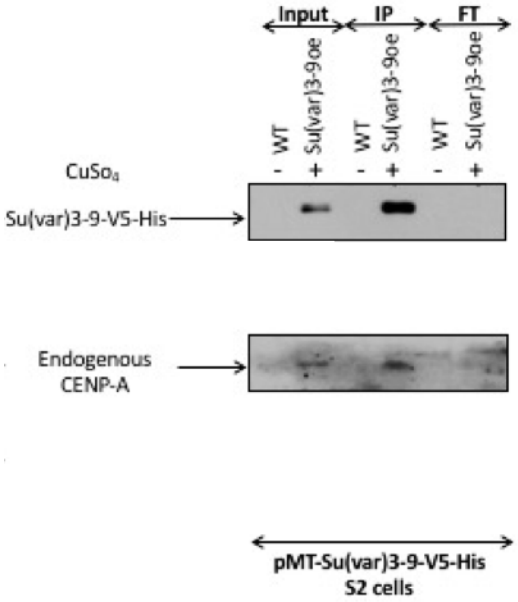

Figure 2.13: **Su(var)3-9 interacts with endogenous CENP-A in Su(var)3-9 overexpression.** S2 cells with Su(var)3-9-V5-His overexpression were subjected to immunoprecipitation using a V5 antibody and then analyzed for presence of Su(var)3-9-V5-His (V5 antibody), CENP-A and H3K9me2, using respective antibodies. The picture is representative of more than 3 repeats.

2.5 Effect of Su(var)3-9 overexpression on cell cycle progression

Next, the effect of Su(var)3-9 overexpression on cell cycle progression was addressed. Propidium iodide (PI) flow cytometry (FACS) was used to analyze the cell cycle phases in WT and Su(var)3-9 overexpressing cells. The results obtained show no significant change in different G1, S, S2/M and SubG1 cell cycle phases (Figure 2.14 A and B).

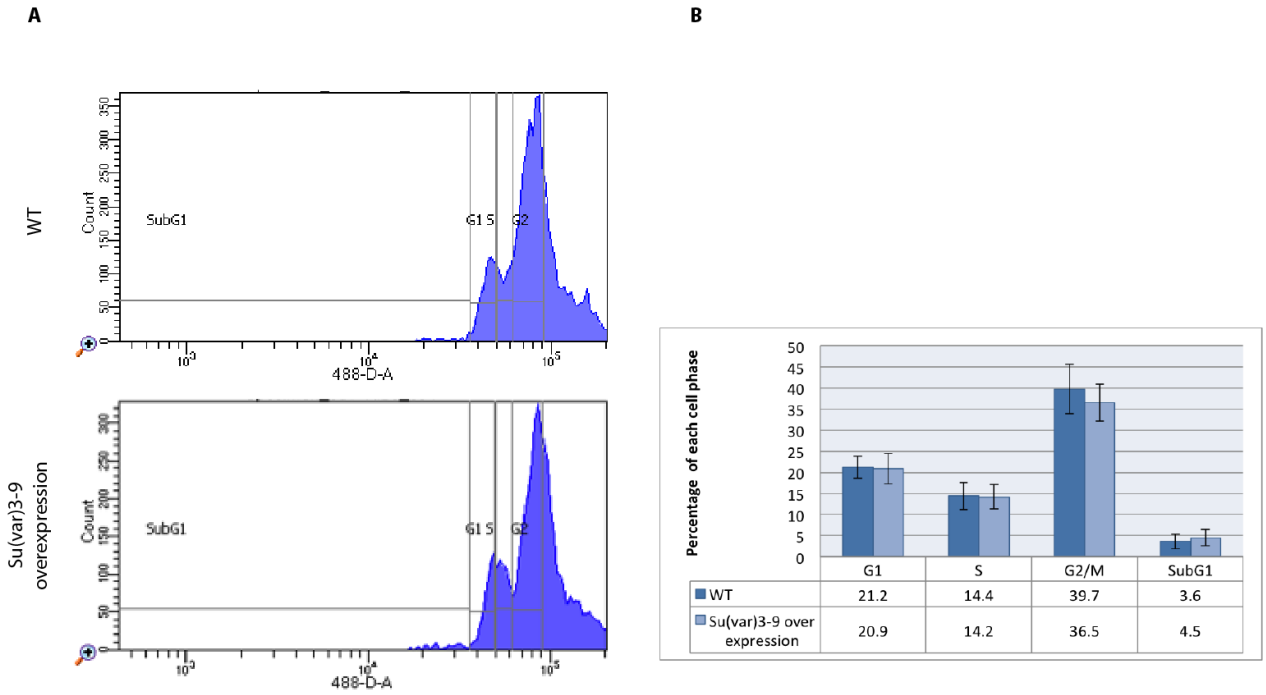

Figure 2.14: High Su(var)3-9 level in S2 cells does not affect the cell cycle progression. A) Flow cytometric analysis indicating the cell cycle profile of control (WT upper panel) and CHRAC14 RNAi (lower panel) cells. The cells from each sample were collected after 4 days of RNAi treatment, processed and analyzed using BD FACS Canto II. The percentage of each cell cycle stage and the number of cells used (10,000 event count) in both samples were as indicated and was analyzed using FlowJo software. The cell cycle profile and the frequency of each stage in both samples were comparable to each other. B) Quantification of average of three biological replicates of the experiment represented in Figure A. Error bars represent ±SEM.

PI dependent FACS analysis cannot be used to differentiate between G2 and M phase in WT and Su(var)3-9 overexpressing cells. To further evaluate the mitotic index of Su(var)3-9 overexpressing cells, it was decided to check for the mitotic marker phospho-Histone 3 (PH3) (Goshima et al. 2007). Cells with and without

Su(var)3-9 overexpression were subjected to IF using an anti-PH3 antibody and nuclei were stained with DAPI (Figure 2.15).

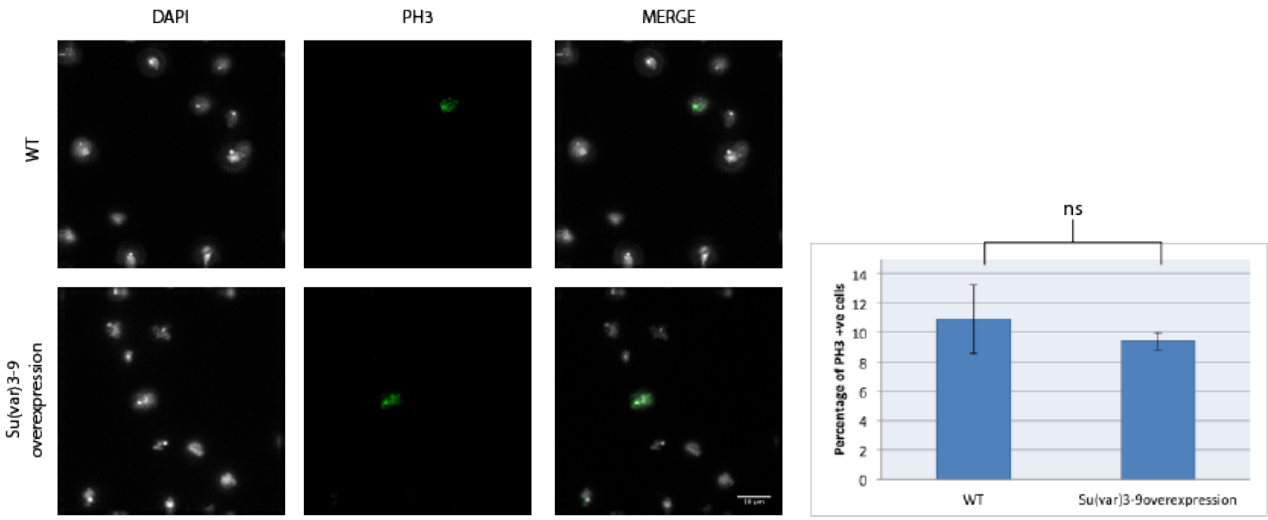

Figure 2.15 Elevated Su(var)3-9 does not affect the mitotic index. S2 cells with and without Su(var)3-9 overexpression were subjected to IF using anti-phospho-Histone 3 (PH3) and co-stained with DAPI (grey). Bar= 10µm. The graph represents the percentage of PH3 positive cells from control and Su(var)3-9 overexpressing cells from 3 biological independent replicates. Total 50 cells/repeat were counted. Error bars represent ±SEM and a p-value >0.05. ns=non-significant

PH3 positive cells were quantified and percentages measured. Results suggest around 10% of mitotic cells present in unsynchronized WT and Su(var)3-9 overexpressing S2 cells, reflecting no significant difference in the mitotic index between the two conditions (Figure 2.15).

3 Discussion

3.1 Role of CHRAC14 in maintenance of heterochromatin

In this study I show that depletion of CHRAC14 results in an increase of H3K9me2 which suggests an overall increase in heterochromatin structure. In addition to this, the CHRAC14 human homolog has been reported to enhance nucleosome sliding effect in *in vitro* experiments (Kukimoto et al. 2004). These evidences all together suggest that CHARC14 alone could play a crucial role in maintaining chromatin structure.

In mammalian and in yeast cells, it has been shown that a defect in nucleosome assembly affects the replication, transcription and genome maintenance (Lewis et al. 2005; Kukimoto et al. 2004; Rocha & Verreault 2008; Burgess & Zhang 2014). Further, CHRAC14 in the CHRAC complex is reported to affect chromatin nucleosome assembly (Guelman et al. 2009; Clapier & Cairns 2009). Depletion of ACF1 (a CHRAC subunit) has also been shown to slow down the replication of heterochromatin region suggesting a role of the CHRAC complex in relaxing heterochromatin structure (Collins et al. 2002). Additionally, in yeast a homolog of CHRAC14 is suggested to anchor the CHRAC complex to specific genomic sites (Dang et al. 2007). It is possible that this role of CHRAC14 is important in relaxing heterochromatin and could be one of the reasons why CHRAC14 depletion shows increased heterochromatin marker.

Further, another CHRAC14 containing complex, ATAC which also contains two HATs, has been shown to be important for maintenance of histone acetylation and thereby maintaining the euchromatin and heterochromatin balance in Drosophila (Ciurciu et al. 2008; Ma et al. 2013; Guelman et al. 2009). Ciurciu et. al. has also reported that an absence of ATAC complex subunits can lead to enhanced heterochromatin structures (Ciurciu et al. 2008). However, it has never been elucidated whether the absence of CHRAC14 either as part of CHRAC complex or ATAC complex can impact the overall chromatin structure. Our study, explicitly, show that the absence of CHRAC14 lead to increased H3K9me2 and HP1 levels

suggesting that the presence of CHRAC14 is required for maintaining the physiological level of heterochromatin and euchromatin.

We have also observed an enhanced expression of Su(var)3-9 mRNA in absence of CHRAC14, as seen via RT-PCR. The increased Su(var)3-9 expression further supports our observation of enhanced H3K9me2 level in CHRAC14 depleted cells. Moreover, ADA2A (subunit of ATAC complex) depletion shows enhanced H3K9me2 (see appendix 6.2) and this is Su(var)3-9 dependent (Ciurciu et al. 2008) which is similar to the CHRAC14$^{-/-}$ phenotype observed in our study. In addition to this, we also observed that the lack of CHRAC14 shows reduced H3K9 acetylation, which indicates the loss of HAT activity. One possible reason could be that the presence of CHRAC14 increases the DNA binding to ATAC complex that in turn becomes crucial for HAT activity. Another possibility could be that an absence of CHRAC14 led disruption of ATAC complex that in turn affects HAT activity. However, a precise understanding CHRAC14 on HAT activity is a subject of further studies.

It would be interesting to analyze the *in vitro* efficiency of the ATAC complex with and without CHRAC14 on H3K9 containing substrate. Our results, together with previous reports, indicate a possible disruption of the ATAC complex or a combination of a defect in CHRAC and ATAC complex activity which leads to an increase in heterochromatin structure.

3.2 Role of CHRAC14 in DNA damage repair

Increase in heterochromatin and decrease in H3K9 acetylation have been shown to impair the DNA damage repair ability of cells (Guo et al. 2011; Klement et al. 2014; Dinant et al. 2008; Chiolo et al. 2011; Sulli et al. 2012; Jakob et al. 2011). Chromatin requires a balance between condensed and decondensed chromatin structures in response to overcome DNA damage stress arising due to biotic and abiotic factors. It is easy to imagine that compact DNA structure can protect DNA against any endogenous DNA damaging factors like reactive oxygen species (ROS) (Harikrishnan et al. 2008; Tsang et al. 2014). However, once the DNA damage occurs, accessing the DNA damage sites by DNA repair proteins is the foremost step, which may involve expansion of heterochromatin along with moving the DNA damage site out of the compact structure (Chiolo et al. 2011; Jakob et al. 2011; Guo et al. 2011). The

repair system may also involve chromatin relaxation by acetylation of histones (Tjeertes et al. 2009; Guo et al. 2011). We have observed that the CHRAC14 knockdown which shows reduced H3K9ac with an increase of H3K9me, suggest defective chromatin relaxing machinery with increased DNA compaction. This could be a possible reason for accumulation of DNA damage seen in absence of CHRAC14. In addition to this, a previously, our research group showed that CHRAC14$^{-/-}$ flies and embryos show a defect in hatching upon heavy IR treatment (10 Gy -30 Gy) but hatch normally when not subjected to a DNA damaging agent, although they have low level of endogenous DNA damage accumulation (Mathew et al. 2014). One possible explanation for this is that when embryos are subjected to strong dose of DNA damaging agent/s, because of high DNA compaction it is not possible for embryos to cope up with high amounts of unrepaired DNA damage and this leads to their death. Altogether, suggesting an important role of CHRAC14 in facilitating appropriate chromatin environment for the repair of damaged DNA.

3.3 **CENP-A, a potential substrate for acetylation**

In Drosophila, global inhibition of histone deacetylation with TSA leads to reduction in ectopic CENP-A localization, in CENP-A overexpressing cells (Olszak et al. 2011). Further, our analysis suggests that TSA treatment reduces the overall CENP-A foci number in CHRAC14 depleted cells when compared to CHRAC14 depleted cells which has been reported to have high CENP-A foci number (Mathew et al. 2014). We also observe that the nuclear localization of CENP-A is negatively affected by TSA treatment, in CENP-A over expressing cells. These experiments, indicating two possibilities; 1) either acetylation/deacetylation of other histones (H4, H2A, H2B) in CENP-A nucleosome plays role in CENP-A localization or 2) acetylation/deacetylation of CENP-A play role in its localization. Recently it has been reported that HAT1 dependent H4 K5 and K12 acetylation is important for centromeric CENP-A localization in chicken cells and human cells (Shang et al. 2016). Similar mechanism is also possible in Drosophila model system which may require CHRAC14 containing complex like ATAC. Additionally, it is also possible that CHRAC14 depletion also affects CENP-A acetylation which in turn could affect the localization in combination with observed reduced H3K9 acetylation.

Very little is known about acetylation of CENP-A. Our preliminary experiments suggest that CENP-A could be a potential acetylation substrate. Further, I attempted to check which HAT could be responsible for this. For this purpose, a Sumo tagged CENP-A was expressed and purified from a bacterial expression system as described in a previous report (Bade et al. 2014). Later, the *in vitro* acetylation assay was performed by Renate Voit (lab of Prof. Ingrid Grummt). Initial results suggested that CENP-A could be acetylated. However, we also found control CENP-A acetylated (without incubation with any HAT), suggesting acetylation via bacterial system (Linda I. et al. 2010). Nevertheless, the experiment still hints that CENP-A could be acetylated but whether Drosophila HATs can acetylate it, still remains a question. Alternative technique like in-vitro translation can be helpful to obtain unmodified CENP-A for repetition of HAT assay. A recent study suggests that Drosophila CENP-A interacts with HAT1 but does not acetylate it (Boltengagen et al. 2015). Although the study detected acetylation of CENP-A at K105 via mass spectrometry, the responsible HAT is yet to be discovered. GCN5 and ATAC2 are two HATs associated with the ATAC complex and it is possible that either of these HATs could be the responsible HAT for CENP-A acetylation. Additionally, in budding yeast, a homolog of GCN5 has been shown to interact with Cse4p (CENP-A homolog) and this interaction is important for kinetochore formation (Vernarecci et al. 2008). This further stresses the idea of GCN5 as a potential HAT for CENP-A acetylation. It would be interesting to further investigate the role of GCN5 in CENP-A acetylation in Drosophila cells via *in-vivo* and *in-vitro* approaches. Further experiments in this direction will reveal the details of CENP-A as a potential acetylation substrate and its significance in Drosophila model system.

3.4 **Role of Su(var)3-9 in facilitating ectopic CENP-A localization**

CHRAC14 depletion leads to an increase in CENP-A foci number in S2 cells and the increased foci were ectopic foci (Mathew et al. 2014). Interestingly, during this study, we have observed that depletion of CHRAC14 increases Su(var)3-9 and H3K9me2, indicating an increase in heterochromatin. This was followed by the observation that raised Su(var)3-9 expression shows potential to facilitate ectopic CENP-A and CENP-C localization. Previously, it has been shown that tethering of HP1

which is downstream to Su(var)3-9 in heterochromatin formation pathway, can lead to de-novo deposition of CENP-A at ectopic sites (Olszak et al. 2011). It is possible that ectopic loading of CENP-A requires Su(var)3-9 activity to create heterochromatin boundaries and this is followed by HP1 recruitment. Additionally, whether HP1 and Su(var)3-9 leads to ectopic loading of CENP-A via same the pathway or separate is a subject to study further. It will also be interesting to ask whether the observed Su(var)3-9 dependent CENP-A ectopic loading requires Satellite III, which has been reported to be important for centromeric CENP-A localization (Rošić et al. 2014).

Further, our live-cell image analysis on Su(var)3-9 overexpressing cells show an enhanced chromosome segregation defect with lagging chromosomes and these lagging chromosomes show an increase in CENP-A foci count. These increased CENP-A sites on chromosomes could be the possible cause of a lagging chromosome defect and should be further characterize for the presence of outer kinetochore proteins. Additionally, further investigation by analyzing chromatin bound to CENP-A using chromatin immunoprecipitation (ChIP) could help us to identify a possible increase in genomic sites for ectopic CENP-A localization. Additionally, it will also help us to understand whether there is some consistency in their preferred sites localization or it is random but more specific to the surrounding epigenetic environment. Previous reports suggest that heterochromatin boundaries are hotspots for CENP-A ectopic localization (Olszak et al. 2011). In agreement with this, my results suggest that ectopic CENP-A foci sites in Su(var)3-9 overexpressing cells were more often near to the telomeres, which are known to be dominant heterochromatin site. This, in turn, indicates that the heterochromatin boundaries might also be favourable sites for ectopic CENP-A localization in given Su(var)3-9 conditions and would be interesting to investigate in future. It is possible that overexpression of Su(var)3-9 gives rise to ectopic heterochromatin chromatin sites by methylating H3K9 slightly away from telomeric heterochromatin and this is followed by recruitment of HP1. This would lead to the formation of a non heterochromatinized chromatin region which is flanked by heterochromatin, similar to centromere which is flanked by pericentric heterochromatin. Further, this "*ectopic heterochromatin-non heterochromatin-telomeric heterochromatin*" region

at telomere might be recruiting CENP-C and CENP-A, and other kinetochore related proteins leading to the formation of potential ectopic microtubule attachment sites. Later, this is resulting in a chromosome segregation defect with lagging chromosomes.

In mammalian cells it has been shown that tethering of heterochromatin forming factors like Su(var)3-9h1 and HP1 does not favour CENP-A deposition (Ohzeki et al. 2016; Ohzeki et al. 2012; Nakano et al. 2008) although it is also interesting to see that tethering of G9a {redundant in Drosophila, its role is taken over by Su(var)3-9} shows ectopic CENP-A deposition as seen in HAC system (Shono et al. 2015). In yeast, the Su(var)3-9 homologue Clr4 promotes CENP-A deposition (Kagansky et al. 2009) and in Drosophila HP1 tethering promotes ectopic CENP-A localization which is converse to the mammalian system (Olszak et al. 2011). Complementary to this my results showed that increased Su(var)3-9 expression can cause ectopic CENP-A localization. In addition to this, in the preliminary data using the Lac-O/Lac-I tethering system, I was able to observe that the tethering of Su(var)3-9 can cause CENP-A deposition (see Appendix 6.1). However, this data should further be validated using metaphase spreads since there is a possibility that it is not due to the tethering of Su(var)3-9 but due to the overexpression of Su(var)3-9 that causes CENP-A deposition at the Lac-O site. Nevertheless, we can conclude from my results that the Su(var)3-9 overexpression is capable of CENP-A deposition at ectopic sites in S2 cells, primarily near telomeres. This suggests a potential role of Su(var)3-9 in facilitating ectopic loading of CENP-A in Drosophila cells by influencing the formation of heterochromatin structure and highlights the importance of maintaining its physiological level in the context of CENP-A localization.

3.5 **Working Model**

It has been postulated that CHRAC14 monitors CENP-A miss-localization in presence of DNA damage, possibly by formation of CHRAC14-CENP-A complex (Mathew et al. 2014). Moreover, results from this study suggest that CHRAC14 depletion also leads to an increase in heterochromatin. Considering our results and previous reports, we can propose that in addition to previously reported CHRAC14's role in monitoring

ectopic CENP-A localization; CHRAC14 also maintains heterochromatin level and its absence leads to an increase in Su(var)3-9 expression which is upstream to HP1 localization in heterochromatin formation. Su(var)3-9 rise leads to ectopic heterochromatin formation which may impair the DNA damage repair ability and also favor the CENP-A and CENP-C ectopic localization. This ectopic CENP-A and CENP-C localization may require SatIII? The non-centromeric CENP-A and CENP-C may recruit kinetochore proteins leading to potential microtubule attachment site/s in addition to centromeric site, in metaphase cells. As a consequence, metaphase chromosomes with more than one microtubule sites results as lagging chromosome defects, which in turn may cause genomic instability (Figure 3.1).

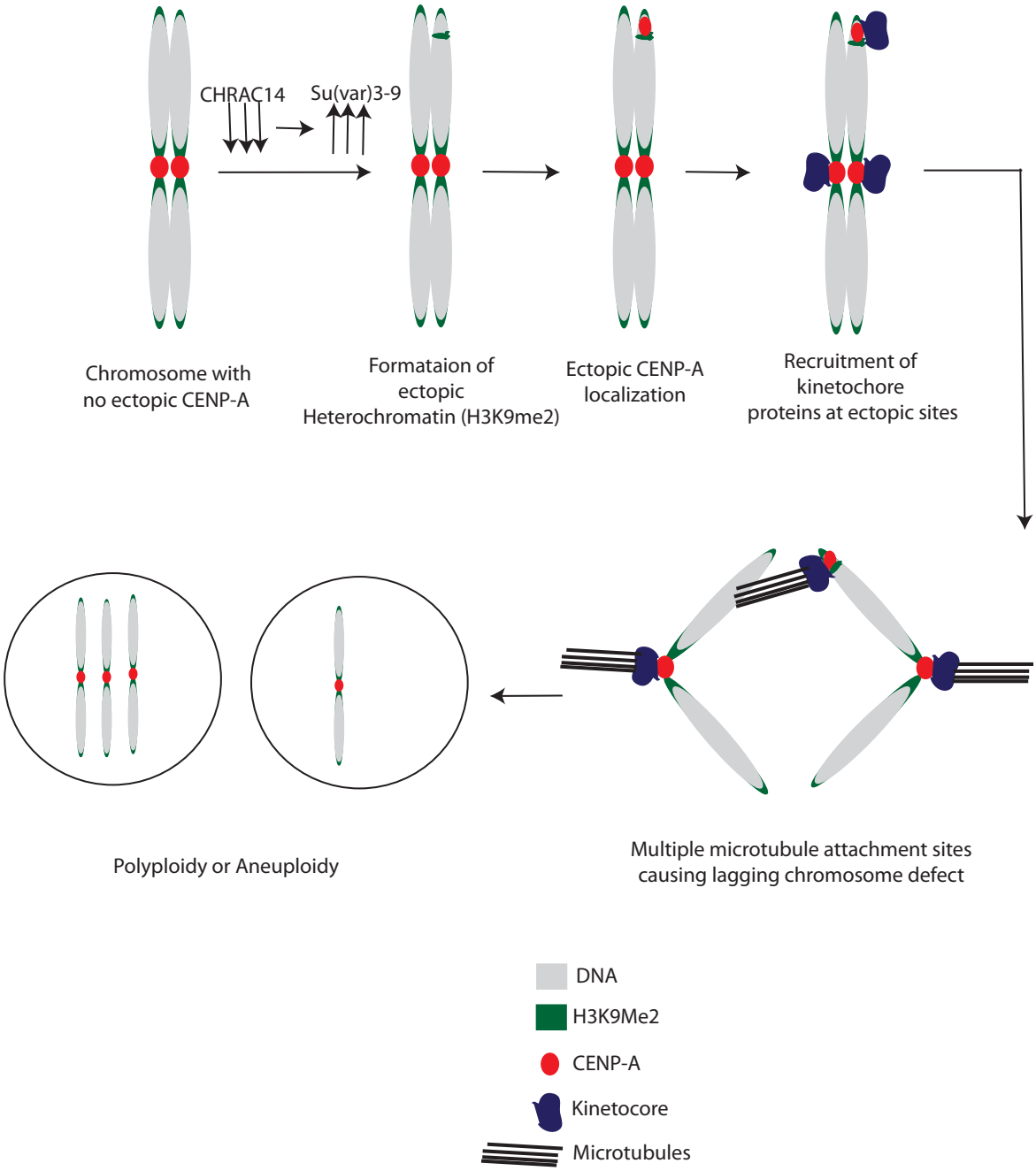

Figure 3.1: Working Model: CHRAC14 depletion leads to increase in Su(var)3-9 expression, resulting in the formation of ectopic heterochromatin near telomeres, leading to the non-heterochromatin region flanked with heterochromatin (similar to centromere). Region flanked with heterochromatin near telomere may favor ectopic CENP-A localization and thereby recruiting kinetochore proteins. This would further lead to microtubule attachment of kinetochore in addition to centromeric attachment causing delayed metaphase and lagging chromosome defect. This may further result in polyploidy or aneuploidy.

3.6 Histone methyltransferases, the possible missing-link between ectopic CENP-A and cancer

Reports on molecular biology of colon cancer suggests that the patients have elevated level of Su(var)3-9H1 and G9a histone methyltransferases (Kang et al. 2007; Zhang et al. 2015), increased H3K9me level (Nakazawa et al. 2012; Tamagawa et al. 2012), defect in DNA mismatch repair pathway (Kerr, D.J. & Midgley, R., 2010) and non-centromeric CENP-A localization (Tomonaga et al. 2003). Interestingly, in colon cancer cells ectopic CENP-A has been mapped at sub-telomeric sites (Athwal et al. 2015). Furthermore, HDAC inhibitors has been shown beneficial for the treatment of colorectal cancer (Barneda-Zahonero & Parra 2012; Chou et al. 2011; Kondo et al. 2003; Fang et al. 2004; He et al. 2013), possibly by promoting hyperacetylation environment. However, whether CENP-A non-centromeric localization could be the result of increased level of HMT and H3K9me has never been investigated in colon cancer. Here, using Drosophila model system, we present evidences which suggest possible link between raised HMT level, H3K9me and CENP-A miss-localization with potential impact on genome stability via cell chromosome segregation defects. It is possible that colon cancer cells which possess combination of DNA mismatch repair defect, increased HMT, H3K9me and non-centromeric CENP-A localization, altogether, creates tumour promoting environment. Our study, address the possible cause of CENP-A mislocalization observed in colorectal cancer, however this should be further investigated in cancer cells.

4 Materials

4.1 Chemicals Used in this study

All the chemicals used in this study were purchased from Roth, Applichem, Merck, Invitrogen/Life Technology (Invitrogen), Sigma Aldrich (Sigma) and Fluka. Details of the specific chemicals are in the table below:

Serial No.	Chemicals	Chemical provider
1	DAPI	AppliChem
2	EDTA	Roth
3	Formaldehyde 37%	AppliChem
4	Ethanol	AppliChem
5	2-Propanol	AppliChem
6	Methanol	ZMBH
7	Mounting medium- Aqua-Polymount	Poly Sciences
8	Milk Powder	AppliChem
9	Triton X-100	Merck
10	Tween 20	AppliChem
11	Trizol	Invitrogen
12	Tris	AppliChem
13	30% Acrylamide solution	AppliChem
14	Albumin Fraction V (pH 7.0)	Invitrogen
15	Phenol/Chloroform	AppliChem
16	Phenylmethylsulfonyl fluoride (PMSF)	Sigma
17	TEMED	AppliChem
18	Sodium tetraborate	Sigma
19	Sodium chloride	AppliChem
20	Sodium citrate	AppliChem

21	Sodiumdodecylsulphate (SDS)	AppliChem
22	Bromphenolblue	AppliChem
23	Protease inhibitor cocktail complete EDTA-free	Roche
24	NP-40	AppliChem
25	Agarose Ultra Pure	Invitrogen
26	Calcium Cloride	Fluka

4.2 Tissue culture reagents

Serial No.	Reagents	Company/Provider
1	Schneider's Drosophila medium	Invitrogen
2	Hygromycin B solution	Invitrogen
3	Fetal Bovine Serum (FBS)	Biochrom AG and Invitrogen
4	Colchemid	PAA
5	Cellfectin II	Invitrogen
6	Trichostatin A	Sigma-Aldrich
7	Methy methanesulfonate (MMS)	Sigma-Aldrich
8	$CuSo_4$	Applichem

4.3 Buffers/Solutions

Below are the details of all the buffers used in this study and all the buffer were prepared using double distilled water (ddH2O)

Serial No.	Buffer	Ingredients
	Buffers used in SDS-PAGE and Western Blot	
1	Separation gel (10.5%)	0.375 M Tris-HCl pH 8.8 10.5% acrylamide/bisacrylamide 30:0.8% 0.1% SDS 0.05% APS 0.05% TEMED

		in ddH2 O
2	Stacking gel	0.123 M Tris-HCl pH 6.8 4.4% acrylamide/bisacrylamide 30:0.8% 0.1% SDS 0.03% APS 0.1% TEMED in ddH2 O
3	4x Laemmli sample loading buffer	50 mM Tris-HCl pH 6.8 10% glycerol 2% SDS 0.5% ß-Mercaptoethanol 0.02% Bromphenolblue in ddH2 O
4	1x SDS gel running buffer	25 mM Tris 190 mM glycine 0.1% SDS in ddH2 O
5	Tris-glycine-methanol transfer buffer	25 mM TrisHCl 0.192 M glycine 20% methanol absolute in ddH2 O
6	20x Borate transfer buffer	20 mM Boric acid 1 mM EDTA 0.1 mM DTT pH 8.8 in ddH2 O
7	10x TBS	30 g/l Tris 88 g/l NaCl 2 g/l KCl pH 7.5 in ddH2 O
8	PBS buffer	137 mM NaCl 2.7 mM Kcl 10 mM Na2 HPO4 1.7 mM KH2 PO4 adjusted to pH 7.5 (HCl)
9	Blocking buffer	1x TBS/PBS 0.1% Tween-20 5% Milk powder
10	Washing buffer	1x TBS/PBS 0-0.1% Tween-20

11	Ponçeau	0.2% Ponçeau 3% TCA
12	Lysis buffer for whole cell extract	50 mM Tris pH 7.5 200 mM NaCl 1% Triton 0.5% Sodium dodecylsulfate 0.1% SDS 2 mM PMSF
13	Mild stripping buffer	15 g/l glycine 0.1% SDS 1% Tween-20 pH 2.2 in ddH2 O
	Acid Histone Extraction	
14	Triton Extraction Buffer	0.5% Triton X 100 (v/v) @mM PMSF, 0.02% $NaNa_3$
	Buffers and Solution used in Gel electrophoresis	
15	50x Tris-acetate-EDTA (TAE)	242 g/l Tris-HCl 18.6 g/l EDTA pH 7.7 adjusted with acetic acid in ddH2 O
	Immunofluorescence	
16	4% paraformaldehyde (PFA) PBS (50ml)	2g PFA 75.7µ l 1N KOH 45ml H2 O + 5ml 10X PBS
17	PBS premeabilization solution	1x PBS 0.1%/2 Triton X 100
18	PBS blocking solution	1x PBS 0.1% Triton X 100 5% Milk powder/5% BSA Fraction V
19	Metaphase spreads Hypotonic swelling solution	0.5 % (w/v) Sodium citrate in ddH2 O
	Immunoprecipitation	
20	Standard RIPA cell lysis buffer for whole cell extracts	50 mM TrisHCl (pH7.5) 150 mM NaCl 1% NP-40 0.5% Sodium dodecylsulfate 0.1% SDS 2 mM PMSF

21	Co-IP buffer/wash buffer	50 mM TrisHCl (pH 7.5) 200 mM NaCl 1% NP-40 2 mM PMSF Roche complete protease inhibitor cocktail
22	RIPA high salt IP buffer	50 mM TrisHCl (pH7.5) 250 mM NaCl 1% NP-40 0.5% Sodium dodecylsulfate 0.1% DOC 2 mM PMSF Roche complete protease inhibitor cocktail 10 mM Na-fluoride 1mM Na-orthovanadate 10 mM N-ethylmalemide

4.4 **Equipment and lab materials**

Serial No.	Equipment/Material/Tools	Provider/Company
1	Agarose gel trays	Workshop ZMBH
2	Balance	Sartorius, Kern EG
3	Blotting materials	BioRad
4	Deltavision microscope	Olympus/GE Healthcare
5	Film development system SRX-101A	Konica Minolta
6	Tabletop centrifuges	Eppendorf
7	Micropipettes	Gilson
8	PCR-cycler	Biorad
9	Vortex	Scientific industries
10	-80°C freezer	Heraeus
11	pH-meter	Sartorius
12	1.5 and 2 ml reaction tubes	Sarstedt
13	15 and 50 ml tubes	Sarstedt
14	0.2 ml PCR reaction tubes	Sarstedt
15	25 cm2 flask (cell culture)	Orange Scientific

16	75 cm2 flask (cell culture)	Orange Scientific
17	150 cm2 flask (cell culture)	Orange Scientific
18	FUJI Medical X-Ray Film	Fujifilm
19	Pipette tips	Sarstedt, TipOne, Avant Gμ ard
20	Superfrost® Plus Slides	Thermo Scientific
21	Protein gel equipment	Biorad
22	Coverslips (18 x 18 mm)	Thermo Scientific
23	Nitrocellulose membrane (0.45 μ m)	Amersham Biosciences
24	PVDF transfer membrane	GE Healthcare
25	UV stratalinker 2400	Stratagene
26	Power supplies	Biorad, EMBL PS143
27	Waterbath	Memmert
28	Microwave	Sharp
29	Micropipettes	Gilson
30	Whatman Paper	Roth
31	Shandon EZ MegafunnelTM	Thermo Scientific
32	Shandon EZ Double CytofunnelTM	Thermo Scientific
33	Bioruptor	

4.5 **Protease, Phosphate and HDAC inhibitors**

Details of the protease and phosphatase inhibitors. These inhibitors were used mainly in preparing samples for western blot or Immunoprecipitation

Serial No.	Inhbitors	Provider/Company
1	Aprotinin	AppliChem
2	Leupeptin	AppliChem
3	Pepstatin	AppliChem
4	PMSF	Sigma
5	NEM	Sigma
6	NaF	AppliChem
7	Protease inhibitors complete	Roche

8	Trichostatin A	Sigma

4.6 Primary and Secondary antibody

List of all the primary and secondary antibody used in western blot (WB) and Immunofluorescence (IF) for this study.

Serial No.	Antibody-reacts with	Dilution	Provider/Company
1	CID-anti rabbit	1:500 (for WB)	Active motif
2	H3K9me2-anti mouse	1:500 (for WB and IF)	Abcam
3	α-Tubulin-anti mouse	1:5000 (for WB) 1:1000 (for IF)	Sigma
4	Actin-anti mouse	1:5000 (for WB)	millipore MAB1501
5	H3K9acetylation-anti rabbit	1:1000 (for WB and IF)	abcam
6	H3K9me3-anti rabbit	1:1000 (for WB)	abcam
7	H3-anti rabbit	1:1000 (for WB)	abcam
8	CENP-C-anti Guinea pig	1:1000 (for IF)	Covance
9	Spc105-anti sheep	1:1000 (for WB)	David M. Glover
10	P55	1:5000 (for WB)	
11	Pan-acetyl Lysine-anti rabbit	1:1000 (for WB)	Stoecklin Lab
12	Histone H2AvD pS137-anti rabbit	1:500 (for WB and IF)	Rockland
13	V5-anti mouse	1:5000 (for WB and IF)	Invitrogen
14	YFP-anti rabbit	1:2500 (for WB)	Bukau Lab
15	CID	1:200 (for IF)	P.Heun
16	Alexa Fluor® 647 goat IgG-mouse	1:500 (for IF)	Invitrogen
17	Alexa Fluor®	1:500 (for IF)	Invitrogen

	647 goat IgG-anti rabbit		
18	Alexa Fluor® 647 goat IgG	1:500 (for IF)	Invitrogen
19	Alexa Fluor® 546 goat IgG-anti rabbit	1:500 (for IF)	Invitrogen
20	Alexa Fluor® 546 goat IgG-anti mouse	1:500 (for IF)	Invitrogen
21	Alexa Fluor® 546 goat IgG-anti chicken	1:500 (for IF)	Invitrogen
22	Alexa Fluor® 488 goat IgG-anti guinea pig	1:500 (for IF)	Invitrogen
23	Alexa Fluor® 488 goat IgG-anti rabbit	1:500 (for IF)	Invitrogen
24	Alexa Fluor® 488 goat IgG-anti mouse	1:500 (for IF)	Invitrogen

4.7 **Kits**

Serial No.	**Kits**	**Provider/Company**
1	NucleoBond PC 100	Macherey-Nagel
2	MEGAscript RNAi Kit	Ambion
3	RevertAidTM H Minus First Strand cDNA synthesis kit	Fermentas
4	Gel Extraction Kit	Fermentas
5	Plasmid Mini Kit	Fermentas
6	Invisorb Spin Plasmid Mini Two	Invisorb

4.8 **Plasmids and DNA vectors**

Name	**Source**
pMT-CID-V5-His	Matthias Spiller-Becker (Erhardt lab)
pCopia-Hygro	Erhardt et al, 2008
pCopia-LAP-CID	Erhardt et al, 2008
H2B-GFP	Goshima et al, 2007
mCherry Tubulin	Goshima et al, 2007

pMT-CHRAC14-V5-His	Mathew et al, 2014 (Erhardt lab)
pMT-CID S46A-V5-His	This Study
pMT-CID S46D-V5-His	This Study
pMT-Su(var)3-9-V5-His	This study

4.9 **Primers**

Details of primers used in this study for RT PCR, preparation of dsRNA, gene amplification and molecular cloning.

Primer Name	**Primer Sequence**
CID qPCR-fw	TCACCGAAGGCGCCCTATTGG
CID qPCR-rv	CTAAAATTGCCGACCCCGGTCGCAG
CHRAC14qPCR-Fw	AGACTTCGAAAGCTTCGTGCCC
CHRAC14qPCR-Rv	TCACTCGGGGGCTTCCTCTGCTG
ATM-T7-R	TAATACGACTCACTATAGGGGCGTTCTGCTGGAAGATG
ATM-T7-F	TAATACGACTCACTATAGGGGCTCATCCAAACTAGCGTAA
CID-S46Dmut_Fw	TCGAATTCACCACCGACCAACTGACGCTTCAGGA
CID-S46Dmut_Rv	TCCTGAAGCGTCAGTTGGTCGGTGGTGAATTCGA
CID S 46 A_ Fw	TCGAATTCACCACCGCCCAACTGACGCTTCAG
CID S 46 A_ Rv	CTGAAGCGTCAGTTGGGCGGTGGTGAATTCGA
NotI_Suv3-9_Fw	ATTTATTGGCGGCCGCATGGCCA
SacII_Suv3-9_Rv	GGGGCCGCGGAAAGAGGACCTTT
Ada2a_1_Fw	CTAATACGACTCACTATAGGGAGACCGCAATAACCACGC TTAC
Ada2a_1_Rv	CTAATACGACTCACTATAGGGAGACTCTCAGACGCCTCG TTGT
ADA2A_4RT_Fw	ACAACGAGGCGTCTGAGAGT
ADA2A_4RT_RV	AATTTGGCTCCGGAAAGAGT
ATM qPCR Fw	ACCACAGCAATCCGGTGAAG
ATM qPCR Rv	CCCGGAAAAAGCATGCAGAG
Su(var)3-9_mid_Fw	AGCATGCAAATCAAGCGGGCCCAATTTGTACG

T7-H2AV-FW T7-H2AV-RV	CTAATACGACTCACTATAGGGAGGAAGGGCAACGTCATTC TGT CTAATACGACTCACTATAGGGAGGTGAGTGTTGGGGAGAT GCT
Actin D Fw Actin D Rv	ATGTGTGACGAAGAAGTTGC AGGATCTTCATCAGGTAGTC
SpeI_Suv39_Fw NOTI_SUV39_RV	AAGGTACTAGTATGGCCACGGCTGAAGCCC AAAGCGGCCGCTAAAGAGGACCTTTCTGCAA
T7-WDS-Fw T7-WDS-Rv	TAATACGACTCACTATAGGGCAACTTGAGCGTATTATCCAG TAATACGACTCACTATAGGGATCAAAATCTGGGGAGCATA C
T7-Su(var)3-9-Fw T7-Su(var)3-9-Rv	TAATACGACTCACTATAGGGCAACGGCGCCTAGCAC TAATACGACTCACTATAGGGAGAGCCAGGCGAAAGAGC

4.10 **Drosophila stocks used for studies:**

Gene	Source	Genotype
CHRAC14	13190	y1 w67c23; P{SUPor-P}mus201KG01051 Chrac-14KG01051
ATM	8625(referred as $ATM3^{-/-}$)	w[*]; P{ry[+t7.2]=neoFRT}82B tefu[atm-3] e[1]/TM6B, Tb[1]
ATM	8626	w[*]; P{ry[+t7.2]=neoFRT}82B tefu[atm-6] e[1]/TM6B, Tb[1]
Oregon R	Erhardt Lab	+/+

5 Methods

5.1 Freezing and Thawing Drosophila S2 cells

5.1.1 Freezing S2 cells

Freshly transfected cells were allowed to grow in selection media for 4-6 weeks, later were frozen in aliquots as soon as possible at -80 °C or -196 °C. S2 cells were grown in 150 cm^2 flask. S2 cells were centrifuged for 5 minutes at 1500 rpm. S2 cell pallet was resuspended in to 45 % serum medium, 45 % conditioned medium (medium in which same cell line have been previously grown for a week) and 10% DMSO. DMSO serves as cryo-protectant. Cells were stored in 1ml aliquots in 2ml NUNC tubes and stored overnight into Mr. Freezer with fresh 2-propanol at -80°C. For term storage frozen cells can be later transferred from -80°C to -196 °C in liquid Nitrogen. This storage of cells is required for regular replacement of running stock of S2 cells after every 60 to 90 days.

5.1.2 Thawing S2 cells

Frozen S2 cells stocks were thawed when required. Thawing was done by quickly subjecting the frozen S2 cells to water bath at 30°C for short 1 to 2 minutes. Cells were immediately transferred to 25 cm^2 flask with 5ml fresh Serum medium. Cells were allowed to settle for 10 to 20 minutes and then medium was replaced with fresh 5 ml serum medium to get rid to DMSO. Freshly thawed S2 cells usually took 2 to 4 weeks to recover from freezing/thawing process and thereafter they were used for planned experiments.

5.2 Preparation of double stranded RNA

Gene of interest was amplified using genomic cDNA obtained from Oregon R flies as PCR template and amplification was analyzed on 1% agarose gel. Amplified gene was used to make dsRNA using reverse transcriptase from Ambion MEGAscript kit. Protocol provided by manufacturer was followed. Prepared dsRNA was aliquoted and frozen at -20°C.

5.3 RNA interference in S2 cells

RNA interference was used to knockdown the expression of gene of interest by introducing double stranded RNA (dsRNA) of 150 to 500bp. For this, 1.5-2.0 x 10^6 S2 cells were plated in six-well plate, were allowed to settle and grow for overnight with 2ml serum medium. Next day cells were washed thrice with serum free medium and further incubated for 1 hour with 20 µg dsRNA containing 1ml serum free medium (dsRNA specific to gene of interest). After 1hour incubation, 2ml of 15% of serum medium was added and cells were incubated for next 4days. After 4days cells were used for planned experiment and further analysis.

5.4 RNA isolation and RT PCR

RNA isolation was done to check the gene specific mRNA level via reverse transcriptase PCR. To achieve this, 5 x 10^6 S2 cells were harvested and centrifuged for 5minutes at 1000rpm at 4°C. Pallet obtained was resuspended in 1ml Trizol. Samples were incubated at room temperature for 5 minutes, then supplemented with 200µl $ChCl_3$/Phenol and incubated for 5minutes at room temperature. Samples were further mixed for 1minute, then incubated for 5minutes at room temperature and centrifuged for 10 minutes at 4°C with 12000rpm. Carefully aqueous phase was then taken and mixed with 500 µl isopropanol. This was followed by 10minutes incubation at room temperature which allows RNA to precipitate. Samples were centrifuged at 12000rpm for 10minutes at 4°C. Samples were then, washed with 75% ethanol and centrifuged at 12000rpm at 4°C for 10minutes. The pallet obtained was then allowed to dry and later resuspended in 30 µl double distilled H_2O. Later the isolated RNA concentration was measured by determining optical density (Nanodrop A260).

5.5 Transfection in S2 cells

Transfection of S2 cells with plasmids containing gene of interest was performed to make stable cell lines. In none of the cases, transient transfection was used for experiments. For stable transfection, 1.5 x 10^6 S2 cells were plated into six well plate with 2ml serum medium for overnight. Prior to transfection two solutions were prepared 1) 200µl serum free medium with 4µl Celfectin II and 2) 200µl serum

free medium with 5µg of DNA to be transfected (plasmid/s with gene of interest + pCopia-Hygro). Both the solutions were mixed and incubated for 30-45 minutes, thereafter 600µl serum free medium was added to make upto 1ml (transfection solution). S2 cells were thrice washed with fresh serum free medium and then incubated for 4hours with transfection solution (DNA, Celfectin II and serum free medium mixture). After which, 1ml of 20% serum medium was added to the cells and incubated for overnight. Next day, 1ml of 10% serum medium was added and cells were grown for next 3 to 4dyas. Following which 250µg/ml Hygromycin-B was added and cells were grown in the same plate for next 3-6 weeks depending upon their recovery rate and are continuously checked under white field microscope. Media was replaced every week and cells were throughout grown in Hygromycin-B containing medium. Expression of transfected gene/s was tested by western blot and further cells were frozen to keep stock and running cells were passaged 1-2 times every week.

5.6 **Immunofluorescence using S2 cells and Larvae tissues**

S2 cells were platted on positively charged glass slides and allowed to settle for 10-15 minutes. Cells were then fixed by subjecting to 4% PFA/PBS for 10minutes. Fixed cells were washed 3 times with PBS, each wash was done by 10minutes incubation at room temperature. Then cells were permeablized by treating them with 0.1% Triton for 10-15minutes, thereafter cells were blocked using 5%BSA-0.1% Triton-PBS for 30 minutes to get rid of unspecific binding. This was followed by overnight incubation with primary antibody solution (Primary Antibody-0.1%Triton-5%BSA in PBS) in moist chamber at 4°C. Primary incubation was followed by 3 times washes with PBS, then cells were incubated with secondary antibody solution (Secondary Antibody-0.1%Triton-5%BSA in PBS) for 1hour in dark. Cells were again washed 3 times with PBS which was then followed by 10minutes incubation with DAPI (1 µg/µl) in PBS, washed once with PBS. Further cells on slides were mounted with mounting medium (Aqua/polymount), covered with cover slip (1.5), allowed to dry completely and further stored at 4°C in dark moist chamber. Cells were imaged using Delta Vision(R) core system.

5.7 Metaphase spreads

Mitotic spreads were used to analyze localization of proteins at chromosome in metaphase. $2x10^5$ S2 cells were plated in six well plate and grown for overnight. Next day, cells were arrested in metaphase via 3.3 µg/ µl Colcemid (1:3 dilution) for 30-90 minutes. Cells were then centrifuged for 5-10minutes at 2000 rpm at 4°C. Subsequently cells were resuspended in 1ml hypotonic sodium citrate solution (0.5% $Na_3C_6H_5O_7$ in ddH_2O) and incubated for 7.5 minutes at room temperature, this makes them cells swelled. 500 µl of swelled cells were subjected to cytospin with 900 rpm, high acceleration for 10 minutes on positively charged slides. This was followed by fixing by 4% PFA/PBS for 10 minutes and then subjected to IF according to section 5.6.

5.8 Microscope and Imaging

Images were taken by Delta Vision (R) Core system (Applied Precision) microscope. Olympus UPlanSApo 100x and 60x objective (n.a. 1.4), 2x2 binning was used to acquire images (for IF and metaphase spreads). For live cell imaging, 60x objective was used. Images were taken as z-stacks, each z-stack ranging between 0.2-0.4µm thickness. If not mentioned specifically, all the images were deconvolved, maximum projected and threshold using the Applied Precisions soft WoRx 3.7.1 suite. Deconvolution was done using enhanced aggressive or conserved, 10 cycles and high noise filtering. Further the images were processes either by Applied Precisions softWoRx 3.7.1 suite or by ImageJ software.

5.9 Quantitative and Qualitative Analysis using ImageJ

Images taken by microscope were later analyzed by Image J software. Deconvoled and quick projected images (Images with ".dv.prj" extension) were opened in Image J software. If not mentioned, then all the cases only DAPI stained regions were taken into consideration for any kind of quantification. These regions were marked as region of interest (ROI) via ImageJ and further used as reference area for the channel of interest. The mean intensities of the signals in the selected regions were then calculated by adjusting the threshold of the intensities by default setting and by analyzing the mean intensities relative to the saved ROIs areas.

Foci/spot detection plugin was used for determining the number and the intensities of CENP-A, CENP-C and other centromeric/kinetochore proteins signals in DPAI regions marked as ROI. Spots in the ROI were enhanced using the DoG spot enhancer plugin. Thereafter threshold was adjusted using "Li". The numbers obtained by this approach were saved on Excel sheet and then the average of spots/nucleus (spot/DAPI) was taken into account for compiling average of three or more biological repeats. The final graph presented in results and appendix were plotted in Microsoft Excel. The statistical significance of the results was analyzed with the student T-test.

5.10 Sample preparation for western blot from S2 cells and adult flies

To analyze the protein levels in S2 cells from whole cell extract, 10^6- 10^7 cells were washed 2-3 times with PBS and resuspended in in RIPA buffer for 5-10minutes for lysis. Cells were later sonicated in Bioruptor (3-5 cycles with 30 sec sonication/30 sec break at level 5). Further, the lysed cells were mixed with 4x SDS laemmli loading buffer and boiled at 95°C for 5 minutes. Samples were either stored in -20°C or directly loading on 10-15% SDS PAGE gel for further analysis of proteins as per requirement of experiments.

To prepare sample from adult flies, flies were homogenized and lysed in 40 µl RIPA buffer using piston. Thereafter the lysate was subjected to sonication using Bioruptor (15 cycle, 30 sec sonication/30sec off at level 5). Lysate was later treated with Benzonase (125U). Thereafter mixed with 4x SDS laemmli buffer and boiled at 95°C for 10 minutes. Later samples were either stored at -20°C or directly loaded on 10-15% gel for protein analysis.

5.11 SDS PAGE and Western Blot

Protein levels were analyzed using western blot techniques and this requires Sodium dodecyl-sulfate (SDS) poly-acrylamide gel electrophoresis (PAGE). Samples were loaded on 8-15% SDS poly-acrylamide gel with Biorad Tetracell system and run at constant 100Volt for 1-1.5hours. Resolved proteins were then transferred to nitrocellulose membrane with 0.45µm thickness using transfer buffer (Tris-glycine-methanol) at constant 100Volt for 1-1.5hours at 4°C via Biorad wet-transfer system.

Transfer involved gel and nitrocellulose membrane sandwiched between Whatman paper (cathode, Whatman paper, gel, membrane, Whatman paper, anode). To check successful transfer, membrane was incubated with Ponceau for 10 minutes at room temperature. The membrane with successful protein transferred was washed 2-3 times with PBST (0.1% Tween-20 in PBS) and thereafter incubated with 5% skimmed dry milk in PBST to get rid of unspecific antibody binding. This was followed by overnight incubation with primary antibody at 4°C. Next day, membrane was washed 3 times with PBST, each wash 10 minutes to remove the residual primary antibody. Membrane was then incubated with secondary antibody for 1hour at room temperature with 5% skimmed dry milk in PBST. Later, secondary antibody was coupled with horseradish peroxidase (HRP). Membrane was later incubated with chemi-luminescence (HRP-ECL) solution for 1 to 3 minutes at room temperature. Membrane was exposed to Fuji X-ray medical film in dark and signals were detected by developed with Konica Minolta film developing machine.

5.12 **Co-Immunoprecipitation**

Co-immunoprecipitation was performed to see potential interaction between two or more proteins, atleast one of which was fused with V5 tag. V5 tag was used at bait to pulldown. This was achieved by cross-linking of V5-antibody to Agarose G beads from Roche. For this, Agarose G beads were washed 2-3 times with PBS. After washing, beads were mixed with V5 antibody (2µg/20µl of dry bead volume) in 250µl PBS and incubated at room temperature on rotating platform for 30 minutes. Beads were then washed twice with 0.2M sodium tetraborate pH 9. Afterward, bound antibody and beads were cross-linked by incubating with 5.2mg Dimethyl pimelimidate (DMP Sigma) mixed in 0.2M sodium tetraborate pH 9 PBS solution for 30 minutes at room temperature. This step was repeated. Cross-linked beads were centrifuged at 1000rpm 4°C, resuspended in 0.1M Glycine pH 7.0 and incubated for 30 minutes at room temperature, this quenches the reaction. Unbound antibody were removed my washing beads with 0.1M glycine pH2.5. Afterwards, either the antibody bound beads were stored in PBS supplemented with 0.02% sodium azide to prevent bacterial growth or directly used to for immunoprecipitation.

(Co)-Immunoprecipitation of V5-tagged proteins

For immunoprecipitation, S2 cells with pMT-protein-V5-His containing construct were induced with 1mM $CuSo_4$ for overnight. 1.5-2.0 x 10^8 S2 cells expressing V5-tagged proteins were washed with cold PBS and then lysed with Co-IP buffer (See section 5.3 Buffer/Solution, serial no. 21). Lysis buffer was supplemented with proteasome inhibitors. Cells were incubated with lysis buffer for 20 minutes at 4°C. Cells were then centrifuged for 30 minutes at 13000rpm. Supernatant was then transferred to precooled tube containing 20 µl of beads coupled with V5 antibody. Supernatant+beads were incubated at 4°C for 3-5hours on rotating platform. Beads were then collected by centrifugation, 1000rpm at 4°C. Thereafter beads were washed 6 times in 1o bed volume of lysis buffer. Proteins were eluted in 2 bed volume and then mixed with 2x SDS laemmili buffer. Followed by 5 minutes boiling at 95°C and separated by SDS-PAGE analyzed by western blot.

5.13 Denaturing Immunoprecipitation

Denaturing immunoprecipitation was performed to get rid of potential indirect interaction between the proteins. 1.5 x 10^8 S2 cells were supplemented with 20mM NEM and centrifuged at 3000rpm for 5minutes and the supernatant was discarded. Cells were washed with cold PBS and pallet was resuspended in 100µl 1x lysis buffer (denaturing, with 1% SDS). Lysate was sonicated using Bioruptor (10 cycles, 30sec sonication/30sec off at level 5). Further the lysates were supplemented with 50mM DTT. Samples were boiled at 97°C for 10minutes. Lysates were then diluted with cold RIPA buffer (1:10) and supplemented with 10mM NEM. Lysates were then centrifuged at 13000rpm at 4°C for 30minutes and later the supernatant were subjected to beads coupled with antibody as mentioned in section 5.12.

5.14 Nuclear Fractionation

For analysis of protein levels in nuclear and cytoplasmic compartment, S2 cells were subjected to nuclear fractionation. 10^6 -10^7 S2 cells were harvested and resuspended in RIPA lysis buffer with protease inhibitors for 10minutes on ice. Cells were then centrifuged at 13000rpm for 30 minutes at 4°C. Supernatant was kept as soluble fraction. Pallet was resuspended into same volume of lysis buffer+

Benzonase, later sonicated via Bioruptor (5 cycles, 30 sec sonication/ 30 sec off at level 5) and mixed with 4x SDS laemmli buffer. Samples were either stored in -20°C or directly loaded on 10-15% SDS.

5.15 **Acid histone extraction from S2 cells.**

4×10^6 S2 cells were subjected to lysis using Triton Extraction Buffer (TEB) (see 5.3 serial no. 14) for 10 minutes at 4°C with gentle stirring. Cells were then centrifuged at 2000 rpm for 10 minutes at 4°C. After removal of supernatant, cells pallet was washed once with TEB and centrifuged at 2000rpm at 4°C. Pallet was resuspended in 0.2N HCl at the density of 4×10^7 cells/ml and incubated at 4°C for overnight. Next day cells were subjected to centrifuged at 6600g for 10 minutes. Obtained supernatant was then mixed with 2x SDS laemmli buffer and boiled at 95°C for 5 minutes and then either stored at -20°C or directly analyzed via western blot using 15% SDS PAGE gel.

5.16 **Molecular cloning**

All the standard techniques were essentially performed as described in *Molecular cloning: A Laboratory Manual* by Sambrook and Russell.

6 Appendix

6.1 Tethering of Su(var)3-9 leads to CENP-A deposition

HP1 can interact with H3K9me and Su(var)3-9 (Schotta et al. 2002). Further, tethering of HP1 results in recruitment of CENP-A as seen via Lac-o/Lac-I system developed for S2 cells (Olszak et al. 2011). In order to probe whether Lac-I-Su(var)3-9-GFP tethering is involved in CENP-A recruitment at the site of Lac-O in S2 cells (Lac-O cells courtesy of Patrick Heuns's Lab), Lac-O/pMT-Lac-I-Su(var)3-9-GFP containing S2 cells were examined for CENP-A foci at GFP sites. The preliminary experiments suggest the presence of CENP-A spots in the vicinity of GFP (Figure 6.1). In contrary, the tethering of Lac-I-GFP did not show recruitment of CENP-A (Figure 6.1), indicating either that Su(var)3-9 tethering can facilitate CENP-A recruitment at the ectopic site or overexpression of Su(var)3-9 can lead to CENP-A deposition at Lac-O site. It is important to note that these are preliminary experiments and need to be repeated for a quantitative analysis.

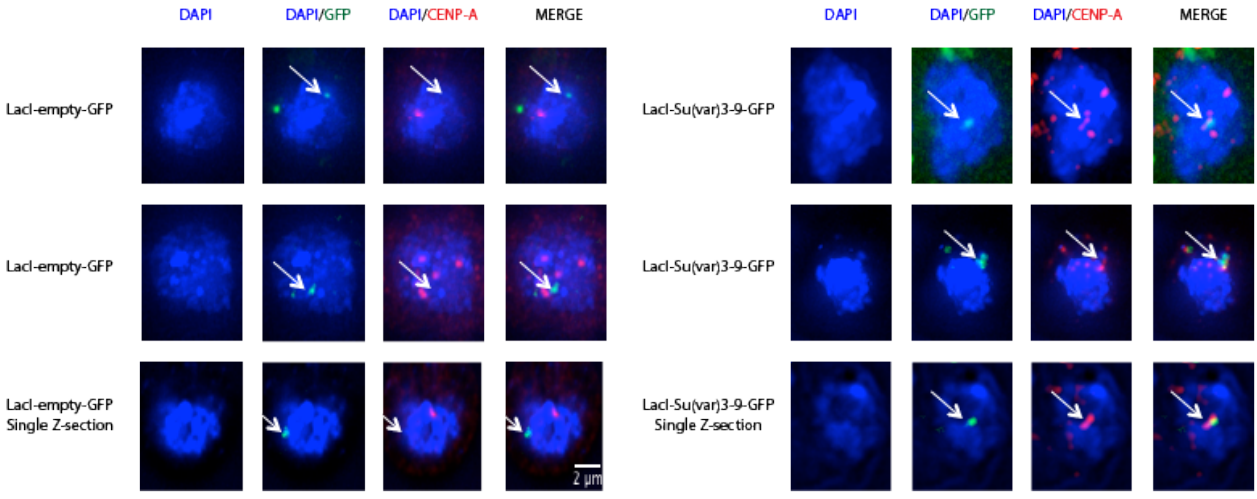

Figure 6.1: **Lac-I-Su(var)3-9-GFP expression causes CENP-A deposition at GFP sites.** Lac-O containing S2 cells were transfected with a control plasmid (pMT-Lac-I-empty-GFP) and pMT-Lac-I-Su(var)3-9-GFP. The cells were subjected to IF using GFP (green) and CENP-A (red) antibody and nuclei were co-stained with DAPI (blue). Cells with GFP foci were imaged. Upper two lanes of control and Lac-I-Su(var)3-9-GFP expressing cells represent quick projection of all the z-stacks. Lower panel represents single z-stack. Bar=2µm.

6.2 **Depletion of ADA2A leads to increase in CENP-A foci and H3K9me2**

Depletion of CHRAC16, which is another subunit of CHRAC complex, does not affect the CENP-A localization (unpublished data from Dr. Veena Mathew's work in our lab). I further examined whether ATAC complex specific subunit depletion could lead to a similar phenotype as CHRAC14 knockdown. For this purpose, I used ADA2A since it is only found in the ATAC complex. Knockdown of ADA2A in S2 cells showed increase in H3K9me2 (in accordance with Ciurciu et al. 2008) as seen in CHRAC14 depleted cells and also increased CENP-A foci as seen via IF (Figure 6.2 and 6.3), indicating the significance of the ATAC complex in maintaining heterochromatin structure and CENP-A localization.

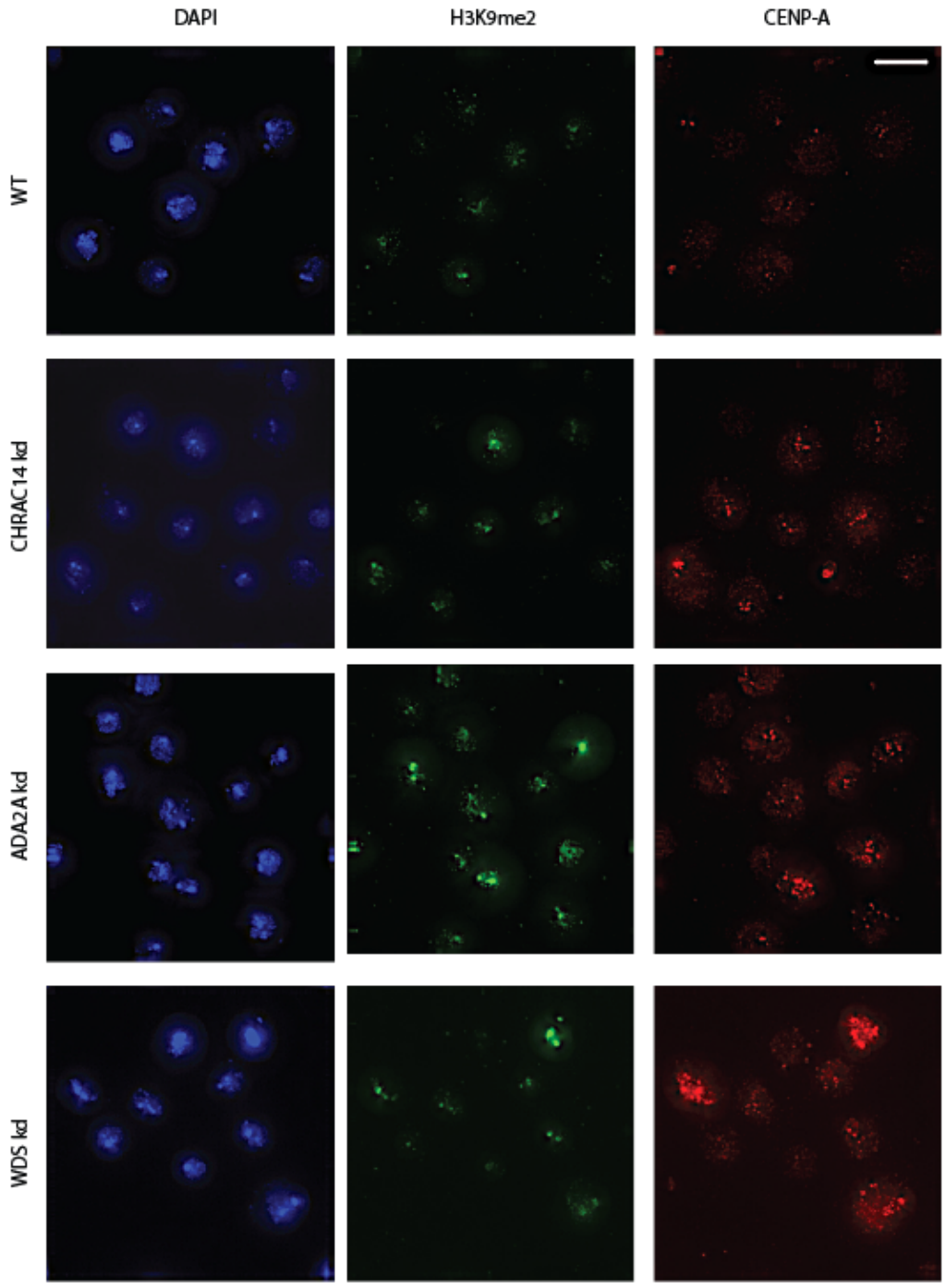

Figure 6.2: Depletion of ADA2A affects the H3K9me2 and CENP-A spots. CHRAC14, ADA2A and WDS RNAi treated S2 cells were subjected to IF using H3K9me2 (green) and CENP-A (red) antibody and nuclei were co-stained with DAPI. CHRAC14 RNAi (represented as CHRAC14 kd), ADA2A RNAi (represented as ADA2A kd), WDS RNAi (represented as WDS kd). Bar=5µm

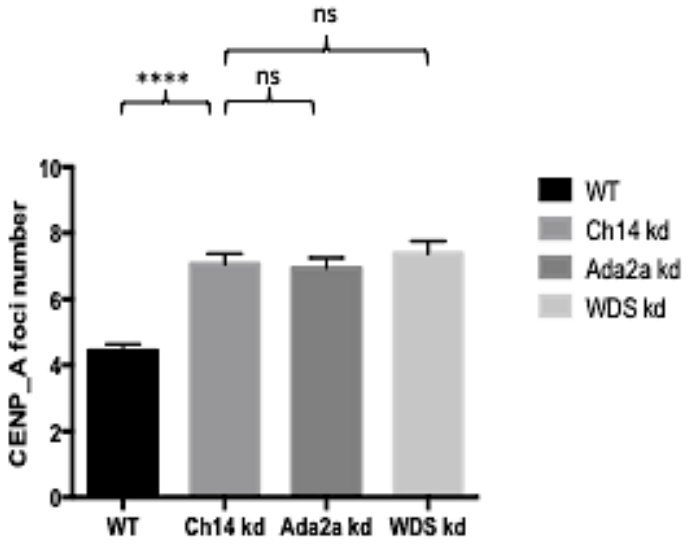

Figure 6.3: Lack of ATAC complex subunits increases the CENP-A foci number in S2 cells. Quantification of average CENP-A foci number count from the experiment shown in Figure 6.2. Total 50 cells/repeat were counted; bar represent average from 3 biological replicates. Error bars represent ±SEM and a p-value >0.05, ns=non-significant.

6.3 Effect of TSA on CENP-A localization in CENP-A overexpressing S2 cells

Overexpression of CENP-A leads to CENP-A ectopic loading and when analyzed by IF it is known that CENP-A localized throughout the chromatin or nucleus reflecting ectopic loading throughout the chromatin (Pauleau & Erhardt 2011; Heun et al. 2006). The HDAC inhibitor TSA is known to create hyperacetylated chromatin environment in Drosophila and mammalian cells (Foglietti et al. 2006; Taddei et al. 2001) Considering this I studied whether TSA would affect the CENP-A localization in CENP-A overexpressing cells.

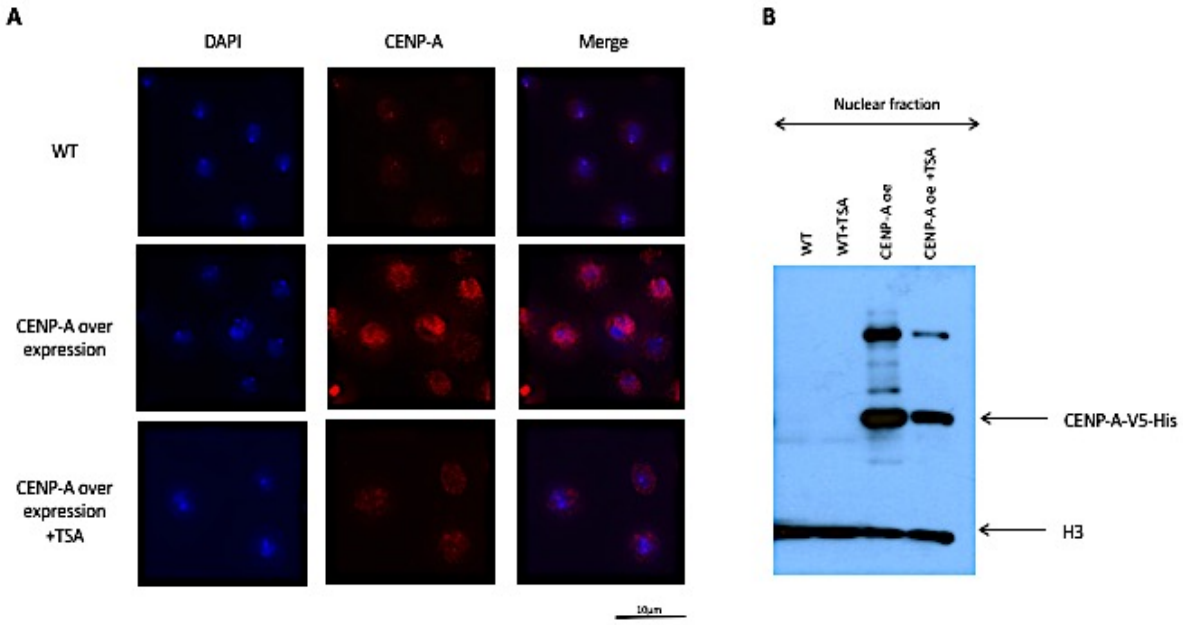

Figure 6.4: TSA affects the CENP-A nuclear localization in CENP-A overexpressing cells . **A)** S2 cells without CENP-A overexpression (WT) and with CENP-A overexpression (CENP-A oe) were subjected to IF. Additionally, CENP-Aoe cells treated with 0.5 µM TSA were subjected to IF. **B)** TSA treatment reduces the level of nuclear CENP-A in CENP-A overexpressing cells. Nuclear fractionation on S2 cells without expression of CENP-A-V5-His (WT) and with CENP-A-V5-His overexpression was performed. Additionally, the effect of 0.5 µM TSA treatment was analyzed. S2 cells after nuclear fractionation were analyzed via western blot using V5 antibody for detection of CENP-A-V5-His and Histone H3 antibody (loading control). Size bar= 10 µm

Cells with pMT-CENP-A-V5-His construct were incubated with 1mM $CuSO_4$ overnight for overexpression of CENP-A. Additionally, cells were treated with 0.5 µM TSA overnight. These cells were subjected to IF and later analyzed under a microscope. As expected, S2 cells with no CENP-A overexpression only showed a CENP-A signal at chromocenter (near bright DAPI region) (Figure 6.4 A). In contrast, CENP-A overexpressing cells showed a CENP-A signal throughout the nucleus or

DAPI stained region suggesting ectopic CENP-A localization (Figure 6.4 A). Furthermore, careful observation of TSA treatment of CENP-A overexpressing cells shows less CENP-A in DAPI region (Figure 6.4 A). This suggested that TSA treatment affects the localization of CENP-A. In other words, hyperacetylation is not favourable for CENP-A localization throughout the nucleus.

In order to further validate the above observations, CENP-A-V5-His overexpressing S2 cells with and without TSA were subjected to nuclear fractionation and later analyzed by immune blotting using V5 antibody. Control with no CENP-A-V5-His expression did not show any band, while cells induced with $CuSO_4$ show a high level of CENP-A-V5-His. Interestingly, the addition of TSA to these cells reduces the CENP-A-V5-His level in observed nucleus (Figure 6.4 B). Further stressing the idea that inhibition of HDAC/ hyperacetylation reduces the CENP-A nuclear localization.

6.4 Identifying interacting partner of CENP-A with and without DNA damage upon CENP-A overexpression

Ectopic loading of CENP-A can also be seen by CENP-A overexpression. DNA damage can enhance CENP-A ectopic localization to DNA damage sites (Mathew et al. 2014). To get the better understanding of the situation, I checked all the direct and indirect CENP-A interacting protein partners. This was achieved by immunoprecipitation of CENP-A using CENP-A overexpressing cells, with and without MMS induced DNA damage (0.4% MMS). The samples were analyzed using Mass Spectrometry and Proteomics at ZMBH core facilities. This provided several potential protein candidates that interact directly/indirectly with CENP-A/kinetochore in the mentioned condition of cells. Moreover, many interacting proteins also showed a change in protein level as detected by peptide hits. A list of the interacting proteins that resulted from mass spectrometry are in section 6.7 (for the complete list see Appendix 6.7). However, it should be noted that few of the known CENP-A interacting partners could not be detected, for example, CAL1, possibly because their interaction is transient or because its occurring in specific cell cycle phase/s. Nevertheless, many interesting interacting proteins were detected in two biological repeats and three independent mass spectrometry analysis are listed in table 1.3.

Few interesting potential interacting proteins	**Function/s**	**Control Protein coverage %(peptide count)**	**0.4% MMS. Protein coverage%(peptide count)**
Chromatin assembly factor 1 (p55)	Chromatin assembly, repression of genes (Anderson et al. 2011; Loyola et al. 2009)	6%(13)	6%(15)
Suppressor of variegation 3-7	Positive regulator of heterochromatin and gene silencing (Cléard & Spierer 2001)	6%(3)	6%(2)
Topoisomerase-2	Accession of DNA for transcription and replication machinery. Chromosome condensation (Soret et al. 2003).	3%(4)	2.3%(2)
Minichromosome maintenance complex component 5	DNA replication initiation and elongation (Forsburg 2004).	4.6%(3)	2.2%(1)
Histone-lysine N-methyltransferase trithorax	Methylates H3K4 and tags for transcription activation (Wang & Zhu 2008).	1.5%(3)	3.4%(5)
Ataxia telangiectasia mutated	Serine/threonine-protein kinase (Shiloh & Ziv 2013).	1.8%(4)	3.3%(4)
Zeste White 10	Kinetochore protein, essential for mitotic checkpoint (Karess 2005).	4.6%(1)	7.6%(3)

Table 1.3: Interesting CENP-A interacting proteins obtained in mass spectrometry analysis. The table represents selected interacting proteins detected in mass spectrometry approach. CAF1(p55), Top-2 and ZW10 have been reported previously by other members in the lab. Su(var)3-7, ATM, MCM5 and TXR were few of the potentially interesting interacting proteins. The candidates presented in table are found in two or more independent mass spectrometry analysis from two biological repeats. Protein peptide counts and protein coverage numbers are presented from one analysis, however were detected in two or more independent mass spectrometry analyses from two biological replicates.

6.5 Effect of ATM depletion on CENP-A

Results from mass spectrometry revealed ATM as one of the potential interacting partners of CENP-A. Following the mass spectrometry results, I checked whether ATM depletion has any effect on CENP-A. Knockdown of ATM in S2 cells upon addition of MMS shows increased CENP-A levels as seen via western blot (Figure 6.5). However, caffeine treatment of S2 cells shows increased CENP-A level without any DNA damaging agent. This was further checked in ATM mutant Drosophila flies,

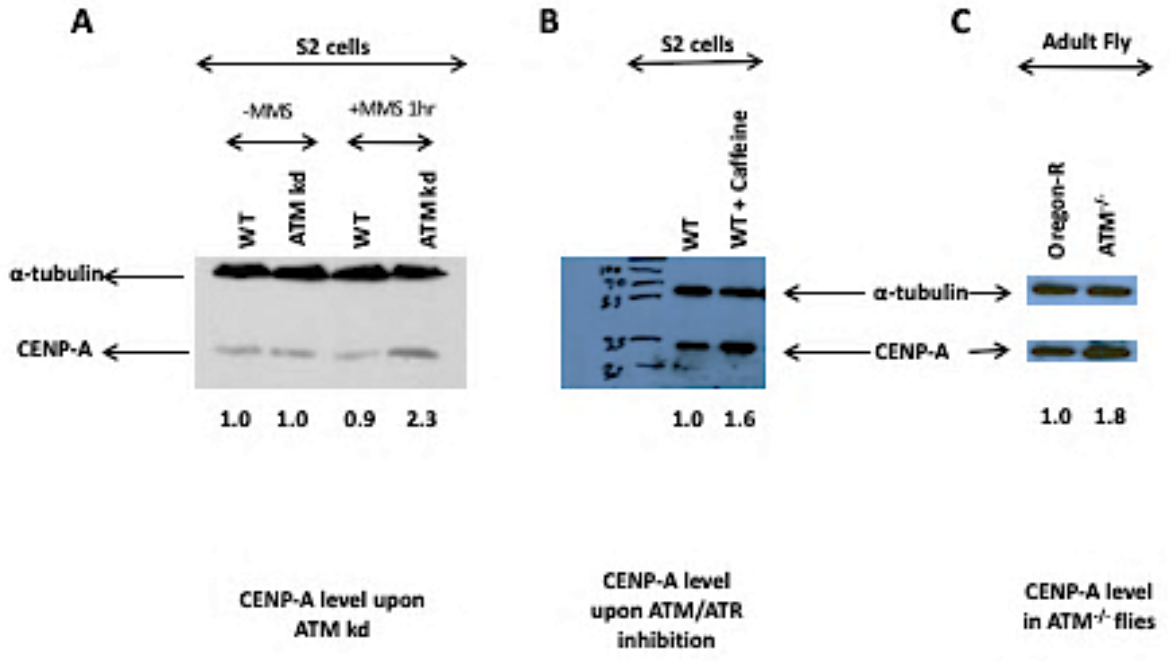

Figure 6.5: Absence of ATM elevates the level of CENP-A. A) S2 cells after 4 days treatment with ATM RNAi were treated with 0.4% MMS for 1 hour and then analyzed by western blot using anti-Tubulin (loading control) and CENP-A. ATM depletion increases CENP-A level upon MMS treatment. **B)** S2 cells were treated with Caffeine and later analyzed via western blot using Tubulin (loading control) and CENP-A antibody. **C)** Whole adult fly lysate from Oregon-R and $ATM^{-/-}$ were subjected to western blot and analyzed using Tubulin and CENP-A antibody. $ATM^{-/-}$ flies show increase in CENP-A level.

the results of which suggests an increase in the level of CENP-A in ATM mutant Drosophila fly.

6.6 List of CENP-A interacting proteins detected by mass spectrometry in presence/absence of DNA damage

To identify CENP-A interacting proteins with and without genotoxic stress (0.4% MMS 1 hour treatment), CENP-A-V5-His overexpressing cells were subjected to Immunoprecipitation with a V5 antibody and samples were then further analysed by Mass Spectrometry and Proteomics ZMBH core facilities. Below is the list of few interesting proteins (82 out of 357) sorted by unique peptide counts, found in one of the mass spectrometry analysis. Proteins presented in the list are related to transcription, replication, phosphorylation, acetylation, chromatin remodelling and DNA damage repair and could be potential player/s in regulation and maintenance of CENP-A in Drosophila cells.

Identified Proteins (82)	Accession Number	Molecular Weight	Peptide count No MMS	Peptide count 0.4% MMS
14-3-3 protein epsilon OS=Drosophila melanogaster GN=14-3-3epsilon PE=1 SV=2	1433E_DROME	30 kDa	3	2
14-3-3 protein zeta OS=Drosophila melanogaster GN=14-3-3zeta PE=1 SV=1	1433Z_DROME	28 kDa	3	2
Serine/threonine-protein phosphatase PP2A 65 kDa regulatory subunit OS=Drosophila melanogaster	2AAA_DROME	65 kDa	3	4
Protein argonaute-2 OS=Drosophila melanogaster GN=AGO2 PE=1 SV=3	AGO2_DROME	137 kDa	53	55
Serine/threonine-protein kinase ATM OS=Drosophila melanogaster GN=tefu PE=2 SV=1	ATM_DROME	318 kDa	2	1
Serine/threonine-protein kinase ATR OS=Drosophila melanogaster GN=mei-41 PE=1 SV=2	ATR_DROME	289 kDa	0	2
Ataxin-2 homolog OS=Drosophila melanogaster GN=Atx2 PE=1 SV=1	ATX2_DROME	118 kDa	7	4
Probable histone-binding protein Caf1 OS=Drosophila melanogaster GN=Caf1 PE=1 SV=1	CAF1_DROME	49 kDa	13	15
Chromodomain-helicase-DNA-binding protein Mi-2 homolog OS=Drosophila melanogaster GN=Mi-2 PE=1 SV=2	CHDM_DROME	224 kDa	2	2

Histone H3-like centromeric protein cid OS=Drosophila melanogaster GN=cid PE=1 SV=2	CID_DROME	26 kDa	3	2
ATP-dependent RNA helicase p62 OS=Drosophila melanogaster GN=Rm62 PE=1 SV=3	DDX17_DROME	79 kDa	11	12
ATP-dependent RNA helicase bel OS=Drosophila melanogaster GN=bel PE=1 SV=1	DDX3_DROME	85 kDa	35	28
Elongation factor 1-alpha 1 OS=Drosophila melanogaster GN=Ef1alpha48D PE=1 SV=2	EF1A1_DROME	50 kDa	20	19
Probable elongation factor 1-beta OS=Drosophila melanogaster GN=Ef1beta PE=1 SV=3	EF1B_DROME	24 kDa	2	0
Probable elongation factor 1-delta OS=Drosophila melanogaster GN=eEF1delta PE=1 SV=1	EF1D_DROME	29 kDa	1	2
Elongation factor 1-gamma OS=Drosophila melanogaster GN=Ef1gamma PE=2 SV=2	EF1G_DROME	49 kDa	5	6
Elongation factor 2 OS=Drosophila melanogaster GN=Ef2b PE=1 SV=4	EF2_DROME	94 kDa	21	23
Eukaryotic translation initiation factor 3 subunit D-1 OS=Drosophila virilis GN=eIF-3p66 PE=3 SV=1	EI3D1_DROVI	64 kDa	4	0
Eukaryotic translation initiation factor 3 subunit A OS=Drosophila melanogaster GN=eIF3-S10 PE=1 SV=1	EIF3A_DROME	134 kDa	6	11
Eukaryotic translation initiation factor 3 subunit B OS=Drosophila virilis GN=eIF3-S9 PE=3 SV=1	EIF3B_DROVI	80 kDa	2	1
Eukaryotic translation initiation factor 3 subunit C OS=Drosophila erecta GN=eIF3-S8 PE=3 SV=1	EIF3C_DROER	106 kDa	9	4
Eukaryotic translation initiation factor 3 subunit L OS=Drosophila mojavensis GN=GI12903 PE=3 SV=1	EIF3L_DROMO	63 kDa	2	1
Putative elongator complex protein 1 OS=Drosophila melanogaster GN=Elp1 PE=1 SV=2	ELP1_DROME	143 kDa	1	2
Probable ubiquitin carboxyl-terminal hydrolase FAF OS=Drosophila melanogaster GN=faf PE=1 SV=2	FAF_DROME	311 kDa	2	1
Cadherin-related tumor suppressor OS=Drosophila melanogaster GN=ft PE=1 SV=3	FAT_DROME	565 kDa	2	1

WD repeat-containing and planar cell polarity effector protein fritz OS=Drosophila melanogaster GN=frtz PE=2 SV=1	FRITZ_DROME	106 kDa	2	0
Zinc finger protein hangover OS=Drosophila melanogaster GN=hang PE=1 SV=3	HANG_DROME	210 kDa	2	1
E3 ubiquitin-protein ligase highwire OS=Drosophila melanogaster GN=hiw PE=1 SV=2	HIW_DROME	566 kDa	3	3
Protein hu-li tai shao OS=Drosophila melanogaster GN=hts PE=1 SV=2	HTS_DROME	128 kDa	21	24
E3 ubiquitin-protein ligase hyd OS=Drosophila melanogaster GN=hyd PE=1 SV=3	HYD_DROME	319 kDa	2	1
Eukaryotic translation initiation factor 2 subunit 1 OS=Drosophila melanogaster GN=eIF-2alpha PE=2 SV=1	IF2A_DROME	39 kDa	2	1
Eukaryotic translation initiation factor 2 subunit 2 OS=Drosophila melanogaster GN=eIF-2beta PE=1 SV=1	IF2B_DROME	35 kDa	2	1
Eukaryotic translation initiation factor 2 subunit 3 OS=Drosophila melanogaster GN=eIF-2gamma PE=2 SV=1	IF2G_DROME	51 kDa	0	2
Eukaryotic initiation factor 4A OS=Drosophila melanogaster GN=eIF-4a PE=1 SV=3	IF4A_DROME	46 kDa	4	7
Inhibitor of nuclear factor kappa-B kinase subunit beta OS=Drosophila melanogaster GN=ird5 PE=1 SV=2	IKKB_DROME	86 kDa	4	3
Importin subunit alpha OS=Drosophila melanogaster GN=Pen PE=1 SV=2	IMA_DROME	58 kDa	2	1
Inositol-3-phosphate synthase OS=Drosophila melanogaster GN=Inos PE=1 SV=1	INO1_DROME	62 kDa	7	4
Arginine kinase OS=Drosophila melanogaster GN=Argk PE=2 SV=2	KARG_DROME	40 kDa	3	5
Kinesin-like protein Klp10A OS=Drosophila melanogaster GN=Klp10A PE=1 SV=1	KI10A_DROME	89 kDa	3	4
Pyruvate kinase OS=Drosophila melanogaster GN=PyK PE=2 SV=2	KPYK_DROME	57 kDa	6	7
Lamin Dm0 OS=Drosophila melanogaster GN=Lam PE=1 SV=4	LAM0_DROME	71 kDa	1	2

RNA-binding protein lark OS=Drosophila melanogaster GN=lark PE=1 SV=1	LARK_DROME	40 kDa	3	2
DNA replication licensing factor Mcm5 OS=Drosophila melanogaster GN=Mcm5 PE=1 SV=1	MCM5_DROME	82 kDa	2	1
Mediator of RNA polymerase II transcription subunit 12 OS=Drosophila melanogaster GN=kto PE=1 SV=2	MED12_DROME	279 kDa	5	1
Mediator of RNA polymerase II transcription subunit 13 OS=Drosophila melanogaster GN=skd PE=1 SV=1	MED13_DROME	280 kDa	5	2
Mediator of RNA polymerase II transcription subunit 14 OS=Drosophila melanogaster GN=MED14 PE=1 SV=4	MED14_DROME	172 kDa	2	1
Mediator of RNA polymerase II transcription subunit 15 OS=Drosophila melanogaster GN=MED15 PE=2 SV=1	MED15_DROME	81 kDa	4	3
Mediator of RNA polymerase II transcription subunit 16 OS=Drosophila melanogaster GN=MED16 PE=1 SV=2	MED16_DROME	90 kDa	1	2
Mediator of RNA polymerase II transcription subunit 17 OS=Drosophila melanogaster GN=MED17 PE=1 SV=1	MED17_DROME	72 kDa	4	1
Mediator of RNA polymerase II transcription subunit 23 OS=Drosophila melanogaster GN=MED23 PE=1 SV=1	MED23_DROME	167 kDa	2	2
Mediator of RNA polymerase II transcription subunit 25 OS=Drosophila melanogaster GN=MED25 PE=2 SV=1	MED25_DROME	97 kDa	2	1
Mediator of RNA polymerase II transcription subunit 26 OS=Drosophila melanogaster GN=MED26 PE=1 SV=2	MED26_DROME	166 kDa	1	2
Mediator of RNA polymerase II transcription subunit 26 OS=Drosophila p	MED26_DROPS	178 kDa	2	1
Mediator of RNA polymerase II transcription subunit 27 OS=Drosophila melanogaster GN=MED27 PE=1 SV=1	MED27_DROME	34 kDa	1	2
DNA mismatch repair protein spellchecker 1 OS=Drosophila melanogaster GN=spel1 PE=3 SV=4	MSH2_DROME	103 kDa	1	2
Probable DNA mismatch repair protein Msh6 OS=Drosophila melanogaster GN=Msh6 PE=1 SV=2	MSH6_DROME	133 kDa	0	2
Methyltransferase-like protein 13 OS=Drosophila pseudoobscura	MTE13_DROPS	76 kDa	2	0

pseudoobscura GN=GA15401 PE=3 SV=1				
Zinc finger protein on ecdysone puffs OS=Drosophila melanogaster GN=Pep PE=1 SV=1	PEP_DROME	78 kDa	5	4
Serine/threonine-protein kinase N OS=Drosophila melanogaster GN=Pkn PE=1 SV=1	PKN_DROME	132 kDa	0	2
Serine/threonine-protein kinase polo OS=Drosophila melanogaster GN=polo PE=1 SV=2	POLO_DROME	67 kDa	2	2
Serine/threonine-protein phosphatase alpha-2 isoform OS=Drosophila melanogaster GN=Pp1-87B PE=1 SV=1	PP12_DROME	35 kDa	1	2
Regulator of nonsense transcripts 1 homolog OS=Drosophila melanogaster GN=Upf1 PE=1 SV=2	RENT1_DROME	130 kDa	4	6
Replication protein A 70 kDa DNA-binding subunit OS=Drosophila melanogaster GN=RpA-70 PE=1 SV=1	RFA1_DROME	67 kDa	4	0
Regulator of telomere elongation helicase 1 homolog OS=Drosophila virilis GN=GJ16649 PE=3 SV=1	RTEL1_DROVI	112 kDa	1	2
Transcription elongation factor SPT5 OS=Drosophila melanogaster GN=Spt5 PE=1 SV=1	SPT5H_DROME	119 kDa	1	2
Transcription elongation factor SPT6 OS=Drosophila melanogaster GN=Spt6 PE=1 SV=1	SPT6H_DROME	209 kDa	2	1
Serine-arginine protein 55 OS=Drosophila melanogaster GN=B52 PE=1 SV=4	SRR55_DROME	43 kDa	1	2
Protein suppressor of variegation 3-7 OS=Drosophila melanogaster GN=Su(var)3-7 PE=1 SV=4	SUV37_DROME	140 kDa	2	1
Polycomb protein Su(z)12 OS=Drosophila melanogaster GN=Su(z)12 PE=1 SV=1	SUZ12_DROME	100 kDa	0	2
Alanine--tRNA ligase, cytoplasmic OS=Drosophila melanogaster GN=Aats-ala PE=2 SV=1	SYAC_DROME	108 kDa	9	8
Probable glutamine--tRNA ligase OS=Drosophila melanogaster GN=Aats-gln PE=1 SV=1	SYQ_DROME	88 kDa	2	2
Probable arginine--tRNA ligase, cytoplasmic OS=Drosophila melanogaster GN=Aats-arg PE=2 SV=1	SYRC_DROME	76 kDa	2	1

General transcription factor IIH subunit 1 OS=Drosophila melanogaster GN=Tfb1 PE=2 SV=1	TF2H1_DROME	66 kDa	1	2
DNA topoisomerase 2 OS=Drosophila melanogaster GN=Top2 PE=1 SV=1	TOP2_DROME	164 kDa	4	1
Histone-lysine N-methyltransferase trithorax OS=Drosophila virilis GN=trx PE=3 SV=1	TRX_DROVI	414 kDa	2	1
Transcription termination factor 2 OS=Drosophila melanogaster GN=lds PE=1 SV=2	TTF2_DROME	118 kDa	3	1
E3 UFM1-protein ligase 1 homolog OS=Drosophila melanogaster GN=CG1104 PE=1 SV=1	UFL1_DROME	87 kDa	2	1
WD repeat-containing protein on Y chromosome OS=Drosophila virilis GN=WDY PE=4 SV=1	WDY_DROVI	133 kDa	2	1
5'-3' exoribonuclease 2 homolog OS=Drosophila melanogaster GN=Rat1 PE=1 SV=2	XRN2_DROME	104 kDa	10	6
Zinc finger protein CG2199 OS=Drosophila melanogaster GN=CG2199 PE=1 SV=1	Y2199_DROME	82 kDa	2	2
Zinc finger protein 423 homolog OS=Drosophila melanogaster GN=Oaz PE=2 SV=2	ZN423_DROME	134 kDa	0	2
Centromere/kinetochore protein zw10 OS=Drosophila melanogaster GN=mit(1)15 PE=1 SV=2	ZW10_DROME	82 kDa	0	2

7 References

Aagaard, L. et al., 1999. Functional mammalian homologues of the Drosophila PEV-modifier Su(var)3-9 encode centromere-associated proteins which complex with the heterochromatin component M31. *The EMBO journal*, 18(7), pp.1923–1938.

Al-Sady, B., Madhani, H.D. & Narlikar, G.J., 2013. Division of labor between the chromodomains of HP1 and Suv39 methylase enables coordination of heterochromatin spread. *Molecular Cell*, 51(1), pp.80–91.

ALLFREY, V.G., FAULKNER, R. & MIRSKY, A.E., 1964. Acetylation and Methylation of Histones and Their Possible Role in the Regulation of Rna Synthesis. *Proceedings of the National Academy of Sciences of the United States of America*, 51(1938), pp.786–94.

Anderson, A.E. et al., 2011. The enhancer of trithorax and polycomb gene Caf1/p55 is essential for cell survival and patterning in Drosophila development. *Development (Cambridge, England)*, 138(10), pp.1957–66.

Andreyeva, E.N. et al., 2007. High-resolution analysis of Drosophila heterochromatin organization using SuUR Su(var)3-9 double mutants. *Proceedings of the National Academy of Sciences of the United States of America*, 104(31), pp.12819–12824.

Athwal, R. et al., 2015. CENP-A nucleosomes localize to transcription factor hotspots and subtelomeric sites in human cancer cells. *Epigenetics & Chromatin*, 8(1), p.2.

Audergon, P.N.C.B. et al., 2015. Epigenetics. Restricted epigenetic inheritance of H3K9 methylation. *Science (New York, NY)*, 348(6230).

Bade, D. et al., 2014. The E3 Ligase CUL3/RDX Controls Centromere Maintenance by Ubiquitylating and Stabilizing CENP-A in a CAL1-Dependent Manner. *Developmental Cell*, 28(5), pp.508–519.

Bailey, A.O. et al., 2015. Identification of the posttranslational modifications present in centromeric chromatin. *Molecular & cellular proteomics : MCP*, p.M115.053710-.

Bailey, A.O. et al., 2013. Posttranslational modification of CENP-A influences the conformation of centromeric chromatin. *Proceedings of the National Academy of Sciences of the United States of America*, 110(29), pp.11827–32.

Bannister, A.J. & Kouzarides, T., 2011. Regulation of chromatin by histone modifications. *Cell research*, 21(3), pp.381–395.

Barneda-Zahonero, B. & Parra, M., 2012. Histone deacetylases and cancer. *Molecular Oncology*, 6(6), pp.579–589.

Bassett, E.A. et al., 2012. HJURP Uses Distinct CENP-A Surfaces to Recognize and to Stabilize CENP-A/Histone H4 for Centromere Assembly. *Developmental Cell*, 22(4), pp.749–762.

Bednar, J. et al., 1998. Nucleosomes, linker DNA, and linker histone form a unique structural motif that directs the higher-order folding and compaction of chromatin. *Proceedings of the National Academy of Sciences of the United States of America*, 95(24), pp.14173–8.

Beisel, C. et al., 2002. Histone methylation by the Drosophila epigenetic transcriptional regulator Ash1. *Nature*, pp.1–7.

Bell, O. et al., 2007. Localized H3K36 methylation states define histone elongation in Drosophila. *Embo J*, 26(24), pp.4974–4984.

Bergmann, J.H. et al., 2011. Epigenetic engineering shows H3K4me2 is required for HJURP targeting and CENP-A assembly on a synthetic human kinetochore. *The EMBO journal*, 30(2), pp.328–340.

Biterge, B., 2016. A Mini Review on Post-Translational Histone Modifications. *MOJ Cell Science & Report*, 3(1), pp.1–4.

Black, B.E. et al., 2007. Centromere Identity Maintained by Nucleosomes Assembled with Histone H3 Containing the CENP-A Targeting Domain. *Molecular Cell*, 25(2), pp.309–322.

Black, J.C., Van Rechem, C. & Whetstine, J.R., 2012. Histone Lysine Methylation Dynamics: Establishment, Regulation, and Biological Impact. *Molecular Cell*, 48(4), pp.491–507.

Blattes, R. et al., 2006. Displacement of D1, HP1 and topoisomerase II from satellite heterochromatin by a specific polyamide. *The EMBO journal*, 25(11), pp.2397–2408.

Blower, M.D., Sullivan, B.A. & Karpen, G.H., 2002. Conserved organization of centromeric chromatin in flies and humans. *Developmental Cell*, 2(3), pp.319–330.

Bodor, D.L. et al., 2014. The quantitative architecture of centromeric chromatin. *eLife*, 2014(3), pp.1–26.

Boltengagen, M. et al., 2015. A novel role for the histone acetyltransferase Hat1 in the CENP-A/CID assembly pathway in Drosophila melanogaster. *Nucleic Acids Research*, 44(5), pp.2145–2159.

Brownell, J.E. et al., 1996. Tetrahymena histone acetyltransferase A: A homolog to yeast Gcn5p linking histone acetylation to gene activation. *Cell*, 84(6), pp.843–851.

Bui, M. et al., 2012. Cell-cycle-dependent structural transitions in the human CENP-A nucleosome in vivo. *Cell*, 150(2), pp.317–326.

Burgess, R.J. & Zhang, Z., 2014. Histone chaperones in nucleosome assembly and human disease. *Nat Struct Mol Biol.*, 20(1), pp.14–22.

Capuano, F. et al., 2014. Cytosine DNA methylation is found in drosophila melanogaster but absent in saccharomyces cerevisiae, schizosaccharomyces pombe, and other yeast species. *Analytical Chemistry*, 86(8), pp.3697–3702.

Carrozza, M.J. et al., 2003. The diverse functions of histone acetyltransferase complexes. *Trends in Genetics*, 19(6), pp.321–329.

Chan, F.L. et al., 2012. Active transcription and essential role of RNA polymerase II at the centromere during mitosis. *Proceedings of the National Academy of Sciences*, 109(6), pp.1979–1984.

Cheeseman, I.M. et al., 2006. The Conserved KMN Network Constitutes the Core Microtubule-Binding Site of the Kinetochore. *Cell*, 127(5), pp.983–997.

Chen, X. et al., 2012. G9a/GLP-dependent histone H3K9me2 patterning during human hematopoietic stem cell lineage commitment. *Genes & Development*, 26(22), pp.2499–2511.

Chin, H.G. et al., 2007. Automethylation of G9a and its implication in wider substrate specificity and HP1 binding. *Nucleic Acids Research*, 35(21), pp.7313–7323.

Chiolo, I. et al., 2011. Double-strand breaks in heterochromatin move outside of a dynamic HP1a domain to complete recombinational repair. *Cell*, 144(5), pp.732–744.

Cho, Y. et al., 2005. Individual histone deacetylases in Drosophila modulate transcription of distinct genes. *Genomics*, 86(5), pp.606–617.

Chou, C.W. et al., 2011. HDAC inhibition decreases the expression of EGFR in colorectal cancer cells. *PLoS ONE*, 6(3), pp.1–12.

Ciurciu, A., Komonyi, O. & Boros, I.M., 2008. Loss of ATAC-specific acetylation of histone H4 at Lys12 reduces binding of JIL-1 to chromatin and phosphorylation of histone H3 at Ser10. *Journal of cell science*, 121(Pt 20), pp.3366–3372.

Clapier, C.R. & Cairns, B.R., 2009. The biology of chromatin remodeling complexes. *Annual review of biochemistry*, 78, pp.273–304.

Cléard, F. & Spierer, P., 2001. Position-effect variegation in Drosophila: The modifier Su(var)3-7 is a modular DNA-binding protein. *EMBO Reports*, 2(12), pp.1095–1100.

Collins, N. et al., 2002. An ACF1-ISWI chromatin-remodeling complex is required for DNA replication through heterochromatin. *Nature genetics*, 32(4), pp.627–632.

Corona, D.F. et al., 2000. Two histone fold proteins, CHRAC-14 and CHRAC-16, are developmentally regulated subunits of chromatin accessibility complex (CHRAC). *The EMBO journal*, 19(12), pp.3049–3059.

Czermin, B. et al., 2001. Physical and functional association of SU (VAR) 3-9 and HDAC1 in Drosophila. *EMBO Reports*, 2(10), pp.915–919.

Dang, W., Kagalwala, M.N. & Bartholomew, B., 2007. The Dpb4 subunit of ISW2 is anchored to extranucleosomal DNA. *Journal of Biological Chemistry*, 282(27), pp.19418–19425.

Das, C. et al., 2009. CBP/p300-mediated acetylation of histone H3 on lysine 56. *Nature*, 459(7243), pp.113–117. Available at: http://dx.doi.org/10.1038/nature07861.

Dillon, S.C. et al., 2005. The SET-domain protein superfamily: protein lysine methyltransferases. *Genome biology*, 6(8), p.227.

Dinant, C., Houtsmuller, A.B. & Vermeulen, W., 2008. Chromatin structure and DNA damage repair. *Epigenetics & chromatin*, 1(1), p.9.

Du, J. et al., 2015. DNA methylation pathways and their crosstalk with histone methylation. *Nature Reviews Molecular Cell Biology*, 16(9), pp.519–532.

Dunleavy, E.M. et al., 2009. HJURP Is a Cell-Cycle-Dependent Maintenance and Deposition Factor of CENP-A at Centromeres. *Cell*, 137(3), pp.485–497.

Dunleavy, E.M., Zhang, W. & Karpen, G.H., 2013. Solo or doppio: how many CENP-As make a centromeric nucleosome? *Nature Structural {&} Molecular Biology*, 20(6), pp.648–650.

E. Vamos, E. & Boros, I.M., 2012. The C-terminal domains of ADA2 proteins determine selective incorporation into GCN5-containing complexes that target histone H3 or H4 for acetylation. *FEBS Letters*, 586(19), pp.3279–3286.

Eberharter, A. & Becker, P.B., 2002. Histone acetylation : a switch between repressive and permissive chromatin Second in review series on chromatin dynamics. *EMBO Reports*, 3(3), pp.224–229.

Ebert, A. et al., 2004. Su(var) genes regulate the balance between euchromatin and heterochromatin in Drosophila. *Genes and Development*, 18(23), pp.2973–2983.

Erhardt, S. et al., 2008. Genome-wide analysis reveals a cell cycle-dependent mechanism controlling centromere propagation. *Journal of Cell Biology*, 183(5), pp.805–818.

Fachinetti, D. et al., 2013. A two-step mechanism for epigenetic specification of centromere identity and function. *Nature cell biology*, 15(9).

Falk, S.J. et al., 2016. CENP-C directs a structural transition of CENP-A nucleosomes mainly through sliding of DNA gyres. *Nature structural & molecular biology*, 23(3), pp.204–8.

Fang, J.Y. et al., 2004. Epigenetic modification regulates both expression of tumor-associated genes and cell cycle progressing in human colon cancer cell lines: Colo-320 and SW1116. *Cell research*, 14(3), pp.217–226.

Felisbino, M.B. et al., 2016. Differential Response of Human Hepatocyte Chromatin to HDAC Inhibitors as a Function of Microenvironmental Glucose Level. *Journal of Cellular Physiology*, (September 2015), pp.2257–2265.

Filion, G.J. et al., 2010. Systematic Protein Location Mapping Reveals Five Principal Chromatin Types in Drosophila Cells. *Cell*, 143(2), pp.212–224.

Fischle, W. et al., 2003. Molecular basis for the discrimination of repressive methyl-lysine marks in histone H3 by polycomb and HP1 chromodomains. *Genes and Development*, 17(15), pp.1870–1881.

Flemming, W., 1882. Zellsubstanz, kern und zelltheilung. *F.C.W. Vogel, Leipzig,*, p.419.

Fogg, P.C.M. et al., 2014. Class IIa histone deacetylases are conserved regulators of circadian function. *Journal of Biological Chemistry*, 289(49), pp.34341–34348.

Foglietti, C. et al., 2006. Dissecting the biological functions of Drosophila histone deacetylases by RNA interference and transcriptional profiling. *Journal of Biological Chemistry*, 281(26), pp.17968–17976.

Folco, H.D. et al., 2008. Heterochromatin and RNAi are required to establish CENP-A chromatin at centromeres. *Science (New York, N.Y.)*, 319(5859), pp.94–97.

Forsburg, S.L., 2004. Eukaryotic MCM proteins: beyond replication initiation. *Microbiology and molecular biology reviews : MMBR*, 68(1), pp.109–131.

Fulco, M. et al., 2003. Sir2 regulates skeletal muscle differentiation as a potential sensor of the redox state. *Molecular Cell*, 12(1), pp.51–62.

Gabor, G.L., And, M. & John, B., 1979. Heterochromatin and Satellite DNA in Man: Properties and Prospects. *Am JHum Genet*, 31(3), pp.264–280.

Gao, L. et al., 2002. Cloning and functional characterization of HDAC11, a novel member of the human histone deacetylase family. *Journal of Biological Chemistry*, 277(28), pp.25748–25755.

Gaydos, L.J., Wang, W. & Strome, S., 2014. H3K27me and PRC2 transmit a memory of repression across generations and during development. *Science*, 345(6203).

Goldberg, A.D., Allis, C.D. & Bernstein, E., 2007. Epigenetics: A Landscape Takes Shape. *Cell*, 128(4), pp.635–638.

Görisch, S.M. et al., 2005. Histone acetylation increases chromatin accessibility. *Journal of cell science*, 118(Pt 24), pp.5825–5834.

Goshima, G. et al., 2007. Genes required for mitotic spindle assembly in Drosophila S2 cells. *Science (New York, N.Y.)*, 316(5823), pp.417–21.

Goutte-Gattat, D. et al., 2013. Phosphorylation of the CENP-A amino-terminus in mitotic centromeric chromatin is required for kinetochore function. *Proceedings of the National Academy of Sciences of the United States of America*, 110(21), pp.8579–84.

Greaves, I.K. et al., 2007. H2A . Z contributes to the unique 3D structure of the centromere. , 104(2), pp.525–530.

Greil, F. et al., 2003. Distinct HP1 and Su (var) 3-9 complexes bind to sets of developmentally coexpressed genes depending on chromosomal location. , 3, pp.2825–2838.

Gu, B. & Lee, M.G., 2013. Histone H3 lysine 4 methyltransferases and demethylases in self-renewal and differentiation of stem cells. *Cell & Bioscience*, 9, pp.1–14.

Guarente, L., 2001. SIR2 and aging - The exception that proves the rule. *Trends in Genetics*, 17(7), pp.391–392.

Guelman, S. et al., 2009. The double-histone-acetyltransferase complex ATAC is essential for mammalian development. *Molecular and cellular biology*, 29(5), pp.1176–1188.

Guo, R. et al., 2011. GCN5 and E2F1 stimulate nucleotide excision repair by promoting H3K9 acetylation at sites of damage. *Nucleic Acids Research*, 39(4), pp.1390–1397.

Guse, A. et al., 2011. In vitro centromere and kinetochore assembly on defined chromatin templates. *Nature*, 477(7364), pp.354–358.

Haaf, T., Warburton, P.E. & Willard, H.F., 1992. Integration of Human a-Satellite DNA into Simian Chromosomes : Centromere Protein Binding and Disruption of Normal Chromosome Segregation. , 70.

Hahnenberger, K.M. et al., 1989. Construction of functional artificial minichromosomes in the fission yeast Schizosaccharomyces pombe. , 86(January), pp.577–581.

Harikrishnan, K.N. et al., 2008. Effect of valproic acid on radiation-induced DNA damage in euchromatic and heterochromatic compartments. *Cell Cycle*, 7(4), pp.468–476.

Hartlepp, K.F. et al., 2005. The histone fold subunits of Drosophila CHRAC facilitate nucleosome sliding through dynamic DNA interactions. *Molecular and cellular biology*, 25(22), pp.9886–9896.

He, G. et al., 2013. Inhibition of autophagy induced by TSA sensitizes colon cancer cell to radiation. *Tumour biology : the journal of the International Society for Oncodevelopmental Biology and Medicine*, pp.1003–1011.

Henikoff, S. et al., 2014. The budding yeast centromere DNA element II wraps a stable Cse4 hemisome in either orientation in vivo. *eLife*, 2014(3), pp.1–23.

Heun, P. et al., 2006. Mislocalization of the drosophila centromere-specific histone CID promotes formation of functional ectopic kinetochores. *Developmental Cell*, 10(3), pp.303–315.

Hood, L. & Galas, D., 2003a. The digital code of DNA. *Nature*, 421(6921), pp.444–448.

Hood, L. & Galas, D., 2003b. The digital code of DNA. *Nature*, 421(6921), pp.444–448.

Hori, T. et al., 2014. Histone H4 Lys 20 Monomethylation of the CENP-A Nucleosome Is Essential for Kinetochore Assembly. *Developmental Cell*, 29(6), pp.740–749.

Huang, H. et al., 2010. Drosophila CAF-1 regulates HP1-mediated epigenetic silencing and pericentric heterochromatin stability. *J Cell Sci*, 123(Pt 16), pp.2853–2861.

Huang, J. et al., 2010. G9a and Glp methylate lysine 373 in the tumor suppressor p53. *Journal of Biological Chemistry*, 285(13), pp.9636–9641.

Hwang, K.K., Eissenberg, J.C. & Worman, H.J., 2001. Transcriptional repression of euchromatic genes by Drosophila heterochromatin protein 1 and histone modifiers. *Proceedings of the National Academy of Sciences of the United States of America*, 98(20), pp.11423–11427.

Izzo, A. & Schneider, R., 2010. Chatting histone modifications in mammals. *Briefings in Functional Genomics*, 9(5–6), pp.429–443.

Jakob, B. et al., 2011. DNA double-strand breaks in heterochromatin elicit fast repair protein recruitment, histone H2AX phosphorylation and relocation to euchromatin. *Nucleic Acids Research*, 39(15), pp.6489–6499.

Jenuwein, T., 2006. The epigenetic magic of histone lysine methylation: Delivered on 6 July 2005 at the 30th FEBS Congress in Budapest, Hungary. *FEBS Journal*, 273(14), pp.3121–3135.

Jørgensen, S., Schotta, G. & Sørensen, C.S., 2013. Histone H4 Lysine 20 methylation: key player in epigenetic regulation of genomic integrity. *Nucleic Acids Research* .

Kagansky, A. et al., 2009. Synthetic heterochromatin bypasses RNAi and centromeric repeats to establish functional centromeres. *Science (New York, N.Y.)*, 324(5935), pp.1716–9.

Kang, M.Y. et al., 2007. Association of the SUV39H1 histone methyltransferase with the DNA methyltransferase 1 at mRNA expression level in primary colorectal cancer. *International journal of cancer. Journal international du cancer*, 121(10), pp.2192–2197.

Karess, R., 2005. Rod-Zw10-Zwilch: A key player in the spindle checkpoint. *Trends in Cell Biology*, 15(7), pp.386–392.

Kasten, M.M., Dorland, S. & Stillman, D.J., 1997. A large protein complex containing the yeast Sin3p and Rpd3p transcriptional regulators. *Molecular and cellular biology*, 17(8), pp.4852–8.

Keller, C. et al., 2013. Noncoding RNAs prevent spreading of a repressive histone mark. *Nature structural & molecular biology*, 20(8), pp.994–1000.

Kerr, D.J. & Midgley, R., 2010. Defective Mismatch Repair in Colon Cancer : A Prognostic Or Predictive Biomarker ? , pp.31–33.

Kevin F. Sullivan, Mirko Hechenberger, K.M., 1994. Human CENP-A Contains a Histone H3 Related Histone Fold Domain That Is Required for Targeting to the Centromere. *The Journal of Cell Biology*, 127(3), pp.581–592.

Kijima, M. et al., 1993. Trapoxin, an antitumor cyclic tetrapeptide, is an irreversible inhibitor of mammalian histone deacetylase. *Journal of Biological Chemistry*, 268(30), pp.22429–22435.

Kleff, S. et al., 1995. Identification of a gene encoding a yeast histone H4 acetyltransferase. *Journal of Biological Chemistry*, 270(42), pp.24674–24677.

Klement, K. et al., 2014. Opposing ISWI- and CHD-class chromatin remodeling activities orchestrate heterochromatic DNA repair. *The Journal of Cell Biology*, 207(6), pp.717–733.

Kondo, Y., Shen, L. & Issa, J.-P.J., 2003. Critical Role of Histone Methylation in Tumor Suppressor Gene Silencing in Colorectal Cancer Critical Role of Histone Methylation in Tumor Suppressor Gene Silencing in Colorectal Cancer. *Molecular and Cellular Biology*, 23(1), pp.206–215.

Kornberg, R.D., 1974. Chromatin structure: a repeating unit of histones and DNA. *Science (New York, N.Y.)*, 184(139), pp.868–871.

Kukimoto, I. et al., 2004. The Histone-Fold Protein Complex CHRAC-15/17 Enhances Nucleosome Sliding and Assembly Mediated by ACF. *Molecular Cell*, 13(2), pp.265–277.

Kunitoku, N. et al., 2003. CENP-A phosphorylation by Aurora-A in prophase is required for enrichment of Aurora-B at inner centromeres and for kinetochore function. *Developmental Cell*, 5(6), pp.853–864.

Kuzmichev, A. et al., 2004. Different Ezh2-Containing Complexes Target Methylation of Histone H1 or Nucleosomal Histone H3. *Molecular Cell*, 14, pp.183–193.

de la Serna, I.L. & Imbalzano, A.N., 2002. Unfolding heterochromatin for replication. *Nature genetics*, 32(4), pp.560–2.

Lachner, M. et al., 2001. Methylation of histone H3 lysine 9 creates a binding site for HP1 proteins. *Nature*, 410(6824), pp.116–20.

Lacoste, N. et al., 2014. Mislocalization of the Centromeric Histone Variant CenH3/CENP-A in Human Cells Depends on the Chaperone DAXX. *Molecular Cell*, 53(4), pp.631–644.

Längst, G. & Becker, P.B., 2001. Nucleosome mobilization and positioning by ISWI-containing chromatin-remodeling factors. *Journal of cell science*, 114(Pt 14), pp.2561–2568.

Lechner, J. & Carbon, J., 1991. A 240 kd Multisubunit Protein Complex , CBF3 , Is a Major Component of the Budding Yeast Centromere. , 64, pp.717–725.

Lee, J. et al., 2013. MLL4 is required for enhancer activation during cell differentiation. *eLife*, 2, pp.1–25.

Lee, K.K. & Workman, J.L., 2007. Histone acetyltransferase complexes: one size doesn't fit all. *Nature reviews. Molecular cell biology*, 8(4), pp.284–295.

Leutz, A. et al., 2011. Crosstalk between phosphorylation and multi-site arginine/lysine methylation in C/EBPs. *Transcription*, 2(1), pp.3–8.

Lewis, L.K. et al., 2005. Reduction of nucleosome assembly during new DNA synthesis impairs both major pathways of double-strand break repair. *Nucleic Acids Research*, 33(15), pp.4928–4939.

Linda I., H., Bruno P., L. & Alan J., W., 2010. Bacterial protein acetylation: The dawning of a new age. *Molecular Microbiology*, 77(1), pp.15–21.

Liu, H. et al., 2015. Mitotic Transcription Installs Sgo1 at Centromeres to Coordinate Chromosome Segregation. *Molecular Cell*, 59(3), pp.426–436.

Liu, Y. & Zhang, D., 2015. HP1a/KDM4A is involved in the autoregulatory loop of the oncogene gene c-Jun. *Epigenetics*, 10(6), pp.453–459.

Locke, D.P. et al., 2011. Comparative and demographic analysis of orang-utan genomes. , pp.10–14.

Lombardi, P. & Cole, K., 2011. Structure, mechanism, and inhibition of histone deacetylases and related metalloenzymes. *Current opinion in Structural Biology*, 21(6), pp.735–743.

Loyola, A. et al., 2009. The HP1alpha-CAF1-SetDB1-containing complex provides H3K9me1 for Suv39-mediated K9me3 in pericentric heterochromatin. *EMBO reports*, 10(7), pp.769–775.

Lu, X. et al., 2013. Drosophila H1 regulates the genetic activity of heterochromatin by recruitment of Su(var)3-9. *Science (New York, N.Y.)*, 340(6128), pp.78–81.

Luger, K. et al., 1997. Characterization of nucleosome core particles containing histone proteins made in bacteria. *Journal of molecular biology*, 272(3), pp.301–11.

Lundberg, L.E., Stenberg, P. & Larsson, J., 2013. HP1a, Su(var)3-9, SETDB1 and POF stimulate or repress gene expression depending on genomic position, gene length and expression pattern in Drosophila melanogaster. *Nucleic Acids Research*, 41(8), pp.4481–4494.

Luo, J. et al., 2001. Negative control of p53 by Sir2alpha promotes cell survival under stress. *Cell*, 107(2), pp.137–48.

Lyko, F., Ramsahoye, B.H. & Jaenisch, R., 2000. DNA methylation in Drosophila melanogaster. *Developmental Dynamics*, 216(1), pp.1–1.

Ma, Y. et al., 2013. Identification of a histone acetyltransferase as a novel regulator of Drosophila intestinal stem cells. *FEBS Letters*, 587(10), pp.1489–1495.

Maeshima, K., Hihara, S. & Eltsov, M., 2010. Chromatin structure: Does the 30-nm fibre exist in vivo? *Current Opinion in Cell Biology*, 22(3), pp.291–297.

Maiato, H. et al., 2004. The dynamic kinetochore-microtubule interface. *Journal of cell science*, 117(Pt 23), pp.5461–77.

Malik, H.S., Vermaak, D. & Henikoff, S., 2002. Recurrent evolution of DNA-binding motifs in the Drosophila centromeric histone. *Proc Natl Acad Sci U S A*, 99(3), pp.1449–1454.

Masumoto, H. et al., 1998. Assay of centromere function using a human artificial chromosome. , pp.406–416.

Mathew, V. et al., 2014. The Histone-Fold Protein CHRAC14 Influences Chromatin Composition in Response to DNA Damage. *Cell Reports*, 7(2), pp.321–330.

McGovern, S.L. et al., 2012. Centromere protein-A, an essential centromere protein, is a prognostic marker for relapse in estrogen receptor-positive breast cancer. *Breast Cancer Research*, 14(3), p.R72.

McKinley, K.L. & Cheeseman, I.M., 2014. Polo-like kinase 1 licenses CENP-a deposition at centromeres. *Cell*, 158(2), pp.397–411.

McKinley, K.L. & Cheeseman, I.M., 2016. The molecular basis for centromere identity and function. *Nat Rev Mol Cell Biol*, 17(1), pp.16–29.

Mellone, B.G. et al., 2011. Assembly of Drosophila Centromeric Chromatin Proteins during Mitosis S. Biggins, ed. *PLoS Genetics*, 7(5), p.e1002068.

Mirza, S. et al., 2012. Alteration/deficiency in activation-3 (Ada3) plays a critical role in maintaining genomic stability. *Cell Cycle*, 11(22), pp.4266–4274.

Miska, E.A. et al., 2001. Differential localization of HDAC4 orchestrates muscle differentiation. *Nucleic Acids Research*, 29(16), pp.3439–3447.

Montefalcone, G. et al., 1999. Centromere Repositioning. , pp.1184–1188.

Murray, K., 1964. The Occurrence of iε-N-Methyl Lysine in Histones. *Biochemistry*, 3(1), pp.10–15.

Nakano, M. et al., 2008. Inactivation of a Human Kinetochore by Specific Targeting of Chromatin Modifiers. *Developmental Cell*, 14(4), pp.507–522.

Nakazawa, T. et al., 2012. Global histone modification of histone H3 in colorectal cancer and its precursor lesions. *Human Pathology*, 43(6), pp.834–842.

Narlikar, G.J., Sundaramoorthy, R. & Owen-Hughes, T., 2013. Mechanisms and functions of ATP-dependent chromatin-remodeling enzymes. *Cell*, 154(3), pp.490–503.

Nguyen, A.T. & Zhang, Y., 2011a. The diverse functions of Dot1 and H3K79 methylation. *Genes & Development*, 3, pp.1345–1358.

Nguyen, A.T. & Zhang, Y., 2011b. The diverse functions of Dot1 and H3K79 methylation. [Genes Dev. 2011] - PubMed - NCBI. *Genes and Development*, 3, pp.1345–1358.

Nielsen, P.R. et al., 2002. Structure of the HP1 chromodomain bound to histone H3 methylated at lysine 9. *Nature*, 416(6876), pp.103–107.

Niikura, Y. et al., 2015. CENP-A K124 Ubiquitylation Is Required for CENP-A Deposition at the Centromere. *Dev Cell*, 32(5), pp.589–603.

O'Byrne, K.J. et al., 2011. Epigenetic regulation of glucose transporters in non-small cell lung cancer. *Cancers*, 3(2), pp.1550–1565.

Ohzeki, J. et al., 2012. Breaking the HAC Barrier: Histone H3K9 acetyl/methyl balance regulates CENP-A assembly. *The EMBO Journal*, 31(10), pp.2391–2402.

Ohzeki, J. et al., 2016. KAT7/HBO1/MYST2 Regulates CENP-A Chromatin Assembly by Antagonizing Suv39h1-Mediated Centromere Inactivation. *Developmental Cell*, 37(5), pp.413–427.

Oliva, R. et al., 1990. Histone hyperacetylation can induce unfolding of the nucleosome core particle. *Nucleic Acids Research*, 18(9), pp.2739–2747.

Okada, T. et al., 2007. CENP-B Controls Centromere Formation Depending on the Chromatin Context. *Cell*, 131(7), pp.1287–1300.

Olins, A.L. & Olins, D.E., 1974. Spheroid chromatin units (v bodies). *Science (New York, N.Y.)*, 183(4122), pp.330–2.

Olszak, A.M. et al., 2011. Heterochromatin boundaries are hotspots for de novo kinetochore formation. *Nature cell biology*, 13(7), pp.799–808.

Orr, B. & Sunkel, C.E., 2011. Drosophila CENP-C is essential for centromere identity. *Chromosoma*, 120(1), pp.83–96.

Padeganeh, A., Ryan, J., et al., 2013. Octameric CENP-A Nucleosomes Are Present at Human Centromeres throughout the Cell Cycle. *Current Biology*, 23(9), pp.764–769.

Padeganeh, A., De Rop, V. & Maddox, P.S., 2013. Nucleosomal composition at the centromere: A numbers game. *Chromosome Research*, 21(1), pp.27–36.

Pankotai, T. et al., 2005. The Homologous Drosophila Transcriptional Adaptors ADA2a and ADA2b Are both Required for Normal Development but Have Different Functions. *Molecular and Cellular Biology*, 25(18), pp.8215–8227.

Pardue, M.L. & Gall, J.G., 1970. Chromosomal localization of mouse satellite DNA. *Science (New York, N.Y.)*, 168(937), pp.1356–1358.

Park, J.-A. et al., 2011. Deacetylation and methylation at histone H3 lysine 9 (H3K9) coordinate chromosome condensation during cell cycle progression. *Molecules and cells*, 31(4), pp.343–349.

Pauleau, A.L. & Erhardt, S., 2011. Centromere regulation: New players, new rules, new questions. *European Journal of Cell Biology*, 90(10), pp.805–810.

Pérez-Toledo, K. et al., 2009. Plasmodium falciparum heterochromatin protein 1 binds to tri-methylated histone 3 lysine 9 and is linked to mutually exclusive expression of var genes. *Nucleic Acids Research*, 37(8), pp.2596–2606.

Peters, A.H.F.M. et al., 2001. Loss of the Suv39h histone methyltransferases impairs mammalian heterochromatin and genome stability. *Cell*, 107(3), pp.323–337.

Peters, A.H.F.M. et al., 2003. Partitioning and Plasticity of Repressive Histone Methylation States in Mammalian Chromatin. *Molecular Cell*, 12(6), pp.1577–1589.

Peterson, C.L., 2002. Chromatin remodeling enzymes : taming the machines Third in review series on chromatin dynamics. *EMBO Reports*, 3(4), pp.319–322.

Pile, L. a, Lee, F.W. & Wassarman, D. a, 2001. The histone deacetylase inhibitor trichostatin A influences the development of Drosophila melanogaster. *Cellular and molecular life sciences : CMLS*, 58(11), pp.1715–1718.

Piras, F.M. et al., 2010. Uncoupling of Satellite DNA and Centromeric Function in the Genus Equus. , 6(2).

Prendergast, L. et al., 2016. The CENP-T/-W complex is a binding partner of the histone

chaperone FACT. *Genes & Development*, 30(11), pp.1313–1326.

Przewloka, M.R. et al., 2011. CENP-C is a structural platform for kinetochore assembly. *Current Biology*, 21(5), pp.399–405.

Quénet, D. & Dalal, Y., 2014. A long non-coding RNA is required for targeting centromeric protein A to the human centromere. *eLife*, 3.

Quivy, J.-P. et al., 2008. The HP1-p150/CAF-1 interaction is required for pericentric heterochromatin replication and S-phase progression in mouse cells. *Nature structural & molecular biology*, 15(9), pp.972–979.

Raddatz, G. et al., 2013. Dnmt2-dependent methylomes lack defined DNA methylation patterns. *Proceedings of the National Academy of Sciences of the United States of America*, 110(21), pp.8627–31.

Rayasam, G.V. et al., 2003. NSD1 is essential for early post-implantation development and has a catalytically active SET domain. *EMBO Journal*, 22(12), pp.3153–3163.

Razin, S. V & Gavrilov, A.A., 2014. Chromatin without the 30-nm fiber. *Epigenetics*, (May), pp.653–657.

Rea, S. et al., 2000. Regulation of chromatin structure by site-specific histone H3 methyltransferases. *Nature*, 406(6796), pp.593–599.

Reinberg, D., 2011. The Polycomb complex PRC2 and its mark in life. *Nature*, 469, pp.342–349.

Ribeiro, S.A. et al., 2010. A super-resolution map of the vertebrate kinetochore. *Proceedings of the National Academy of Sciences of the United States of America*, 107(23), pp.10484–10489.

RIGGS, M.G. et al., 1977. n-Butyrate causes histone modification in HeLa and Friend erythroleukaemia cells. *Nature*, 268(5619), pp.462–464.

Rocha, W. & Verreault, A., 2008. Clothing up DNA for all seasons: Histone chaperones and nucleosome assembly pathways. *FEBS Letters*, 582(14), pp.1938–1949.

Rošić, S. & Erhardt, S., 2016. No longer a nuisance: Long non-coding RNAs join CENP-A in epigenetic centromere regulation. *Cellular and Molecular Life Sciences*, 73(7), pp.1387–1398.

Rošić, S., Köhler, F. & Erhardt, S., 2014. Repetitive centromeric satellite RNA is essential for kinetochore formation and cell division. *Journal of Cell Biology*, 207(3), pp.335–349.

Ruesch, C.E. et al., 2015. The Histone H3 Lysine 9 Methyltransferase DIM-5 Modi fi es Chromatin at frequency and Represses Light-Activated Gene Expression. , 5(January),

pp.93–101.

Saitoh, H. et al., 1992. CENP-C, an autoantigen in scleroderma, is a component of the human inner kinetochore plate. *Cell*, 70(1), pp.115–125.

Samb, B. et al., 2015. CENP-C reshapes and stabilizes CENP-A nucleosomes at the centromere. , 348(6235), pp.699–703.

Samel, a. et al., 2012. Methylation of CenH3 arginine 37 regulates kinetochore integrity and chromosome segregation. *Proceedings of the National Academy of Sciences*, 109(23), pp.9029–9034.

Sanders, S.L. et al., 2004. Methylation of Histone H4 Lysine 20 Controls Recruitment of Crb2 to Sites of DNA Damage. *Cell*, 119, pp.603–614.

Sandstrom, R.S. et al., 2014. Epigenetic Regulation by Chromatin Activation Mark H3K4me3 in Primate Progenitor Cells within Adult Neurogenic Niche. , pp.1–9.

Scheffer, M.P., Eltsov, M. & Frangakis, A.S., 2011. Evidence for short-range helical order in the 30-nm chromatin fibers of erythrocyte nuclei. *Proceedings of the National Academy of Sciences of the United States of America*, 108(41), pp.16992–7.

Schneider, R. & Grosschedl, R., 2007. Dynamics and interplay of nuclear architecture, genome organization, and gene expression. *Genes and Development*, 21(23), pp.3027–3043.

Schotta, G. et al., 2002. Central role of Drosophila SU(VAR)3-9 in histone H3-K9 methylation and heterochromatic gene silencing. *EMBO Journal*, 21(5), pp.1121–1131.

Schotta, G., Ebert, A. & Reuter, G., 2003. SU(VAR)3-9 is a conserved key function in heterochromatic gene silencing. *Genetica*, 117(2–3), pp.149–158.

Sekulic, N. et al., 2010. The Structure of (CENP-A/H4)2 Reveals Physical Features that Mark Centromeres. *Structure*, 467(7313), pp.347–351.

Seum, C. et al., 2007. Drosophila G9a is a nonessential gene. *Genetics*, 177(3), pp.1955–1957.

Shang, W.-H. et al., 2016. Acetylation of histone H4 lysine 5 and 12 is required for CENP-A deposition into centromeres. *Nature Communications*, 7, p.13465.

Shareef, M.M. et al., 2001. Drosophila Heterochromatin Protein 1 (HP1)/ Origin Recognition Complex (ORC) Protein Is Associated with HP1 and ORC and Functions in Heterochromatin- induced Silencing. , 12(June), pp.1671–1685.

Shilatifard, A., 2008. Molecular implementation and physiological roles for histone H3 lysine 4 (H3K4) methylation. *Current Opinion in Cell Biology*, 20(3), pp.341–348.

Shiloh, Y. & Ziv, Y., 2013. The ATM protein kinase: regulating the cellular response to genotoxic stress, and more. *Nature reviews. Molecular cell biology*, 14(4), pp.197–210.

Shono, N. et al., 2015. CENP-C and CENP-I are key connecting factors for kinetochore and CENP-A assembly. *Journal of cell science*, (November 2015), p.jcs.180786-.

Silva, M.C.C. et al., 2012. Cdk Activity Couples Epigenetic Centromere Inheritance to Cell Cycle Progression. *Developmental Cell*, 22(1), pp.52–63.

Soret, J. et al., 2003. Altered Serine/Arginine-Rich Protein Phosphorylation and Exonic Enhancer-Dependent Splicing in Mammalian Cells Lacking Topoisomerase I. *Cancer Research*, 63(23), pp.8203–8211.

Spedale, G., Timmers, H.T.M. & Pijnappel, W.W.M.P., 2012. ATAC-king the complexity of SAGA during evolution. *Genes and Development*, 26(6), pp.527–541.

Suganuma, T. et al., 2008. ATAC is a double histone acetyltransferase complex that stimulates nucleosome sliding. *Nature structural & molecular biology*, 15(4), pp.364–372.

Sulli, G., Di Micco, R. & di Fagagna, F. d'Adda, 2012. Crosstalk between chromatin state and DNA damage response in cellular senescence and cancer. *Nature Reviews Cancer*, 12(10), pp.709–720.

Sullivan, B. a & Karpen, G.H., 2004. Centromeric chromatin exhibits a histone modification pattern that is distinct from both euchromatin and heterochromatin. *Nature structural & molecular biology*, 11(11), pp.1076–1083.

Sullivan KF, Hechenberger M, M.K., 1994. Human CENP-A Contains a Histone H3 Related Histone Fold Domain That Is Required for Targeting to the Centromere. *The Journal of Cell Biology*, 127(3), pp.581–592.

Swygert, S. & Peterson, C., 2014. Chromatin dynamics: Interplay between remodeling enzymes and histone modifications. *Biochim Biophys Acta.*, 1839(8), pp.728–736.

Szyf, M., 2003. DNA methylation and cancer therapy. *Drug resistance updates : reviews and commentaries in antimicrobial and anticancer chemotherapy*, 6(6), pp.341–353.

Tachibana, M. et al., 2002. G9a histone methyltransferase plays a dominant role in euchromatic histone H3 lysine 9 methylation and is essential for early embryogenesis. *Genes and Development*, 16(14), pp.1779–1791.

Tachibana, M. et al., 2001. SET Domain-containing Protein, G9a, is a Novel Lysine-preferring Mammalian Histone Methyltransferase with Hyperactivity and Specific Selectivity to Lysines 9 and 27 of Histone H3. *Journal of Biological Chemistry*, 276(27), pp.25309–25317.

Tachiwana, H. et al., 2011. Crystal structure of the human centromeric nucleosome containing CENP-A. *Nature*, 476(7359), pp.232–235.

Taddei, A. et al., 2005. The effects of histone deacetylase inhibitors on heterochromatin: implications for anticancer therapy? *EMBO reports*, 6(6), pp.520–524.

Taddei, a et al., 2001. Reversible disruption of pericentric heterochromatin and centromere function by inhibiting deacetylases. *Nature cell biology*, 3(2), pp.114–120.

Takayama, S. et al., 2014. Genome methylation in D. melanogaster is found at specific short motifs and is independent of DNMT2 activity. *Genome Research*, 24(5), pp.821–830.

Tamagawa, H. et al., 2012. The global histone modification pattern correlates with overall survival in metachronous liver metastasis of colorectal cancer. *Oncology Reports*, 27(3), pp.637–642.

Tao, D. et al., 2004. Trichostatin A extends the lifespan of Drosophila melanogaster by elevating hsp22 expression. *Acta biochimica et biophysica Sinica*, 36(9), pp.618–622.

Thornton, J.L. et al., 2014. Context dependency of Set1 / COMPASS-mediated histone H3 Lys4 trimethylation. *Genes & Dev.*, pp.1–7.

Tjeertes, J. V, Miller, K.M. & Jackson, S.P., 2009. Screen for DNA-damage-responsive histone modifications identifies H3K9Ac and H3K56Ac in human cells. *The EMBO journal*, 28(13), pp.1878–89.

Tomonaga, T., Matsushita, K. & Yamaguchi, S., 2003. Overexpression and Mistargeting of Centromere Protein-A in Human Primary Colorectal Cancer Overexpression and Mistargeting of Centromere Protein-A in Human Primary. , pp.3511–3516.

Tóth, K.F. et al., 2004. Trichostatin A-induced histone acetylation causes decondensation of interphase chromatin. *Journal of cell science*, 117(Pt 18), pp.4277–4287.

Tsang, C.K. et al., 2014. Superoxide dismutase 1 acts as a nuclear transcription factor to regulate oxidative stress resistance. *Nature communications*, 5, p.3446.

Varga-Weisz, P.D. et al., 1997. Chromatin-remodelling factor CHRAC contains the ATPases ISWI and topoisomerase II. *Nature*, 388(October), pp.598–602.

Vermaak, D., Hayden, H.S. & Henikoff, S., 2002. Centromere Targeting Element within the Histone Fold Domain of Cid. *Molecular and Cellular Biology*, 22(21), pp.7553–7561.

Vernarecci, S. et al., 2008. Gcn5p plays an important role in centromere kinetochore function in budding yeast. *Molecular and cellular biology*, 28(3), pp.988–996.

Ververis, K. et al., 2013. Histone deacetylase inhibitors (HDACIS): Multitargeted anticancer agents. *Biologics: Targets and Therapy*, 7(1), pp.47–60.

Vigushin, D.M. et al., 2001. Trichostatin A Is a Histone Deacetylase Inhibitor with Potent Antitumor Activity against Breast Cancer in Vivo 1. , 7(April), pp.971–976.

Wagner, E.J. & Carpenter, P.B., 2012. Understanding the language of Lys36 methylation at histone H3. *Nature Publishing Group*, 13(2), pp.115–126.

Wang, a H. et al., 1999. HDAC4, a human histone deacetylase related to yeast HDA1, is a transcriptional corepressor. *Molecular and cellular biology*, 19(11), pp.7816–7827.

Wang, X. & Zhu, W.G., 2008. Advances in histone methyltransferases and histone demethylases. *Ai zheng = Aizheng = Chinese journal of cancer*, 27(10), pp.1018–1025.

Wang, Y., Li, X. & Hu, H., 2014. H3K4me2 reliably defines transcription factor binding regions in different cells. *Genomics*, 103(2–3), pp.222–228.

Wang, Z. et al., 2008. Combinatorial patterns of histone acetylations and methylations in the human genome. *Nature genetics*, 40(7), pp.897–903.

Whitaker, R. et al., 2013. Increased expression of Drosophila sir2 extends life span in a dosedependent manner. *Aging*, 5(9), pp.682–691.

Woodcock, C.L., 1994. Chromatin fibers observed in situ in frozen hydrated sections. Native fiber diameter is not correlated with nucleosome repeat length. *Journal of Cell Biology*, 125(1), pp.11–19.

Wu, H. et al., 2011. Histone methyltransferase G9a contributes to H3K27 methylation in vivo. *Cell research*, 21(2), pp.365–367.

Wu, L.-P. et al., 2008. Histone deacetylase inhibitor depsipeptide activates silenced genes through decreasing both CpG and H3K9 methylation on the promoter. *Molecular and cellular biology*, 28(10), pp.3219–35.

Xue-Franzén, Y. et al., 2013. Distinct roles of the Gcn5 histone acetyltransferase revealed during transient stress-induced reprogramming of the genome. *BMC genomics*, 14(1), p.479.

Yamamizu, K. et al., 2012. Protein kinase A determines timing of early differentiation through epigenetic regulation with G9a. *Cell Stem Cell*, 10(6), pp.759–770.

Yan, H. & Jiang, J., 2007. Rice as a model for centromere and heterochromatin research. , pp.77–84.

Yoshidas, M., 1990. Potent and Specific Inhibition of Mammalian in Vivo and in Vitro by Trichostatin A * Histone Deacetylase Both. *October*, 265(28), pp.17174–17179.

Yu, Z. et al., 2015. Dynamic phosphorylation of CENP-A at Ser68 orchestrates its cell-cycle-dependent deposition at centromeres. *Developmental Cell*, 32(1), pp.68–81.

Yuan, K. & O'Farrell, P.H., 2016. TALE-light imaging reveals maternally guided, H3K9me2/3-independent emergence of functional heterochromatin in Drosophila embryos. *Genes and Development*, 30(5), pp.579–593.

Yunis, J.J. & Yasmineh, W.G., 1971. Heterochromatin, satellite DNA, and cell function. Structural DNA of eucaryotes may support and protect genes and aid in speciation. *Science (New York, N.Y.)*, 174(15), pp.1200–1209.

Zeitlin, S.G. et al., 2001. Differential regulation of CENP-A and histone H3 phosphorylation in G2/M. *Journal Of Cell Science*, 114(Pt 4), pp.653–661.

Zhang, J. et al., 2015. Down-regulation of G9a triggers DNA damage response and inhibits colorectal cancer cells proliferation. *Oncotarget*, 6(5), pp.2917–27.

Zhang, X. et al., 2005. Phosphoserines on maize CENTROMERIC HISTONE H3 and histone H3 demarcate the centromere and pericentromere during chromosome segregation. *The Plant cell*, 17(2), pp.572–583.

Zhou, Y. et al., 2009. Reversible acetylation of the chromatin remodelling complex NoRC is required for non-coding RNA- dependent silencing. *Nature Publishing Group*, 11(8), pp.1010–1016.

8 Abbreviations

Ac	Acetylation
ACF	assembly and remodeling factor
Asf1	anti-silencing factor
CAF-1	Chromatin assembly factor 1
CATD	CENP-A targeting domain
CCAN	Constitutive centromere associated complex
CenH3	Centromeric histone H3
CENP	Centromere protein
CHD	Chromodomain, helicase, DNA binding
ChIP	Chromatin Immunoprecipitation
CHRAC	Chromatin accessibility complex
CID	Centromere identifier
DDR	DNA damage response
DNA	Deoxyribonucleic acid
ds	Double stranded
DSBs	DNA Double Stranded Breaks
E (z)	Enhancer of Zeste
FACT	facilitates chromatin transcription
GFP	Green fluorescent protein
h	hour
H2A	Histone 2A
H2B	Histone 2B
H3	Histone 3
H4	Histone 4
HAC	Human artificial chromosome
HAT	Histone acetyltransferase
HDAC1/2	Histone deacetylase 1/2
HJURP	Holliday Junction Recognition Protein
HP1	Heterochromatin protein 1
IF	Immunofluorescence
IN080	Inositol Requiring 80
IP	Immunoprecipitated
ISWI	Imitation SWI
K	Lysine
Me	Methylation
min	Minutes
MMS	Methy Methane Sulfonate
P	Phosphorylation

PEV	Position effect variegation
R	Arginine
S	Serine
Scm3	Scm3
Su(var)	Suppressor of variegation
SWI/ SNF	switching defective/sucrose nonfermenting
T	Threonine
Tip60	Tat-interactive protein 60
Trx	Trithorax
WDS	will die slowly
µl	micro litre

Erklärung

Hiermit erkläre ich, dass ich die vorliegende Dissertation selbstständig und ohne unerlaubte Hilfsmittel angefertigt habe

Heidelberg, den Abhishek Sharma